ECOPHYSIOLOGY OF (PERI)ORAL BACTERIA AND IMPACT OF OTIC COLONIZATION

By

Kristin Marie Jacob

A DISSERTATION

Submitted to
Michigan State University
in partial fulfillment of the requirements
for the degree of

Microbiology and Molecular Genetics – Doctor of Philosophy

2022

ABSTRACT

ECOPHYSIOLOGY OF (PERI)ORAL BACTERIA AND IMPACT OF OTIC COLONIZATION

By

Kristin Marie Jacob

The middle ear is assumed sterile in health due to its secluded location, closed off from external forces by the tympanic membrane & from the naso/oropharynx by a collapsed Eustachian tube (ET). However, the periodic opening of the ET to the naso/oropharyngeal space, releasing pressure across the eardrum & draining otic fluids, could introduce bacteria. Previous studies tested for the presence of bacteria in the uninfected otic cavity using samples collected via invasive surgeries. These studies' findings are controversial due to contradictory results, lack of critical experimental controls, & sampling of participants with underlying ailments (that could impact the microbiology of the otic mucosa. The studies reported herein bypass these limitations by using samples of otic secretions collected non-invasively healthy young adults. This dissertation describes cultivation-dependent methods investigating the microbiology of the middle ear in health to collect otic secretions to sequence their microbiome and recover in pure culture otic bacteria for further characterization. As controls, we also collected buccal & oropharyngeal swabs from each participant. Of the collected secretions, samples from 19 individuals were used for culture independent studies, while the remaining 3 participant samples were subjected to culture dependent studies. 16S rRNA-V4 sequencing detected a diverse & distinct microbiome in otic secretions comprised primarily of strictly anaerobic bacteria (Bacteroidetes, Firmicutes & Fusobacteria) &, to a lesser extent, facultative anaerobes (*Streptococcus*). Thirty-nine isolates of predominantly facultative anaerobes belonging to Firmicutes (*Streptococcus* & *Staphylococcus*), Actinobacteria (*Micrococcus* &

Corynebacterium), & Proteobacteria (*Neisseria*) phyla were recovered from secretions. Partial 16S rRNA amplicon sequences to demonstrate the distinct phylogenetic placement of otic streptococci compared to the oral ancestors (Ch. 2), consistent with the ecological diversification of oral streptococci once in the middle ear microenvironment. The recovery of streptococci & transient migrants (*Staphylococcus*, *Neisseria*, *Micrococcus* & *Corynebacterium*) from otic secretions prompted us to study the adaptive responses giving streptococcal migrants a competitive advantage during the middle ear colonization (Ch. 3). Here, full length 16s rRNA phylogenetic analyses demonstrated the oral ancestry of the otic streptococci, which retained from the otic adaptive traits critical for growth & reproduction in the middle ear mucosa giving oral streptococci a colonization advantage over competing (peri)oral migrants. Additionally, the ability of staphylococcal migrants to breach the middle ear mucosal barrier & cause infections prompted us to study the environmental factors that facilitate the spreading of staphylococci from the nasal to the middle ear mucosa (Ch. 4). I show that mucins induce rapid spreading & dendritic expansion of clinical isolates in a process dependent on the secretion of surfactant-active, phenol-soluble modulins via the agr-quorum sensing two-component system. The work described in this dissertation provides needed understanding of the adaptive responses that allow (peri)oral bacteria to colonize the middle ear. The studies add to the accumulating evidence that the middle ear mucosa harbors a commensal microbiota in health. These commensal community shares many metabolic similarities with ancestors in oral biofilms & retain adaptive traits critical for growth in the otic mucosa & inhibition of otopathogens. Additionally, this work identifies environmental factors that could contribute to staphylococcal virulence, broadening the understanding of newly identified motility phenotypes in the genus that could provide novel pharmaceutical targets.

‘Promise me you’ll always remember:
You’re braver than you believe, stronger than you seem, and smarter than you think.’
-Winnie-the-Pooh

This work is dedicated to family who have supported me along the winding path, through all the doubts and the obstacles set in my way, and for always believing in me even when I couldn’t believe in myself.

ACKNOWLEDGEMENTS

Pursing a PhD has shared many resemblances to a difficult hike in the wood; the long trails twist and turn, sometimes disappearing completely forcing you to push yourself through until you can put yourself back on the right track. Somedays it's easy and somedays its hard to find your way again. But in the end, the view (thesis) is something that can simply take your breath away, filling you with pride and joy in the growth you sustained to reach the end. None of this would have been possible without the continued support, encouragement and guidance from my mentor, Gemma Reguera. She pushed me to be my own scientist, allowing me the freedom to work through the puzzles the results provided me and with the understanding and support that I needed to stumble my own way through with gentle guidance, knowing I would ask for help when I needed it. She has supported me not only through achieving my academic and research goals, but in my non-academic ambitions as well. Also, I could not have come all this way without the support of Dr. Kazem Kashefi, not only for his guidance in anaerobic and pressure growth and culturing conditions utilized in this study. I would also like to thank Dr. Neal Hammer and my committee members, Dr. George Mias and Dr. Chris Waters, for their support, guidance, and expertise that they brought to my project.

Additionally, I am thankful to be a part of the Reguera lab and work closely with incredible and wonderful people, who happily put up with me not only on my best days, but on my worst days. This project wouldn't have been possible without the dedicated collaboration with Dr. Joo-Young Lee who alongside me to begin expanding our understanding of the present otic microbiota through culture independent 16S V4-rRNA amplicon sequencing and metagenomics outlined in my second chapter. Although not a part of our otic team, I am especially thankful to Michael Hunter Dulay and Morgan Clark for always being discussing

experimental parameters, editing papers, inoculating transfers, image plates and overall supporting me, inside and outside of the lab, even when it was to simply talk out my thoughts when my brain was working in a caffeinated overdrive. I exceptionally grateful to Marcela Diana Ruiz Tabares for not only discussing bioinformatics, suffering R-scripting with me (especially helping identify my pitfalls when I delete half the code on accident just when the cat turns off my computer), being my "COVID lab buddy", staying with me on late nights just to keep me company while we dance and sing to salsa until my late timepoints are complete, and overall being the best friend I could have ever asked for. No lab is perfect, but I feel immensely fortunate to not have found just a research lab here at MSU, but instead I found a family.

I would like to thank the staff at the Michigan Department of Health and Human Services for their help and support in completion of this project. Dr. Marty Soehnlen and Dr. Heather Blankenship provided me with the opportunity to expand my knowledge of public health, and I am thankful that they allowed me to immerse myself into the field and broaden my knowledge of infectious disease. Elizabeth Burgess, Dr. Batsiri Mabvakure and Dr. Arianna Miles-Jay helped perform library preparation and oxford nanopore whole genome sequencing of isolates, bioinformatics and pipeline development for sequencing and data analysis included in the study.

Funding for this work came from the Office of Naval Research and Michigan State University. Additional funding was provided through the College of Natural Science Academic Achievement Graduate Assistantship, Department of Microbiology and Molecular Genetics Phillip and Vera Gerhard Research Award, Hsuing-Kimball Award, and Bertina Wentworth Travel Award, and Michigan State University BEST program.

Finally, I must than my friends and family who have showed me love and support during this latest adventure. No matter the distance between us, you all were there for me to share in the

good days and the bad days. Thank you to my best friend Danielle for the late-night phone calls to another state when the pressure took my away my ability to sleep, staying up until I could finally shut my eyes. No matter how far apart we are, whether it is in a northern paradise or across state lines, you've never stopped being there for me. And to Savanna for the "wine and whine" nights, supporting me virtually when the trying times wouldn't make traveling to different cities possible. To my oldest friend, Stephanie, you've been there to support your "starving grad student" through my scientific career since our northern adventures in the UP. To Eric, my virtual study (drinking) buddy, for always finding a way to make me relax and have fun when we hang out, no matter how stressed I am. And to Heather and Marcela, for making me dinner (or breakfast), ensuring I have eaten that day, and pushing me through the crippling procrastination with a steady supply of caffeine, and fun when I don't allow myself to have it, I am forever thankful for the friendship and support I have found in you both. And finally, to the friends I have made during my time as MSU, you all have a special place in my heart, and I cherish all the love and support you've shown me.

A special thank you to my family. I have saved this thank you for last because there are really no words to show my appreciation for your continuous love and support. To my parents, John and Patricia, for putting up with not one but two cycles of graduate school research and thesis writing. The phone calls to check in, the impromptu lunches and dinners and surprise puppy visits with Olya, even when research made you wait for hours after our dinner dates. To my sister Jennifer and her husband Bobby for listening to my venting and making me laugh between meme wars and visits. To my brother Jonathon and his wife Jennifer, for constantly showing me love and support. The saying "it takes a village" has never been so well placed as

when applied to pursuing a PhD, and I am thankful for all those who have been a part of this journey.

TABLE OF CONTENTS

LIST OF TABLES

LIST OF FIGURES

KEY TO ABBREVIATIONS

A550	Absorbance 550nm
BLAST	Basic Local Alignment Search Tool
ET	Eustachian tube
16S rRNA	16S Ribosomal Ribonucleic Acid
RTSF	MSU Research Technology Support Facility
CI	Confidence Interval
CIDT	Culture Independent Test
CV	Crystal Violet
RTA	Illumina Real Time Analysis
OTU	Operational Taxonomic Units
PCoA	Principal Coordinate Analysis
TSA	Tryptic Soy Agar
LB	Luria Bertani Broth
TSB	Tryptic Soy Broth
PCR	Polymerase Chain Reaction
LTP	Living Tree Project
GPAC	Gram Positive Anaerobic Cocci
OD 600/630	Optical Density 600/630nm
ANOVA	Analysis of Variance
HPLC	High Performance Liquid Chromatography

NTHi	Non-Typeable Haemophilus influenzae
BHI/sBHI	Brain Heart Infusion/Supplemented Brain Heart Infusion
NCBI	National Center for Biotechnology Information
PSM	Peptide Soluble Modulins
CA-MRSA	Community-Associated Methicillin-Resistant Staphylococcus aureus
WGS	Whole Genome Sequencing

CHAPTER 1

LITERATURE REVIEW: MIDDLE EAR AND THE HISTORY OF MICOBIOTA IDENTIFICATION AND BACTERIAL COLONIZATION

MIDDLE EAR ANATOMY

The middle ear (tympanic cavity and extended tube – the Eustachian tube [ET]) houses the small, vibrating bones (the ossicles) that propagate sound from the eardrum to the hearing organ (cochlea) in the inner ear (Fig. 1.1). Physical isolation is critical to sound propagation in the middle ear. The cavity is isolated from the external ear canal via the eardrum. As sounds concentrate at the eardrum, the membrane vibrates and the sound-induced vibrations are passed to the ossicle chain and, from there, to the inner ear so "hearing" occurs [1]. Physical isolation sound-proofs the middle ear cavity and enables high-frequency hearing in mammals [2]. Seclusion is also important to prevent the entry of microbes from the neighboring perioral regions. Perhaps because of its secluded location, the middle ear was assumed to be sterile. However, the tympanic space is not completely isolated from the oral cavity. Rather, it extends into the nasopharynx as a tube with the shape of an inverted flask (the Eustachian tube) to provide a mechanism for aeration that periodically supplies oxygen to the otic mucosa [3]. The tube is collapsed at rest to minimize sound interference but opens everytime we swallow or yawn to introduce air from the lungs[3]. As gas is consumed by the otic epithelium, negative pressure builds in the middle ear that retracts the eardrum and draws fluids out of the mucosa. The periodic opening of the ET relieves pressure across the eardrum and drains excess fluids in the back of the throat [3]. The cycles of ET aperture are brief (400 ms) to minimize interference from respiratory and cardiac noise yet essential for mucosal aeration, depressurization, and fluid drainage [3]. The periodic openings of the ET (every minute while awake or 5 minutes during sleep) introduce air from the lower airways, offering opportunities for microorganisms in the naso/oropharynx to disperse aerially into the middle ear and colonize its mucosa. Furthermore, although mucociliary clearance in the ET lumen is vigorous and the periodic openings of the

tube promote muscular clearance of otic fluids [3, 4], microbes from the neighboring perioral regions could potentially move on the mucosal surface to reach the tympanic cavity. Both aerial dispersal and mucosal translocation may in fact contribute to the entry of otopathogens into the middle ear and lead to infections such as otitis media in at risk (e.g., asthma, ET disfunction, inflammation, etc.) patients [3]. Thus, the middle ear mucosa may harbor a microbial community. Whether transient, as in the lungs, or established (as in oral biofilms or the gut microbiome), it is unlikely the middle ear mucosa is sterile, as assumed for long. We posit instead that the middle ear provides conditions optimal for the establishment of a commensal community in health.

Nutrients in the middle ear mucosa that could support the growth of a commensal community

As the mucosae of other body sites, the middle ear mucosa contains host-derived glycoproteins (mucins) and proteins [5] that can support the growth of microbial colonizers. Gel-forming mucins provide a viscous medium (the mucus layer) to cover the epithelial lining throughout the body [3, 6, 7]. As glycoproteins, they also provide an abundant source of carbohydrates and proteins for microbial colonizers. Otic mucin is composed of 39.5% protein and 60.5% carbohydrate [5] thus providing sources of carbon and nitrogen for colonizing bacteria. Not surprisingly, the ability of mucosal residents to break down and assimilate mucin is widespread [8-10]. In general, enzymatic (host or bacterial) degradation interactions between the mucin glycoarray and resident bacteria select for symbiotic relationships and mutualistic partnerships between the host mucosa and bacteria, promoting protection of mucosal lining against pathogens. The mucus layer is typically separated into a lower, more viscous “sterile” layer near the mucosal epithelium, and a less gelatinous top layer abundant with partially degraded mucin, where bacteria can reside [6]. Driving the symbiosis between host and

microbiota, natural host enzymatic processes driving mucosal turnover drive the partial degradation of mucin providing monosaccharides for metabolic use[6]. Additionally, bacterial enzymes contribute to mucosal turnover[6]. Bacterial interactions with the mucosa can determine whether the cells remain commensals or disrupt normal homeostasis and trigger disease [6]. Given the distinct composition of mucosa at each body site, the interactions between the microbial community and the mucosa are diverse. Therefore, each mucosal environment needs independent study. Mucins, for example, can be very diverse and characteristic of the body site, which in turn influences the composition of the resident microbiota. Microbial cells may directly adhere to specific mucins or secrete enzymes for their degradation (i.e., glycosidases, glycosufatases, sialidases) and metabolic assimilation (e.g., sugar/amino acid transport and metabolism) [6, 11]. One of the best studied mucus-bacterial interactions is that of Bacteroidetes in the gut mucosa [12]. Utilizing the enzyme glycosidase, *Bacteroidetes,* and enteric microbiota, degrade mucin within the mucosal lining, utilizing oligosaccharide substrates carbon as a nutrient source [13]. Other microorganisms associated with mucolytic properties include *Candida albicans* (gastrointestinal), *Prevotella* sp. (intestinal, *Arkkermansia mucinphlia* (intestinal), *Vibrio cholerae* (intestinal), *Streptococcus pneumoniae* (ocular), and *Moraxalla catarrhalis* (ocular) [11, 13-16]. Therefore, mucins and other proteins of the middle ear mucosa could provide nutritional support for microbial colonizers. Furthermore, although oxygen availability is limited to brief periods of aeration [3] the pulses of air may enrich for bacteria with aerobic or facultatively anaerobic metabolisms. Obligate anaerobes may also thrive under these conditions, particularly if aerotolerant. Mucin fermentation may in fact be favored under these conditions and provide a primary mechanism for growth and reproduction in the middle ear mucosa.

Mucin structure and distribution in mucosa

Mucin is a glycoprotein comprised of a core protein backbone (39.5% in the otic mucins) and branches O-linked glycans, contributing to its overall carbohydrate content (60.5% in the otic mucins) [5]. Branched O-glycans contain repeating subunits of *N*-acetylgalactosamine (7.8%), *N*-acetylglucosamine (19.9%), galactose (16.1%), fucose (9%), and are often decorated with saliac acid (7.7%) at the branch tip (Fig. 2.2) [5, 6, 8]. Mucins are integral component of the mucus gel that covers the mucosal epithelium throughout the body (i.e. gastrointestinal, otic surface, airwaus, oro- and naso-pharyngeal, ocular surface). The glycoproteins can be secreted to the mucus layer or bound to the membrane of the secretory cells, providing a variety of functions in mucosal protection [6]. All of the 20 mucin types identified in human mucosa to date fall into one of three categories; (1) gel-forming, secreted (MUC2, MUC5AC, MUC5B, MUC6, MUC19), (2) non-gel-forming, secreted (MUC7, MUC8, MUC9) and (3) membrane bound (MUC1, MUC3AB, MUC4, MUC12, MUC13, MUC15, MUC16, MUC17, MUC20, MUC21) [6]. Mucosal surfaces control the secretion of mucins in response to environmental factors (i.e. host nutritional impact, gas exchanges, etc.) to modulate the properties of the mucosal surface locally and adapt to specific physiological needs [6].

The middle ear mucins are an integral part of the mucocilliary transport system and play a key role in clearing biological or inert particles introduced with air through the open ET. Though studies have mostly looked at the distribution of otic mucins in response to infections, a few studies have characterized MUC secretion in the tympanic cavity and ET of non-infected adults [7, 17-20]. Whether these individuals can be considered ‘healthy’ is debatable. Given the secluded location of the middle ear space, many studies relied on samples collected surgically though the eardrum and considered as healthy controls patients receiving cochlear implants [17,

18]. These patients can however be regarded as lacking mucosal inflammation, a condition that increases the risk of otological infections. Early studies based on immunohistochemistry and norther blot analysis detected some low levels of membrane bound MUC1 and MUC4 mucins and a higher abundance of secreted, gel-forming mucins (MUC5AC and MUC5B) in the healthy ET [7]. Only MUC5B was detected in the epithelium of the tympanic cavity, consistent with an increased mucocilia [7]. This suggested that the mucus layer thickens as the mucosa transitions from the tympanic cavity to the ET lumen, consistent with the increased density of ciliated cells in the tubal regions [20]. Infected patients (i.e. otitis media) had 4.2-fold increases in MUC5B and also secreted MUC4 in the tympanic cavity [7]. This finding supports the notion that the mucins control the thickness of the mucus layer to protect the mucosal epithelium against infections. Further supporting this, MUC5B readily binds bacterial cells and is the primary protein involved in mucociliary clearance [7]. MUC4's role is less clear but also appears to be protection, possibly modulating epithelial cell proliferation and differentiation or forming gel matrices with MUC5B [7]. More recent studies demonstrated the upregulation of MUC1 and MUC2 during middle ear infections, where MUC2 functions as a gel-forming mucin alongside MUC5B and MUC5AC to thicken the mucus barrier [17]. Additionally, secretion of these MUC proteins, particularly MUC2, is induced in response to inflammatory cytokines [17]. Collectively, these studies indicate that the middle ear epithelium is protected by a mucin hydrogel whose thickness and rheological properties are modulated by the differential secretion of gel-forming mucins. Furthermore, a spatial gradient exists whereby the mucin hydrogel is likely thinner in the tympanic cavity but thickens and more viscous down the ET. This suggests that microbial colonization of the middle ear mucosa may also follow a spatial gradient.

THE DIVERSITY OF MIDDLE EAR MICROBIOMES

The National Institutes of Health (NIH) defines *microbiome* as a collection of all the microorganisms (bacteria, virus, fungi), and their genes, that naturally reside in an environment. Microbiome research has flourished in the past two decades due to the advent of sequencing methods to investigate the structure and function of host-associated microbial communities [21]. These studies have shed light on the composition of the microbial communities without the need to culture them and have identified correlations between community structure and health or disease, which is important to guide treatment strategies [22]. Knowledge gained from these studies have advanced understanding of not only microbial diversity present in a particular environment, but also the complex molecular, gene, and metabolic networks that sustain the microbiomes and how they respond to and/or influence disease. The human microbiome is to date the best studied of all host-associated microbiomes [21]. The human body harbors a complex collection of microorganisms comprised of many "individual microbiomes", each adapted to the unique microenvironment provided by the part of the body they inhabit (e.g., gut, skin, lung, vaginal mucosa, oral surfaces, etc.). Genome-level understanding of the communities that are present at each body site is also important to understand functional metabolic processes that occur within the community [23, 24]. Such studies often rely on shotgun sequencing approaches to recover metagenomes, but they have mostly focused on microbiomes (i.e. gut, oral or nasopharyngeal mucosa) with the species richness, abundance and accessibility that is needed to collect large sample volumes for high DNA yields and sequencing coverage [25-28]. Body sites harboring lowly abundant microbiomes or limiting sample size (e.g., lungs) make microbiome studies more challenging [29-32].

CULTURE-DEPENDENT VS CULTURE INDEPENDENT APPROACH MICROBIOME RESEARCH

Cultivation-independent (sequencing) approaches can provide high resolution of microbial patterns and diversity, helping identify and study rare taxa or unculturable microorganisms withing a community [33]. This information is also important for building databases that catalog the known microbial diversity and help advance future studies. Though community profiling and metabolic analysis can be readily inferred from sequencing data, intra- and inter-population interactions are more difficult to predict and often require culture-based studies with representative strains [34]. Models derived from cultivation-dependent studies can be used to confirm or gain better understanding in microbe-microbe or microbe-host relationships that help structure the microbiome and provide useful information about the local environment where these microbes live [35-37]. However, only a small fraction of all microorganisms can be grown under laboratory conditions, and cultivation may bias the enrichment of fast-growing, heterotrophic bacteria that may not necessarily be the most abundant and/or functionally important members of the microbiome [38]. Thus, culture-dependent approaches only recover a subset, a very small one, of the native microbial community. The advantages and limitations of each approach highlight the importance of combining cultivation-independent and dependent techniques to gain a more complete understanding of the diversity and functions that host-associated communities play in health and disease.

Sequencing of a diverse and robust microbiome in otic secretions collected from healthy, young adults

Using an institutionally approved protocol, we collected otic, oropharyngeal and buccal samples from 19 individuals (20 years old on average; Table 2.1) for amplicon sequencing of the 16S rRNA variable 4 region (V4). All of the participants reported no recent history of respiratory

infections and/or antibiotic treatment and passed an onsite physical exam that ruled out nasal congestion/dripping as well as inflammation and abnormalities of the nose, mouth, and ears. We also asked the participants to report recreational activities that could affect middle ear aeration and homeostasis such as swimming and diving. The survey identified 9 certified scuba divers who reported similar training in middle ear equalization techniques and diving experience at depths of >60 ft (Table 2.2). Subjects who met the eligibility criteria and passed the onsite physical exam were asked to rinse their mouths with sterile saline to remove food debris and performed a series of equalization exercises (deep inhaling, yawning and swallowing) to maximize otic drainage. The team's physician used a tongue depressor to improve spatial access and introduced a sterile flocked swab behind the left and right palatopharyngeal arch to collect the otic secretions in the mucosal channel (torus tubarius) around the ET orifice (Fig. 2.1). The physician then used separate swabs to collect samples from the center of the oropharynx and buccal mucosae (inner lining of the cheeks, upper gums and palate). Illumina sequencing of 16S-V4 amplicons from all the samples yielded a total of 12,219,721 reads, with an average number of 214,381 (±8,132) reads for each region sampled per participant. To normalize differences in read number and therefore diversity among the samples, we rarified the sequences to a depth of 2,313 reads per sample prior to assigning operational taxonomic units (OTUs). We identified in the otic samples an average of 95 (±26) genus-level OTUs compared to 100 (±28) and 113 (±20) in the center of the oropharynx and the buccal samples, respectively. Thus, genus-level diversity in the otic samples was within the levels obtained for the richly colonized mucosae of the oral cavity [27].

Alpha diversity analyses based on observed species, Shannon diversity and Simpson evenness provided evidence for the presence of a diverse and robust otic community (Fig. 2.2a).

The number of observed otic species was within the ranges measured for the oropharyngeal and buccal microbiomes but Shannon and Simpson diversity tended to be higher in the otic than oral communities. The most notable differences were for Simpson's evenness, which showed the greatest distribution of taxa in the otic communities compared to the oropharynx ($p < 0.01$) and buccal ($p < 0.001$) samples. Estimation plots of the standardized mean differences (Δ) among alpha diversity indices per site confirmed these differences (Fig. 2.2a). Notably, the distributions of Simpson's evenness consistently followed the trend otic>oropharyngeal>buccal. Thus, the otic communities were more even than the oral (oropharyngeal and buccal) populations, a trait associated with microbiomes with the robustness and adaptability needed to function in a fluctuating environment [28]. Beta diversity analyses, on the other hand, highlighted similarities in the phylogenetic distribution of the otic and neighboring communities that agree well with a model of otic mucosal colonization by oral migrants (Fig. 2.2b). Principal Coordinates Analysis (PCoA) transformation plots of weighted UniFrac distances showed, for example, site-specific clustering of otic and buccal samples but some overlap in PCoA space along the variance obtained for the first axis. In contrast, the oropharyngeal sequences spread across the two axes to overlap with both the otic and buccal clusters. This is expected from the central role that the oropharynx is predicted to have in microbial immigration from the oral cavity to the middle ear. The periodic seeding of the oropharynx with saliva facilitates the aerial dispersal of aerosols with oral migrants, seeding the lower aerodigestive tract during inhalation and the middle ear cavity during exhalation. This shows as a substantial spatial overlap between the oropharyngeal and the otic and buccal communities in the PCoA ordination graphs (Fig. 2.2b).

MICROBIOME CHARACTERIZATION WITH NEXTGEN SEQUENCING

There are multiple approaches to characterizing known and novel microbiomes, each with their own advantages and limitations. All methods share a commonality: they align genomic fragments or sequences to a reference database for taxonomic identification and/or functional annotation. The most common approaches for taxonomic identification are 16S rRNA amplicon sequencing analyses or shotgun sequencing of all the microbial DNA in a sample (metagenomics) [39]. Amplicon sequencing has been primarily used for taxonomic and phylogenetic identification of bacterial communities and most often targets the conserved 16S rRNA gene due to its small size (~1542 bp) and functional conservation across bacterial phyla [24, 39]. By amplifying the target genes via PCR, amplicon sequencing facilitates the analyses of low-biomass samples, even from samples with substantial host DNA contamination. It also lowers the cost of the sequencing project. The high conservations of regions along the 16S rRNA gene permits the use of multiple primer sets for the amplification of one or more of the nine hypervariable regions (V1-9), as needed for the particular study. For example, highly diverse communities can be readily profiled by targeting the V4 or V3-V4 regions [40, 41]. Some studies report the suitability of the V2 and V3 regions for taxonomic identification of *Streptococcus* spp., while the V1 is more sensitive for identification of *Staphylococcus aureus* [42]. However, the variable region sequences typically limit taxonomic identification to at most genus levels [24, 43, 44]. For some bacterial genera (e.g., *Streptococcus*) not even the full-length 16S rRNA gene sequence is enough to differentiate between species [45-47]. Thus, there is interest in identifying other conserved genes that can be used as taxonomic markers for taxonomic identification of some bacterial groups, such as *rpoB* in *Corynebacterium*, *Streptococcus* and *Enterococcus* [45, 46]. Finally, though this approach is commonly used among microbiome studies and there are

programs to predict potential functional analysis, these analysis aren't thorough and thus this method is usually regarded as limited to its phylogenetic assessment [24]. Therefore amplicon analysis is commonly utilized solely for taxonomic identification (often genus-level) and remains a useful method for initial microbiome studies [24].

One of the key advantages of the metagenomics approach is that it can assembles short reads from the same genome into one or more contigs to capture the genomic diversity of the sample without the need to amplify and sequence specific genes or gene regions [22]. The method can be applied for *de novo* microbiome studies (assembly without reference strain) or combined with sequencing projects of reference strains to improve contig assembly and recover complete genomes from the metagenomic data [22]. Additionally, the metagenomics approach can provide a wider depth of bacterial detection by increasing the accuracy of species or strain level identification [24]. Metagenomics provides a more in-depth taxonomic analysis of the community and predicts metabolic function and niche adaptations with higher accuracy [24]. However, this approach is limited by the high DNA concentrations required per sample, high sequencing costs, large computing resources to compensate large data output, and the need to use analyses programs in the linux computing platform [24].

Amplicon or metagenomic approaches also face limitations in the analysis pipelines. These pipelines are a series of scripts or programs organized in a particular order to process, assemble, and analyze sequence data [23, 24]. While amplicon sequencing has relatively small data output and quicker, easier analysis options, metagenomics approaches have high data outputs and less intuitive analysis processes [24]. With the rise of sequencing techniques and bioinformatic capabilities, more resources are now available for computational analyses of sequencing data, such as open source tools built from scratch by researchers and commercial

platforms custom-tailored to all experience levels [24]. As more tool choices become available, there is little standardization (i.e. programs) of analysis pipelines, and the differences in program used, program settings, and poor pipeline reporting can lead to inconsistent and unreproducible results [22]. Therefore, it is important to take these limitations into consideration when building assembly and analysis programs for microbiome research.

MIDDLE EAR MICROBIOTA

Eustachian tube dynamics and microbial entry in the tympanic cavity

The secluded location of the middle ear makes for a compelling argument in support of sterility. Yet, this entrenched dogma is incongruent with the periodic ventilation of the space when the ET opens and the fact that bacteria do enter the cavity and cause infections. The ET anatomy and physiology plays an important role in the health of the middle ear and preventing infections [3]. The ET is sometimes defined as "part of a system of contiguous organs, including the nose, pharynx, palate, middle ear and mastoid gas cells", that is, it is an extension of the tympanic cavity into the back of the nasopharynx [3].

The anatomy of the adult ET is adapted to minimize bacterial colonization. Positioned at an angle (45˚) to facilitate downward fluid and mucus draining, it is long enough (avg. 38 mm) and shaped as an inverted S to provide a mechanical barrier to nasal and perioral microbes [3]. The tube is also wider as it opens into the nasopharynx and the orifice is surrounded by an elevated cartilage (like an inverted horseshoe – the torus tubarius) to prevent the aspiration of nasal discharges and drain otic fluids in the back of the throat [3]. A "flask model" is typically used to illustrate how the tube's shape regulates the flow of fluids (gas or liquid) (Fig. 1.3). In this model, the ET is imagined as a flask with long narrow neck, where the flow of fluid is dependent on the pressure differential at either end of the tube (positive or negative), controlling

direction of flow, and viscously of fluids. With increased length of the "neck" (tube), it becomes more difficult for fluid to move through. As gas (air) has a lower viscosity than liquid, allowing it to flow easier[3]. Impairment in the length and angle of the tube have been related to inhibition of the tube's protective functions of the tympanic cavity, making it more susceptible to diseases.

The lumen and mucous membrane of the ET also play important roles in the tube's protective function. As part of the respiratory system, the ET is lined with a respiratory mucosa [3]. The lumen, which connects the tympanic membrane to the nasopharynx, is covered by a dense ciliated epithelium whose function is to "sweep" mucus-bound material away from the tympanic cavity (mucociliary clearance) [3]. Interspersed with the ciliated cells are the goblet that secrete mucins to the mucosa and mucous glands that secrete mucopolysaccharides, lysozymes, secretory immunoglobulins and surface-active molecules [3, 48]. Otic surfactants are complex mixes of peptides, lipids and phospholipids that play key functional roles in human cell health, bacterial colonization, motility and biofilm production [48]. These surfactants control the surface tension of the mucosa, the innate immune system and some also have antimicrobial activity (SP-A and SP-D peptides) [48-50]. Out of the four surfactant peptides secreted in the human mucosa (SP-A through SP-D), SP-A is the most abundant in the ET [48]. SP-A has also been shown to induce phagocytosis of common otopathogens such as *Streptococcus pneumonia* and *Haemophilus influenzae.* Although SP-A reduces the surface tension of the mucus layer, SP-B, also secreted by the ET mucosa, is the major contributor to this function in the ET [48]. [48]. By reducing the surface tension of the mucus layer, these surfactants prevent the walls of the collapsed ET from sticking to each and facilitate the expansion of the mucosa when the tube opens [3].

The unique anatomy and dynamics of the ET perpetuated, clearly adapted as a barrier to microbial infiltration, helped perpetuate the idea that the middle ear mucosa is sterile in health. Previous studies have explored the presence of an otic microbiome using samples collected using invasive procedures (surgery through or around the eardrum) [51-54]. Findings were often contradictory, with some studies detecting bacteria in biopsy specimens collected from the mucosa of the tympanic cavity in healthy individuals [54] and others detecting them only in patients that had recovered from otitis media [54, 55]. Two studies that sequenced 16S rRNA-V3-V4 amplicon region from the tympanic cavity mucosal swabs identified a bacterial community dominated by Proteobacteria and Actinobacteria, regardless of history of middle ear infections [51, 52]. These sequencing studies introduced swabs through the ear canal, which could contaminate the samples. Furthermore, the study did not include controls from the outer ear canal, where Proteobacteria and Actinobacteria sequences are prevalent. Lastly, all previous studies of the otic microbiome sampled individuals undergoing surgery for otological conditions (e.g., cochlear implant) that can affect the middle ear mucosa and the functioning of the ET. Therefore, whether the middle ear harbors an otic microbiome in health remained debatable.

Middle ear pathogens

Middle ear infections, or otitis media, occur at all ages of life but are more common in children due to the shorter length (~18 mm, roughly half the length of the adult tube) and lack of incline of the immature ET [3]. These anatomical differences impair the proper protective functions (reflux, aspiration, or expulsion of nasopharyngeal secretions) of the ET and increase the risk of infections [3]. While acute otitis media is transient, frequent episodes can develop into chronic otitis media, sometimes with effusion, that impair ET functioning and can lead to hearing loss [3]. Frequently, a dysfunctional ET often leads to primary or secondary infections and

pressure imbalances (most commonly under pressurization) in the tympanic cavity [3]. ET dysfunction can be the result of a pathophysiology (e.g., allergy induced inflammation) or a functional obstruction either because of an anatomical predisposition (floppy cartilage, dysfunction of tensor veli palatini muscle, etc) or external force (barotrauma) [3]. Host factors (e.g., genetic predisposition, age, gender, race, allergy, immunocompetence and craniofacial abnormalities) as well as environmental factors (e.g., upper respiratory illnesses, season of the year, exposure to smoking, socioeconomic status, etc.) also contribute to the etiology and pathogenesis of middle ear disease [3, 56]. In all cases, however, one of the most common route of infection is 1) the reflux of nasal secretions carrying otopathogens [3].

Middle ear infections can be bacterial or viral in nature, and are often triggered by nasal congestion or other conditions that lead to ET inflammation and disruption of the normal cycles of tubal aperture [3]. With a dysfunctional ET, mucus clearance from the tympanic cavity is reduced, fluids and mucus accumulate, and otopathogens grow. Due to the frequency of otitis media in young children, most studies have focused on the identification and treatment of otopathogens implicated in pediatric infections [3]. Bacterial otitis media is primarily caused by a single infection of *Streptococcus pneumonia*, or coinfection of *S. pneumoniae* with *Moraxella catarrhalis* or non-typeable *Haemophiles influenzae* [57-60]. *Staphylococcus aureus, Staphylococcus epidermidis,* Group A *Streptococcus, Enterobacter agglomerens, Streptococcus viridans,* and *Neisseria* spp. have also been isolated from mucosa of patients with acute otitis media patients [59-62].

Interestingly, the observation that children with recurrent acute otitis media (rAOM) showed significantly lower levels of nasopharyngeal α-hemolytic streptococci. The correlation between the low abundance of the staphylococci and rAOM was further investigated to identify

potential of inhibition of otopathogens [63, 64]. Two studies analyzed the effects of recolonization, in an effort to determine if returning bacterial homeostasis could aid in rAOM treatment, using a saline nasal spray containing alpha-hemolytic streptococci (AHM) in 2001 and 2002. It was initially shown that the use of AHM nasal spray reduced recurrence of rAOM by 50% [65], however these results were contradicted in a smaller study comparing ASM treatment to a placebo group [63]. Though these studies highlighted the importance of bacterial homeostasis in maintaining a healthy middle ear mucosa, more studies are needed to identify the potential use of bacterial replacement therapies to help combat antibiotic resistance that can lead to chronic or recurrent otitis media.

APPENDIX

Figure 1.1: Eustachian tube dynamics. Cartoon representation of the ear anatomy showing the tympanic cavity (A; blue circles) and the closed (A) and open (B) Eustachian tube (ET). At rest, the collapsed ET prevents air flow and negative pressure builds inside the tympanic cavity. Swallowing contracts, the muscles around the ET and opens the ET to allow air to flow, depressurizing the tympanic cavity and draining excess fluids. Yawning creates positive pressure of air at the ET orifice and opens the ET. Image adapted from Microsoft Word's Creative Commons Pictures.

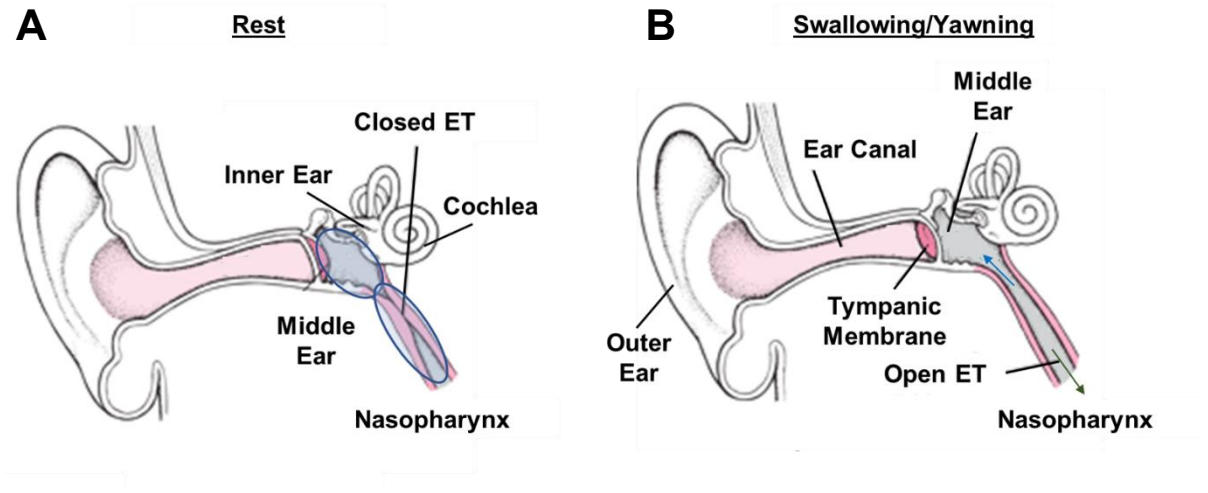

Figure 1.2: **Structure and predicted cleavage sites of membrane bound and secreted mucin glycoproteins**. Cartoon representation of the structure and composition of membrane bound or secreted mucins. Predicted cleavage sites by either *Bacteroidetes* (blue dashed line) or *Streptococcus* (grey dashed line) by either mucolytic (glycosidase; orange pac-man) or proteolytic (yellow pac-man) activity. Image adapted from [8].

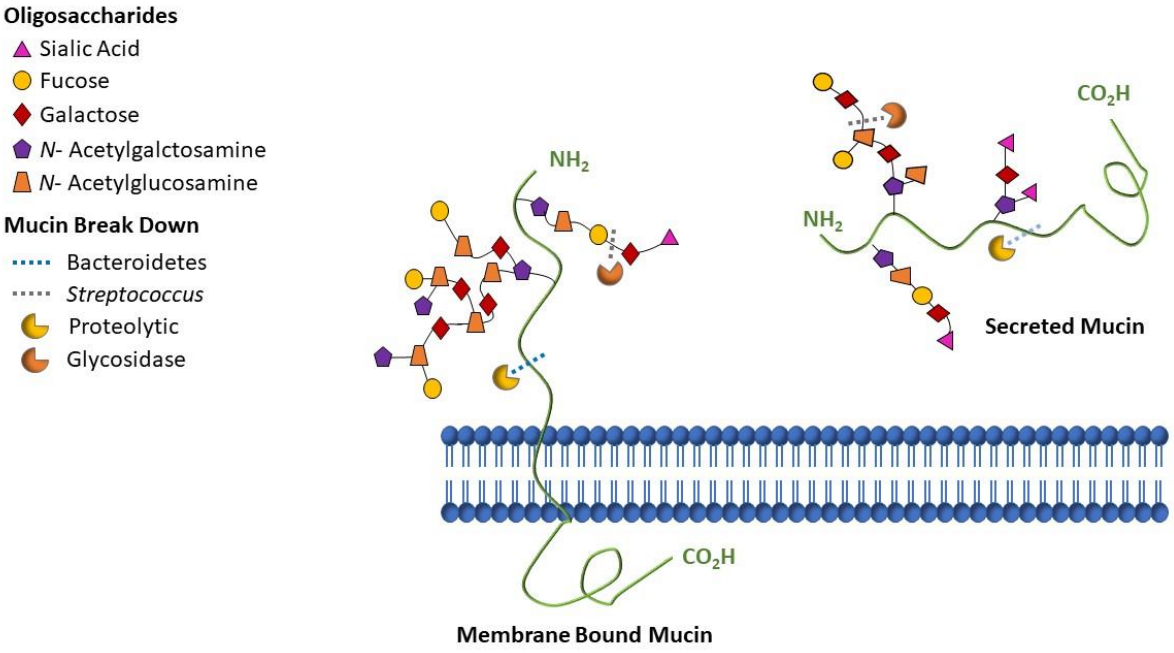

Figure 1.3: Illustration of the Flask Model. Image adapted from [3]. The mouth of the flask represents the nasopharyngeal opening of the Eustachian tube, the neck represents the lumen of the tube and the balbous portion represents the tympanic cavity. Factors influencing the flow of fluid include pressure at either side of the neck, length and radius of the neck, and viscosity of the fluid flowing through it. The rigidity (compliance) of the neck also influences the flow of fluid. The type of pressure (negative or positive) influences the direction of fluid flow.

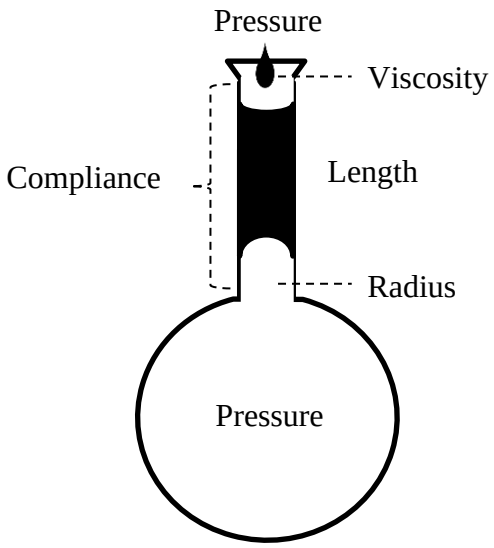

REFERENCES

REFERENCES

1. Christensen-Dalsgaard, J. and C.E. Carr, Evolution of a sensory novelty: tympanic ears and the associated neural processing. Brain Res Bull, 2008. 75(2-4): p. 365-70.

2. Masterton, B., H. Heffner, and R. Ravizza, The evolution of human hearing. J Acoust Soc Am, 1969. 45(4): p. 966-85.

3. Bluestone, C.D., Eustachian tube: structure, function, role in otitis media, ed. M.B. Bluestone. 2005, Hamilton; Lewiston, NY: BC Decker. 219.

4. Sadé, J., Mucociliary Flow in the Middle Ear. Annals of Otology, Rhinology & Laryngology, 1971. 80(3): p. 336-341.

5. Reddy, M.S., et al., Middle ear mucin glycoprotein: purification and interaction with nontypable *Haemophilus influenzae* and Moraxella catarrhalis. Otolaryngol Head Neck Surg, 1997. 116(2): p. 175-80.

6. Corfield, A.P., Mucins: A biologically relevant glycan barrier in mucosal protection. Biochimica et Biophysica Acta (BBA) - General Subjects, 2015. 1850(1): p. 236-252.

7. Lin, J., et al., Characterization of mucins in human middle ear and Eustachian tube. Am J Physiol Lung Cell Mol Physiol, 2001. 280(6): p. L1157-67.

8. Carlson, T.L., J.Y. Lock, and R.L. Carrier, Engineering the Mucus Barrier. Annu Rev Biomed Eng, 2018. 20: p. 197-220.

9. van Muijlwijk, G.H., et al., Identification of Allobaculum mucolyticum as a novel human intestinal mucin degrader. Gut Microbes, 2021. 13(1): p. 1966278.

10. Png, C.W., et al., Mucolytic bacteria with increased prevalence in IBD mucosa augment in vitro utilization of mucin by other bacteria. Am J Gastroenterol, 2010. 105(11): p. 2420-8.

11. Roberton, A.M., et al., A novel bacterial mucinase, glycosulfatase, is associated with bacterial vaginosis. J Clin Microbiol, 2005. 43(11): p. 5504-8.

12. Thomas, F., et al., Environmental and gut bacteroidetes: the food connection. Front Microbiol, 2011. 2: p. 93.

13. Selwal, K.K., M.K. Selwal, and Z. Yu, Mucolytic bacteria: prevalence in various pathological diseases. World Journal of Microbiology and Biotechnology, 2021. 37(10): p. 176.

14. Paone, P. and P.D. Cani, Mucus barrier, mucins and gut microbiota: the expected slimy partners? Gut, 2020. 69(12): p. 2232-2243.

15. Colina, A.R., et al., Evidence for degradation of gastrointestinal mucin by Candida albicans secretory aspartyl proteinase. Infect Immun, 1996. 64(11): p. 4514-9.

16. van Passel, M.W., et al., The genome of Akkermansia muciniphila, a dedicated intestinal mucin degrader, and its use in exploring intestinal metagenomes. PLoS One, 2011. 6(3): p. e16876.

17. Ubell, M.L., et al., MUC2 expression in human middle ear epithelium of patients with otitis media. Arch Otolaryngol Head Neck Surg, 2008. 134(1): p. 39-44.

18. Kerschner, J.E., et al., MUC5AC expression in human middle ear epithelium of patients with otitis media. Arch Otolaryngol Head Neck Surg, 2010. 136(8): p. 819-24.

19. Preciado, D., et al., MUC5B Is the Predominant Mucin Glycoprotein in Chronic Otitis Media Fluid. Pediatric Research, 2010. 68(3): p. 231-236.

20. Lim, D.J., et al., Cell biology of tubotympanum in relation to pathogenesis of otitis media - a review. Vaccine, 2000. 19 Suppl 1: p. S17-25.

21. Methé, B.A., et al., A framework for human microbiome research. Nature, 2012. 486(7402): p. 215-221.

22. Galloway-Peña, J. and B. Hanson, Tools for Analysis of the Microbiome. Digestive Diseases and Sciences, 2020. 65(3): p. 674-685.

23. Thomas, T., J. Gilbert, and F. Meyer, Metagenomics - a guide from sampling to data analysis. Microb Inform Exp, 2012. 2(1): p. 3.

24. Liu, Y.-X., et al., A practical guide to amplicon and metagenomic analysis of microbiome data. Protein & Cell, 2021. 12(5): p. 315-330.

25. Moss, E.L., D.G. Maghini, and A.S. Bhatt, Complete, closed bacterial genomes from microbiomes using nanopore sequencing. Nature Biotechnology, 2020. 38(6): p. 701-707.

26. Bachmann, N.L., et al., Advances in Clinical Sample Preparation for Identification and Characterization of Bacterial Pathogens Using Metagenomics. Front Public Health, 2018. 6: p. 363.

27. Payne, A., et al., Nanopore adaptive sequencing for mixed samples, whole exome capture and targeted panels. bioRxiv, 2020: p. 2020.02.03.926956.

28. Ranjan, R., et al., Analysis of the microbiome: Advantages of whole genome shotgun versus 16S amplicon sequencing. Biochem Biophys Res Commun, 2016. 469(4): p. 967-77.

29. Luhung, I., et al., Experimental parameters defining ultra-low biomass bioaerosol analysis. npj Biofilms and Microbiomes, 2021. 7(1): p. 37.

30. Karstens, L., et al., Controlling for Contaminants in Low-Biomass 16S rRNA Gene Sequencing Experiments. mSystems, 2019. 4(4): p. e00290-19.

31. Caruso, V., et al., Performance of Microbiome Sequence Inference Methods in Environments with Varying Biomass. mSystems, 2019. 4(1): p. e00163-18.

32. Selway, C.A., R. Eisenhofer, and L.S. Weyrich, Microbiome applications for pathology: challenges of low microbial biomass samples during diagnostic testing. J Pathol Clin Res, 2020. 6(2): p. 97-106.

33. Sharma, N., et al., Oral microbiome and health. AIMS Microbiol, 2018. 4(1): p. 42-66.

34. Sommer, M.O.A., Advancing gut microbiome research using cultivation. Current Opinion in Microbiology, 2015. 27: p. 127-132.

35. Wolfe, B.E., Using Cultivated Microbial Communities To Dissect Microbiome Assembly: Challenges, Limitations, and the Path Ahead. mSystems, 2018. 3(2): p. e00161-17.

36. Deo, P.N. and R. Deshmukh, Oral microbiome: Unveiling the fundamentals. J Oral Maxillofac Pathol, 2019. 23(1): p. 122-128.

37. Costa, O.Y.A., et al., Cultivation-independent and cultivation-dependent metagenomes reveal genetic and enzymatic potential of microbial community involved in the degradation of a complex microbial polymer. Microbiome, 2020. 8(1): p. 76.

38. Dickson, R.P., et al., Analysis of Culture-Dependent versus Culture-Independent Techniques for Identification of Bacteria in Clinically Obtained Bronchoalveolar Lavage Fluid. Journal of Clinical Microbiology, 2014. 52(10): p. 3605-3613.

39. Bharti, R. and D.G. Grimm, Current challenges and best-practice protocols for microbiome analysis. Brief Bioinform, 2021. 22(1): p. 178-193.

40. Fadeev, E., et al., Comparison of Two 16S rRNA Primers (V3–V4 and V4–V5) for Studies of Arctic Microbial Communities. Frontiers in Microbiology, 2021. 12.

41. Graspeuntner, S., et al., Selection of validated hypervariable regions is crucial in 16S-based microbiota studies of the female genital tract. Scientific Reports, 2018. 8(1): p. 9678.

42. Chakravorty, S., et al., A detailed analysis of 16S ribosomal RNA gene segments for the diagnosis of pathogenic bacteria. J Microbiol Methods, 2007. 69(2): p. 330-9.

43. Edgar, R.C., Updating the 97% identity threshold for 16S ribosomal RNA OTUs. Bioinformatics, 2018. 34(14): p. 2371-2375.

44. Stackebrandt, E. Taxonomic parameters revisited: tarnished gold standards. 2006.

45. Khamis, A., D. Raoult, and B. La Scola, Comparison between rpoB and 16S rRNA gene sequencing for molecular identification of 168 clinical isolates of *Corynebacterium*. J Clin Microbiol, 2005. 43(4): p. 1934-6.

46. Church, D.L., et al., Performance and Application of 16S rRNA Gene Cycle Sequencing for Routine Identification of Bacteria in the Clinical Microbiology Laboratory. Clin Microbiol Rev, 2020. 33(4).

47. Carlos, N., Y.-W. Tang, and Z. Pei, Pearls and pitfalls of genomics-based microbiome analysis. Emerging Microbes & Infections, 2012. 1(1): p. 1-3.

48. McGuire, J.F., Surfactant in the middle ear and eustachian tube: a review. Int. J. Pediatr. Otorhinolaryngol., 2002. 66(1): p. 1-15.

49. Li, L., et al., Expression of Surfactant Protein-A during LPS-Induced Otitis Media with Effusion in Mice. Otolaryngol Head Neck Surg, 2015. 153(3): p. 433-9.

50. Schicht, M., et al., Detection of surfactant proteins A, B, C, and D in human nasal mucosa and their regulation in chronic rhinosinusitis with polyps. Am J Rhinol Allergy, 2013. 27(1): p. 24-9.

51. Liu, C.M., et al., The otologic microbiome: a study of the bacterial microbiota in a pediatric patient with chronic serous otitis media using 16SrRNA gene-based pyrosequencing. Arch Otolaryngol Head Neck Surg, 2011. 137(7): p. 664-8.

52. Minami, S.B., et al., Microbiomes of the normal middle ear and ears with chronic otitis media. Laryngoscope, 2017. 127(10): p. E371-E377.

53. Chan, C.L., et al., Identification of the Bacterial Reservoirs for the Middle Ear Using Phylogenic Analysis. JAMA Otolaryngol Head Neck Surg, 2017. 143(2): p. 155-161.

54. Tonnaer, E.L., et al., Detection of bacteria in healthy middle ears during cochlear implantation. Arch. Otolaryngol. Head Neck Surg., 2009. 135(3): p. 232-7.

55. Westerberg, B.D., et al., Is the healthy middle ear a normally sterile site? Otol Neurotol, 2009. 30(2): p. 174-7.

56. Lazaridis, E. and J.C. Saunders, Can you hear me now? A genetic model of otitis media with effusion. J. Clin. Invest., 2008. 118(2): p. 471-474.

57. Ngo, C.C., et al., Predominant Bacteria Detected from the Middle Ear Fluid of Children Experiencing Otitis Media: A Systematic Review. PLoS One, 2016. 11(3): p. e0150949.

58. Laufer, A.S., et al., Microbial Communities of the Upper Respiratory Tract and Otitis Media in Children. Mbio, 2011. 2(1).

59. Celin, S.E., et al., Bacteriology of Acute Otitis Media in Adults. JAMA, 1991. 266(16): p. 2249-2252.

60. Niedzielski, A., L.P. Chmielik, and T. Stankiewicz, The Formation of Biofilm and Bacteriology in Otitis Media with Effusion in Children: A Prospective Cross-Sectional Study. International Journal of Environmental Research and Public Health, 2021. 18(7): p. 3555.

61. Ding, Y.L., et al., Molecular characterization and antimicrobial susceptibility of *Staphylococcus aureus* isolated from children with acute otitis media in Liuzhou, China. BMC Pediatrics, 2018. 18(1): p. 388.

62. Kurono, Y., K. Tomonaga, and G. Mogi, *Staphylococcus epidermidis* and *Staphylococcus aureus* in Otitis Media With Effusion. Archives of Otolaryngology–Head & Neck Surgery, 1988. 114(11): p. 1262-1265.

63. Tano, K., et al., A nasal spray with alpha-haemolytic streptococci as long term prophylaxis against recurrent otitis media. Recent Advances in Otitis Media, Proceedings, 2001: p. 397-402.

64. Grahn, E., et al., Interference of α-hemolytic streptococci isolated from tonsillar surface on β-hemolytic streptococci (*Streptococcus* pyogenes) — A methodological study. Zentralblatt für Bakteriologie, Mikrobiologie und Hygiene. 1. Abt. Originale. A, Medizinische Mikrobiologie, Infektionskrankheiten und Parasitologie, 1983. 254(4): p. 459-468.

65. Roos, K., E.G. Hakansson, and S. Holm, Effect of recolonisation with "interfering" alpha streptococci on recurrences of acute and secretory otitis media in children: randomised placebo controlled trial. BMJ, 2001. 322(7280): p. 210-2.

CHAPTER 2

ORAL SEEDING AND NICHE-ADAPTATION OF THE MIDDLE EAR BIOFILMS IN HEALTH

PUBLICATION NOTICE

The following dissertation chapter describes cultivation-independent and culture-based approaches to investigate the microbiology of the middle ear. The author i) assisted with sample collection, ii) isolated the otic, oropharyngeal, and buccal strains, iii) performed the hemolysis assays, iv) curated 16S rRNA amplicon sequences for each cultivar, v) and did the phylogenetic analyses. The 16S rRNA-V4 amplicon sequencing study was conducted by Dr. Joo-Young Lee (past member of Dr. Gemma Reguera's laboratory, Michigan State University). Additionally, Dr. Lee isolated genomic DNA and amplified the 16S rRNA genes from the cultivars with assistance from undergraduate student Hugh McCullough.

The following chapter was published in "*Lee, JY., Jacob, K., Kashefi, K., and Reguera, G. 2021. Oral seeding and niche-adaptation of the middle ear biofilms in health. Biofilm. 3:100041* https://doi.org/10.1016/j.bioflm.2020.100041" and reprint permission was granted for use in this dissertation.

ABSTRACT

The entrenched dogma of a sterile middle ear mucosa in health is incongruent with its periodic aeration and seeding with saliva aerosols. To test this, we sequenced 16S rRNA-V4 amplicons from otic secretions collected at the nasopharyngeal orifice of the tympanic tube and, as controls, oropharyngeal and buccal samples. The otic samples harbored a rich diversity of oral keystone genera and similar functional traits but were enriched in anaerobic genera in the Bacteroidetes (*Prevotella* and *Alloprevotella*), Fusobacteria (*Fusobacterium* and *Leptotrichia*) and Firmicutes (*Veillonella*) phyla. Facultative anaerobes in the *Streptococcus* genus were also abundant in the otic and oral samples but corresponded to distinct, and sometimes novel, cultivars, consistent with the ecological diversification of the oral migrants once in the middle ear microenvironment. Neutral community models also predicted a large contribution of oral dispersal to the otic communities and the positive selection of taxa better adapted to growth and reproduction under limited aeration. These results challenge the traditional view of a sterile middle ear in health and highlight hitherto unknown roles for oral dispersal and episodic ventilation in seeding and diversifying otic biofilms.

INTRODUCTION

The notion that the healthy middle ear is sterile, like the entrenched dogma of lung sterility before [1], has been spread in the literature without strong scientific justification [2]. This tenet is also incongruent with the anatomy of the middle ear (Fig. 2.1a), which has adaptively evolved as an acoustic chamber (the tympanic cavity) while maintaining air exchange with the lower respiratory airways through its extended tube, the tympanic or Eustachian tube (ET). The tympanic cavity houses a delicate chain of small bones (ossicles) to transmit sound-induced vibrations from the eardrum to the hearing organ (cochlea) in the inner ear [3]. A porous bone structure (mastoid antrum) with gas-filled, interconnected spaces communicates the cavity to the mastoid gas cell system to increase resonance and to provide a medium for acoustic insulation and sound dissipation [4]. Yet, the ET extension of the tympanic cavity connects the middle ear to the nasopharynx and, by extent, to the noisy background of the aerodigestive system. To prevent noise interference, the ET is passively closed at rest and times its opening to the cycles of swallowing to periodically aerate the otic tissues and relieve negative pressure building up in the tympanic cavity [5]. Yawning or inhaling deeply can also exert positive pressure at the tube's nasopharyngeal orifice, increasing the differential pressure with the tympanic cavity and forcing the opening of the tube (tubal patency) [5]. ET patency is also facilitated by the lubrication of the tubal walls with surfactants that reduce the surface tension of the mucoid layer [5]. Collectively, these physical and chemical mechanisms ensure that the tube dilates briefly (~400 milliseconds) to minimize acoustic interference yet frequently (approximately every minute when we swallow) to provide adequate ventilation and pressure relief [5,3,6]. As a result, the middle ear mucosa (both the tympanic cavity and ET) is periodically seeded by microorganisms of the aerodigestive system.

To minimize microbial colonization, ET patency is timed to clear otic mucus and fluids that accumulate in the tympanic cavity as negative pressure builds. Mucociliary clearance facilitates the downward drainage of the secretions through the tube and, with them, foreign particles introduced with air [2]. Drainage is also facilitated by the pumping force exerted by the episodic contraction and extension of muscles around the tube [7]. As in other mucosal tissues, the otic epithelium secretes to the mucosa glycoproteins (mucins) and proteins with antimicrobial activity or that bind viral or bacterial surface motifs to promote their recognition by macrophages and neutrophils [8-11,2]. The ET is narrower closer to the tympanic cavity, preventing the reflux of the mucus [5]. It also grows longer [12], curves slightly [5] and increases its tilt [13] into adulthood to facilitate drainage. Furthermore, the ET orifice emerges into the nasopharynx as an elevated cartilage covered by mucosa (torus tubarius) that prevents mixing with nasal secretions (Fig. 2.2.1b). Additionally, this mucosal elevation is shaped like an inverted horseshoe that vertically drains the otic secretions behind the palatopharyngeal arch and prevents their re-aspiration (Fig. 2.2.1c).

The specialized anatomy of the middle ear and mechanisms for mucociliary and muscular clearance have been assumed to maintain the otic mucosa free of microbes in health [2]. Several studies [14-17] have attempted to confirm this, albeit with inconclusive results. All of these earlier studies collected samples from individuals undergoing transcanal surgical procedures designed to treat a number of otic conditions. These interventions reached the middle ear cavity through or around the eardrum [18], limiting sampling to small mucosal areas of the cochlear promontory that can be reached without perturbing the ossicular chain (Fig. 2.2.1a). Two independent pediatric studies that surgically collected biopsy mucosal specimens from this region confirmed the presence of bacterial microcolonies in patients with a history of otitis media

[14,15]. One of the studies also detected microbial cells in samples from healthy individuals [15]. Non-invasive optical techniques also detected signals from bacterial biofilms in the middle ear of patients with a history of chronic ear infections but not in uninfected controls [19]. To improve the sensitivity of detection, Minami et al. [16] used transcanal surgery to collect middle ear mucosal swabs from pediatric and adult patients with or without a history of chronic ear infections. The detection in all the samples of a phylogenetically diverse pool of 16S rRNA amplicon sequences supported the conclusion that "the human middle ear is inhabited by more diverse microbial communities than was previously thought" [16]. However, the study did not include controls from the outer ear canal, which a more recent study showed to contaminate the swabs during sampling [17]. Contamination could explain why the otic samples were enriched (85%) in Proteobacteria and Actinobacteria [16], which are also the most abundant phyla in the outer ear canal [20,21]. Importantly, all of these earlier studies [14-17] considered as healthy controls, individuals undergoing surgery to treat otic conditions (e.g., otosclerosis, middle ear malformation, Bell's palsy and deafness) that are associated with local inflammation and viral and bacterial infections [22-25]. Hence, the assumption that these individuals are healthy is questionable.

The uncertainty surrounding these earlier studies prompted us to design alternative approaches to investigate the microbiology of the middle ear. We reasoned that the growth of microcolonies in the middle ear mucosa in health would enrich for otic bacteria in secretions drained during the cycles of ET patency. To test this, we designed a pilot study and received institutional approval to non-invasively (through the mouth) collect otic secretions from the nasopharyngeal orifice of the ET. As a proof of concept, we collected otic, oropharyngeal and buccal samples from 23 healthy young adults for cultivation-independent analyses (16S-V4

amplicon sequences from 19 of the individuals) and recovery of otic and oral cultivars from the other 4 participants. The participants filled out a questionnaire and passed an onsite physical exam to establish health eligibility. The questionnaire also collected information about sports and recreational diving activities, which have been associated with increased pulmonary rates and, thus, more frequent middle ear ventilation [26]. The oral samples were collected from the oropharynx, the central hub for the distribution of saliva aerosols in the aerodigestive tract, and from the buccal mucosae (inner lining of the cheeks, upper gums and palate) that best represent the flexible and keratinized epithelia of the oral cavity that seed the salivary microbiome [27]. Amplicon sequencing of the 16S rRNA V4 region identified in the otic secretions a rich bacterial community of predominantly anaerobic taxa and revealed changes in community structure that correlated well with the frequency of otic aeration predicted for the participants. Furthermore, all of the subjects shared a core otic community taxonomically and metabolically similar to the oropharyngeal and buccal communities, albeit substantially different from the nasal microbiome. We also isolated from the three collection sites phylogenetically distinct species of facultative anaerobes, consistent with niche-specific adaptations to each body site. These results challenge the long-held view of a sterile otic mucosa and suggest instead that the middle ear is a dynamic ecosystem seeded by oral microbes and enriched in organisms better suited for growth and reproduction under episodic aeration.

MATERIALS AND METHODS

Study design

Eligible participants (*n*=23) were asked to rinse their mouth with a sterile saline solution to remove food debris and to follow a series of deep inhalation and yawn cycles that forced the opening the tympanic tube (they had to hear a “pop”) and the drainage of the middle ear fluids.

They were then asked to swallow to naturally open the ET one more time and to open their mouth to initiate sample collection. We used a sterile tongue depressor to improve access to the back of the mouth and prevent oral and/or tonsil contamination. Sample collection was with FLOQSwabs™ (Copan) and storage was in collection tubes filled with eNAT™ (DNA sequencing; 19 participants) or ESwab™ (cultivation; 4 participants) collection tubes (Copan). We first collected in a single swab the left and right otic secretions, using an ascending motion to swab the mucosal channels that laterally drain the otic fluids behind the palatopharyngeal arch. The physician then used separate swabs to collect control samples from the central region of the oropharynx and from the inner lining of the cheeks and upper gingiva and palate (buccal samples). To preserve the anonymity of the participants, we barcoded the swab samples and all the forms and questionnaire collected for each individual. All samples were stored in the collection tubes at 4^{o}C for 8-24 h before transport to the lab for immediate processing.

DNA extraction and 16S rRNA amplicon sequencing

We vortexed the transport tubes at medium speed for 1 min to detach the specimens and used a 400-µl aliquot of the cell suspension for DNA extraction with the FastDNA™ Spin kit (MP Biomedicals). The protocol for DNA extraction followed manufacturer's recommendations, except that cell lysis used 800 µl of cell lysis buffer instead of the recommended 1 ml. Sample homogenization used a Mini-Beadbeater (BioSpec Products) operated at maximum speed for 40 seconds and followed three cycles of mechanical homogenization interspersed with sample cooling on ice for 1 min. DNA quantification in the samples was with a NanoDop™ (Thermo Fisher Scientific) and a Qubit™ dsDNA HS assay (Thermo Fisher Scientific). The quality of the extracted DNA for amplification of the V4 region of the 16S rRNA genes was tested using dual indexed Illumina compatible primers (515f [GTGCCAGCMGCCGCGGTAA] and 806r

[GGACTACHVGGGTWTCTAAT]) [1] in a 25-µl PCR reaction containing 12.5 µl 2xGoTaq® Green Master Mix (Promega), 0.1 µM of each primer, 0.2-20 ng of DNA template, and nuclease-free water. The PCR amplification also included controls that replace the DNA template with the elution buffer used in DNA extraction, sterilized water and eNAT transport medium. Visualization of PCR products was on 1.2% agarose gels. Library preparation and amplicon sequencing were performed by the Genomics Core staff at Michigan State University's Research Technology Support Facility (RTSF) and followed standard protocols for PCR-amplification of the V4 hypervariable region of the 16S rRNA gene using the 515f/806r primer pair, normalization of the PCR products in SequalPrep DNA Normalization plates (Thermo Fisher Scientific), and cleaning of the pooled samples with AMPureXP magnetic SPRI beads (Beckman Coulter). Quality control and DNA amplicon quantification used the Qubit™ dsDNA HS assay, LabChip® GX DNA HS assay (PerkinElmer), and Kapa Library Quantification kit for Illumina platforms (Kapa Biosystems). Sequencing of the pooled amplicons was on an Illumina MiSeq v2 standard flow cell using a 500 cycle v2 reagent cartridge for 250 bp paired-end reads and used standard Illumina quality control steps, including base calling by Illumina Real Time Analysis (RTA) v1.18.54, demultiplexing, adaptor and barcode removal and RTA output conversion to FastQ format with Illumina Bcl2fastq v2.19.1.

Sequence data processing and analysis

We used USEARCH (v10.0.240) [70] to process the paired-end reads (FASTQ files) and merge paired-end sequences, quality-filter, dereplicate, remove singletons, pick OTUs and match them against the Silva database. Briefly, processing of raw reads and quality filtering used the UPARSE pipeline [71] and clustered into operational taxonomic units (OTUs) at 97% identity against the Silva Database (v. 1.19) [72] using previously outlined protocols [73,74]. Reads

without a database match were clustered in de novo mode at 97% identity [72]. Taxonomic assignment and diversity analyses used the QIIME workflow [75]. A summary of the script used in this study is available on Github (https://github.com/mutantjoo0/RegueraLab_ONR).

Intra-group (alpha) and inter-group (beta) diversity analyses used the functions available in the QIIME pipeline [72]. Alpha diversity analyses measured in each sample the species richness (number of observed species), their abundance and evenness (Shannon diversity index, H) and evenness (Simpson). Beta diversity analyses applied the weighted UniFrac metrics [76] to calculate pairwise phylogenetic distances between sets of sequences and generate a distance matrix for Principal Coordinates Analysis (PCoA). MS Excel 2016 was then used to visualize the inter-group relatedness in PCoA plots and calculate the statistical significance of the Unifrac distance between the otic and control samples with the t-test (*, $p < 0.05$; **, $p < 0.01$; ***, $p < 0.001$). InteractiVenn [77] was used to generate Venn diagrams and identify the core microbiome. When indicated, we applied estimation statistics (www.estimationstats.com) to assess the effect of size distribution and generate two-group estimation plots, as described elsewhere [78,79]. The estimation plots show the mean difference (Δ), the bootstrapped distribution of the mean difference and the bootstrapped 95% confidence interval of mean difference.

We analyzed the 16S-V4 phylogenetic data with the PICRUSt software package [80] to predict functional traits based on the Kyoto Encyclopedia of Genes and Genomes Orthology (KO) classification [81] on the Nephele cloud platform [82]. Visualization of the taxonomic and functional profiles for each sample used heatmaps generated with the HemI toolkit [83]. To illustrate the normalized distribution across the values, we used row Z-score normalized relative abundances and relative proportions or applied the average linkage clustering method and

Euclidean distance metric to calculate pair wise distance and similarity for hierarchical clustering in heatmaps. The neutral community model applied in this study was adapted from Sloan et al. [35] using custom R scripts developed by Venkataraman et al. [36]. Briefly, the analyses calculated OTU abundance in the source (number of OTU sequences with OTU in source community/total no. of sequences in source community) and the frequency of detection of each OTU in the otic communities (no. of participants with that OTU detected in the otic sample/total no. of individuals surveyed). A beta probability distribution was then used to predict the frequency of detection of each OTU in the otic samples as a result of neutral processes (dispersal and ecological drift) [35]. After optimization of the fitting parameter using a least-squares approach, we calculated the 95% binomial proportion confidence intervals for the neutral model and the goodness-of-fit coefficient of determination (R2), which ranges from 0 (no fit) to 1 (perfect fit). OTUs that fall outside the upper or lower confidence intervals are not neutrally distributed and identify OTUs likely to undergo positive or negative selection in the target community, respectively.

Cultivation and isolation procedures

We vortexed the ESwab™ collection tubes for 30 sec to detach the cells from the flocked swabs and transferred 200 µl aliquots of the cell suspension to a sterile cryovial containing an equal volume of freezing medium (Luria-Bertani [LB] broth-50% glycerol; filter sterilized) and stored at -80°C for long-term preservation. Using the sample collection swab, we streaked the remaining cell suspension onto solidified TSA medium (30g Tryptic Soy Broth (Sigma Aldrich); 15g Bacto Agar (BD); 1000 ml double distilled water) and incubated at 37oC for 48-72 h until colonies were visible. Single colonies showing different morphological traits (size, color, shape, texture) were re-streaked up to three times to ensure purity and reproducibility of the colony

phenotype. The isolates were then grown overnight in liquid Tryptic Soy Broth medium (TSB; Sigma Aldrich) at 37oC with gentle agitation. A 200-µl aliquot of the culture was transferred to a sterile cryovial, mixed with an equal volume of LB-50% glycerol and stored at – 80ºC for long-term preservation.

Phylogenetic analyses

DNA extraction was from cells harvested by centrifugation from 2 ml TSB cultures grown at 37°C for 24 h and used the FastDNATM Spin kit (MP Biomedicals) following manufacturer's recommendations. The DNA served as template for PCR-amplification of 16S rDNA fragments using bacterial universal primers (27F: AGAGTTTGATCMTGGCTCAG; 1492R: TACGGYTACCTTGTTACGACTT) [84] and GoTaq® Green Master Mix (Promega). The amplicons were then purified and concentrated with DNA Clean & ConcentratorTM-5 (Zymo Research) prior to Sanger sequencing with the forward or reverse primers using ABI Prism BigDyeTM Terminator v3.1 Cycle Sequencing Kit on an ABI 3730xl DNA Analyzer (Applied Biosystems) at Michigan State's Research Technology Support Facility Genomic Core. To remove sequencing errors, we trimmed the 3' end of the amplicons to retrieve the first 900-bp sequence. We also removed the 50 nt at the 5' end to produce a high quality 850-bp amplicon sequence for sequence homology searches in the GenBank database. For ambiguous matches, we aligned the forward and reverse contigs and repeated the search. Taxonomic assignation used a species cutoff value of 98.65% and a genus cutoff of 97% [85]. We used the Living Tree Project (LTP) database (https://www.arb-silva.de) [40,41] to identify the type strain for each of the closest species relatives and used their 16S rRNA genes as reference sequences for phylogenetic analysis with the 850-bp forward amplicons. We used the MUSCLE tool [86,87] in the software [88] to align the sequences before building a maximum likelihood tree and calculating the

bootstrap confidence values at each node using 1,000 replications. The tree shows bootstrap values above the 50% confidence threshold.

Hemolysis assays

The hemolytic activity of the cultivars was tested in microcolonies grown on blood agar plates prepared with 30 g of TSB (Sigma Aldrich), 15 g of Bacto Agar (BD) and 50ml sheep's blood (Sigma Aldrich). The bacterial strains were first grown overnight in TSB at 37°C with gentle agitation before spot-plating 5 µl of the culture on the blood agar plates. The culture drops were allowed to dry at room temperature for 30 min before incubation at 37°C for 24 hours in a CO2 incubator. The hemolytic activity was characterized as either alpha (media discoloration around the area of growth), beta (clearing around the area of growth) or gamma (no hemolysis).

Availability of data and materials

Raw sequence reads have been deposited in the NCBI Sequence Read Archive under BioProject ID: PRJNA473788.

RESULTS

Otic community structure and evidence for adaptative responses to episodic aeration

Taxonomic analyses of the OTUs assigned to the amplicon sequences identified the same dominant genera in all the samples but their abundance changed with the body site (Fig. 2.3a). Genera in the Bacteroidetes, Fusobacteria, Proteobacteria, and Firmicutes phyla collectively accounted for >95% of the OTUs identified in the otic, oropharyngeal and buccal communities. However, those in the obligate anaerobic phyla (Bacteroides and Fusobacteria) were more prevalent in the otic than in the oropharyngeal samples (55% and 48%, respectively) (Table 2.3). These two phyla had the lowest representation in the more aerated buccal communities (24%), which enriched instead for facultative anaerobic and aerobic genera in the Proteobacteria and

Firmicutes (72% of all the phylotypes). Furthermore, all of the samples shared the same dominant genera, though their relative abundance was site-specific (Fig. 2.3b). These differences could not be attributed to the sex of the participants (Fig. 2.7) but matched well with the frequency of aeration (therefore, oxygen availability) predicted at each body site (Fig. 2.3b). For example, the otic samples were dominated by strict anaerobes in the family Prevotellaceae (Prevotella and Alloprevotella), an oral group that can only proliferate in the low-oxygen communities of the subgingival plaque [29]. Similarly, obligate anaerobic genera in the Fusobacteria phylum (*Fusobacterium* and Leptotrichia) were more highly represented in the otic than in the oropharyngeal and buccal microbiomes. Conversely, *Haemophilus*, a genus enriched in the aerated regions of the buccal mucosa [29], was less abundant in the otic samples than in the oropharynx and buccal microbiomes. *Veillonella* was also one of the dominant genera in all the samples (Fig. 2.3b). Despite their obligate anaerobic metabolism, *Veillonella* survive in the oral cavity in metabolically-dependent aggregates with lactate-producing *Streptococcus* species in the dental plaque [27,30]. The presence of both *Veillonella* and *Streptococcus* in the otic communities suggests similar metabolic associations in the middle ear mucosa. Yet, the facultatively anaerobic metabolism of *Streptococcus* allows it to colonize more aerated regions of the oral cavity, increasing their abundance in the buccal samples (Fig. 2.3b).

The presence of 9 certified divers in the cohort of participants prompted us to separately reconstruct the structure of their otic communities for comparisons with the non-divers group. Scuba divers are trained in equalization techniques that promote the frequent opening of the ET and the aeration of the middle ear cavity. Enhanced pulmonary functions in these individuals independently of diving habits have also been reported [26] that could impact the otic community structure. Indeed, despite the small number of participants in each subgroup, we

observed significant changes in the representation of taxa based on their predicted metabolic response to aeration. In general, the otic communities of divers had less representation of anaerobic taxa that correlated well with increases in facultative anaerobic groups (Fig. 2.8). For example, the mean relative abundance of the anaerobic Bacteroidetes and Fusobacteria phyla decreased ($p = 0.02$) from 62% in non-divers to 48% in divers (Table 2.3). These decreases correlated well with changes in the relative abundance of two of the most abundant Bacteroidetes genera (Prevotella and Alloprevotella) and the Fusobacterial genus *Fusobacterium* (Fig. 2.8b). Divers also had a higher representation of oral genera such as *Streptococcus* and *Veillonella* (Fig. 2.8b), whose metabolic dependence and co-aggregation in the oral cavity could facilitate their co-dispersal in aerosols.

The oral cavity as a seeding source for the otic communities

We gained insights into the contribution of oral bacteria to the seeding of the middle ear by defining the core microbiomes at each collection site and the degree of shared membership among the core communities (Fig. 2.4). We included in these analyses, genera represented in at least half of the participants within each group (non-divers and divers) and used this information to identify core members for each collection site (Fig. 2.4a). The core otic diversity comprised 76 genera and included 66 taxa from the oropharyngeal and buccal core communities (Fig. 2.4b). Thus, 87% of the otic genus diversity was shared with the neighboring oral communities. The remaining 13% consisted of low abundant OTUs (<0.1%) that were present in one or two sites only (Supplementary Files). Transience could explain the detection of some of these low abundant taxa in the otic samples. We detected, for example, *Massilia*, an aerobic genus that is ubiquitous in soils and enters and disperses through the aerodigestive tract via aerosols [31]. Also, among the rare taxa was *Peptococcus*, a Firmicutes genus within the Gram-positive

anaerobic cocci (GPAC) group that enters the aerodigestive tract via saliva or saliva aerosols [32]. Similarly, some of the otic OTUs were assigned to the Eubacterium brachy group, within the Firmicutes, and to uncultured *Leptotrichiaceae* within the Fusobacteria, which are groups of obligate anaerobes known to disperse through the aerodigestive tract as well [33,34].

We next implemented a neutral community assembly model, adapted from Sloan et al. [35] by Venkataraman et al. [36], to predict the contribution of unbiased (neutral) processes such as random dispersal and ecological drift (i.e., stochastic birth and death) to the otic core composition (Fig. 2.4c). A goodness-of-fit test (R2) determines how well (0, no fit; 1, perfect fit) these neutral processes explain the relative abundance of each otic OTU when the oropharyngeal or the buccal communities are considered as sources of migrants. We obtained similar R2 values when considering the oropharynx (R2 = 0.37) and buccal (R2 = 0.44) samples as source communities. This coefficient of determination is modest yet expected from inter-personal variation in microbial seeding, both in terms of the type and abundance of oral migrants (influenced by dietary preferences, among other factors) and the host physiology (e.g., frequency of aeration). Despite this uncertainty, the coefficient of determinations could explain the presence of at least 70% of otic OTUs as the result of dispersal from the oral communities and ecological drift once in the middle ear environment. Most of the remaining OTUs fell above the confidence interval and, therefore, represent taxa over-represented in the otic communities compared to the two sources considered (green symbols in Fig. 2.4c). More than half of these OTUs (38 in all) deviated positively from the neutral model with both the oropharyngeal and buccal source communities (Supplemental Files). These taxa are predicted to have a competitive advantage in the middle ear, either because they are better fitted for growth in the otic mucosa and/or have a greater dispersal ability relative to other members of the source communities. The

fact that most of these OTUs are rare oral taxa enriched in the otic samples (Fig. 2.9) suggests, however, that they are not dispersal-limited but rather they have a growth advantage in the middle ear microenvironment.

The central location of the oropharynx in the aerodigestive system permits the seeding of its mucosa with saliva and the micro-aspiration of saliva aerosols into the middle ear. Therefore, we expected the oropharynx to contribute to the seeding of the middle ear more strongly than the buccal communities. To test this, we compared the mean relative abundance of the 66 genera that are shared by the three core communities (Fig. 2.10). These analyses revealed a stronger positive association of otic taxa abundance with the oropharyngeal (Pearson's correlation coefficient, R2=0.97) than with the buccal (R2=0.62) source communities, supporting the idea that the oropharynx serves as primary source for microbial immigration to the middle ear. The most significant deviations (at least two-fold increases or decreases in otic abundance compared to the oropharyngeal source) were for taxa with mean relative abundance <3 % (Fig. 2.10). Five of these OTUs (Treponema 2, *Corynebacterium, Porphyromonas, Parvimonas,* and *Stenotrophomonas*) were over-represented in the middle ear while the other 8 (*Acidibacter*, *Corynebacterium* 1, *Ralstonia, Catonella, Rothia, Eubacterium yurii* group, and other groups) were under-represented. Not surprisingly, these positive and negative deviations from the linear correlation of OTU abundance were exacerbated when considering the buccal communities (Fig. 2.10), which are more distant sources of microbial immigration.

Analyses of the abundance patterns among the dominant genera also provided evidence for the oropharynx serving as a central hub for the dispersal of oral migrants into the middle ear. For these analyses, we normalized taxa abundances per individual using the z-score method to generate a heatmap of the most abundant genera shared by the three core communities (Fig.

2.4d). We identified the same 20 dominant genera in all the samples, but the average abundance of each taxon changed with the collection site (Fig. 2.4e). The representation of the otic genera more closely mirrored the oropharyngeal than the buccal communities, further supporting the notion that the oropharynx is a primary seeding source for the otic communities. These analyses revealed abundance trends that supported, once again, the positive selection in the middle ear of obligate anaerobes such as those in the Bacteroidetes (family Prevotellaceae), Fusobacteria (*Fusobacterium* and Leptotrichia) and Firmicutes (*Veillonella*) phyla. By contrast, facultative anaerobic Proteobacteria (*Haemophilus*) and Firmicutes (*Streptococcus*) were most prevalent in the buccal samples. *Neisseria* OTUs provided an example of a genus that is similarly represented in the three locations and, therefore, neutrally distributed. This is a proteobacterial group of oropharyngeal and oral commensals that grows best aerobically [37] yet can disperse into the lower respiratory airways and lungs via saliva aerosols [38]. A similar mechanism of dispersal could explain the transience of these commensals in the middle ear.

Evidence for ecological diversification in the middle ear

As part of the study, we also collected otic, oropharyngeal and buccal samples from 4 participants for cultivation experiments. These individuals went through the same eligibility criteria, physical exam and sample collection protocol as the rest of participants but the swabs were collected in a transport medium that preserved the viability of the cells for cultivation studies. We directly streaked freshly collected swabs with the samples onto plates of tryptic soy agar (TSA), a medium that supports the growth of *Streptococcus* and other heterotrophic bacteria dispersing through the respiratory airways [2]. After incubating the plates at 37°C for 72 h, we visually inspected the colonies for morphology, color, shape and texture and ensured their purity through three passages on fresh TSA plates. This approach resulted in the recovery in pure

culture of 20 otic, 10 buccal and 9 oropharyngeal isolates. We next sequenced almost full-length amplicons of the 16S rRNA gene from each of the isolates for taxonomic classification at the genus and species levels using >95% and >98.7% identity cutoffs, respectively [3]. All of the isolates were closely related to species in the genera *Streptococcus, Staphylococcus, Neisseria*, *Micrococcus* and *Corynebacterium*. The majority of the isolates (79.5%) were Firmicutes in the *Streptococcus* (56.4%), consistent with their abundance in the three microbiomes (Fig. 2.3) and growth advantage under the cultivation conditions used for their recovery. We also isolated novel species of *Staphylococcus* (23.1%), *Neisseria* (15.4%) and Actinobacteria (*Micrococcus* and *Corynebacterium*, 5.1%) (Fig. 2.5, inset). Phylogenetic analysis of the 16S rRNA sequences obtained from the isolates and most closely related valid species showed a similar taxonomic distribution at the three collection sites but separation of otic, oropharyngeal and buccal isolates that is consistent with ecological diversification of oral migrants in the middle ear (Fig. 2.5).

The nearest neighbors to the *Streptococcus* sequences were species or subspecies within the Mitis group (*Streptococcus mitis, Streptococcus infantis, Streptococcus oralis, Streptococcus pseudopneumoniae, Streptococcus parasaguinis* and *Streptococcus rubneri*), the Salivarius group (*Streptococcus salivarius*), and the Lancefield's group B *Streptococcus* or GBS (*Streptococcus agalactiae*) [4, 5]. Given the low discriminatory power of 16S rRNA gene to classify human streptococcal isolates [6], we also screened the streptococcal isolates for hemolytic activity (Table 2.5). All of the *Streptococcus* cultivars were α-hemolytic except for three γ-hemolytic isolates most closely related to *S. oralis* (Mitis group), *S. salivarius* (Salivarius group), and to *S. agalactiae* (GBS group). These results are consistent with the classification of streptococci within the Mitis and Salivarius groups as either α- or γ-hemolytic [4, 7]. Furthermore, although

nearly all strains of the GBS group are β-hemolytic [4], isolates of *S. agalactiae* have been recovered that are non-hemolytic (thus, they are classified as γ) [8].

The staphylococcal cultivars (20% otic, 22.2% oropharynx, 30% buccal) were all strains of *Staphylococcus aureus*, *Staphylococcus epidermidis* and *Staphylococcus hominis* (Fig. 2.5). Staphylococci are common residents of the nasal flora [9] and readily disperse into the neighboring oral cavity via the pharynx [10]. As a result, they are frequently isolated from oral and perioral regions [10, 11]. The genus was however poorly represented in the otic, oropharyngeal or buccal 16S-V4 survey (Fig. 2.3), supporting the idea that they are transient members of these communities. We also recovered otic (10%), oropharyngeal (11%) and buccal (30%) strains more closely related to *Neisseria perflava* (Fig. 2.5), an abundant member of the oropharyngeal flora [12] that disperses into the respiratory tract via saliva aerosols [13] and appeared transiently in the microbiome sequenced from otic secretions (Fig. 2.3b). Our cultivation approach also recovered in pure culture two otic Actinobacteria in the *Micrococcus* and *Corynebacterium* genera (Fig. 2.5). Actinobacteria is the most abundant nasal phylum [14] but only accounts for ~1% of the otic OTUs (Fig. 2.3). This is not unexpected considering that *Micrococcus* and *Corynebacterium* species are obligate or facultative aerobes and, therefore, they are more likely to be negatively selected under the anaerobic conditions that prevail in the middle ear.

Similar functional structure of the otic and oral microbiomes

Given the similarities in community membership among the three collection sites, we predicted a high degree of functional redundancy among their members as well. To test this, we used metabolic inference methods to predict the metabolic structure of the microbiome from otic secretions and describe relationships with the spatially close communities of the oropharynx and

buccal mucosae. A heatmap of Z-score transformed relative proportion of functions represented at each collection site (1% cutoff) revealed a high degree of redundancy in core functions (Fig. 2.11) and similar trends in non-divers and divers (Fig. 2.12). All of the microbiomes had a high representation of membrane transport functions and modules associated with the metabolism of amino acid and carbohydrates (Fig. 2.11). These metabolic functions often prevail in mucosal-associated communities, whose members support their growth using proteins and mucin glycoproteins secreted in the mucosa as sources of amino acids and carbohydrates [51]. Also with high representation in the three microbiomes were essential functions for genetic processing and information (replication and repair and, to a lesser extent, translation), which are critical to support cell growth (Fig. 2.11). By contrast, cell motility functions were low. This is not unexpected given the primary contribution of passive mechanisms of dispersal (i.e., aerial dispersal of saliva aerosols) to microbial immigration in these body sites.

Despite the overall similarity in core functions at the three collection sites, we identified in pairwise comparisons some significant changes in the otic communities compared to the oropharyngeal and buccal sources (Fig. 2.6). The most notable differences were the lower representation of membrane transport functions yet higher relative proportion of amino acid and energy metabolism modules in the otic and oropharyngeal communities compared to the buccal communities. These differences likely reflect quantitative and qualitative changes in the nutrients that are available to support the growth of the resident microorganisms. Dietary substrates, which are abundant in the oral cavity, are less accessible in the oropharynx due to disturbance by the frequent cycles of air inhalation and exhalation. Dietary nutrients are also scarce in the middle ear due to the limited carriage of external nutrients in saliva aerosols. The oropharyngeal and, even more so, the otic communities are more likely to sustain their trophic webs with host-

derived nutrients such as proteins and mucin glycoproteins secreted to the mucosa [51]. This helps explain why the relative proportion of membrane transport functions decreased while modules for amino acid and energy metabolism were more represented in the otic and oropharyngeal communities.

DISCUSSION

The identification of a diverse yet distinct microbiome in otic samples collected from healthy young adults challenges the entrenched view of a sterile middle ear mucosa and suggests instead that microorganisms colonize the otic mucosa and establish a site-specific community adapted to episodic ventilation. Our results thus validate earlier studies, which reported the presence of bacterial microcolonies in otic mucosal samples collected from individuals that had no history of chronic otic infections [15]. We initially reasoned that these microcolonies could have resulted from the colonization and growth of oral bacteria introduced in the middle ear during the cycles of ventilation. As in other regions of the upper respiratory tract [52], mucociliary activity promotes the clearance of the otic mucus and, with it, bacteria residing in the mucosa. The periodic contraction and expansion of muscles around the ET also contributes to the clearance of mucus and fluids from the tympanic cavity and their drainage [7]. Non-invasive sampling of these secretions permitted the amplification of 16S-V4 rRNA bacterial sequences and the identification of an otic community with genus-level diversity comparable to the neighboring oral communities, which are among the richest and most diverse in the human body [27]. PCoA plots revealed the spatial clustering of the otic communities expected for site-specific populations and overlap with the oropharyngeal and, to a lesser extent, buccal communities that we predicted to serve as seeding sources (Fig. 2.2b). However, the taxonomic composition of the otic communities differed substantially from that reported for nasal microbiomes [50], despite

the closer proximity of the ET orifice to the nasopharynx (Fig. 2.2.1b). Actinobacteria, for example, is the most abundant nasal phylum [50] but only accounted for ~1% of the otic OTUs (Table 2.3). Instead, the otic secretions enriched (~38%) for genera in the Bacteroidetes, a strictly anaerobic phylum with lower representation (<10%) in the more aerated mucosae of the nasal cavity [50]. The relative abundance of Firmicutes in the otic samples (~21%) was within the ranges reported in the nasal microbiome [50] but while nasal Firmicutes are dominated by *Staphylococcus* [47], this genus was not significantly represented among the otic OTUs (Fig. 2.3). Rather, otic Firmicutes were dominated by *Streptococcus* and *Veillonella,* which are two of the most abundant genera in the oral cavity (Fig. 2.3). The otic communities also shared most of the keystone taxa of the core oral communities that we hypothesized would serve as sources of dispersal (Fig. 2.4). Indeed, the three mucosal sites sampled in this study harbored microbial communities dominated by the same 9 genera (*Prevotella* 7, *Prevotella*, *Alloprovetella, Fusobacterium*, *Leptotrichia*, *Haemophilus*, *Veillonella*, *Streptococcus*, and *Neisseria*) (Fig. 2.3). These genera represented four phyla (Bacteroidetes, Fusobacteria, Proteobacteria and Firmicutes) that collectively accounted for >90% of all the OTUs at each collection site. However, the relative abundance of anaerobic taxa (e.g., all of the Bacteroidetes and Fusobacterial genera) was higher in the otic secretions than in the neighboring oral mucosae, which selected instead for facultative aerobes in the Proteobacteria (*Haemophilus*) and Firmicutes (*Streptococcus*) (Fig. 2.5).

Alpha diversity analyses (Fig. 2.2a) provided additional evidence for the presence of an otic community as rich and diverse as the oral communities yet adapted to the fluctuating aeration of the middle ear environment. The analyses revealed, for example, increases in species evenness in the otic communities that are often associated with microbiomes having the

robustness and functional stability needed to adapt to environmental fluxes [28]. Redox fluctuations are expected in the middle ear, due to the periodic pulses of air that enter the tympanic cavity when the ET opens. Episodic exposure of the otic mucosa to air provides a reasonable explanation for the enrichment in the otic communities of strict anaerobes, particularly those in the Bacteroidetes phylum (Fig. 2.3). The brief cycles of tubal dilation limit the volume of air entering the tympanic cavity to 4-5 µl [5]. Moreover, otic ventilation uses exhaled air [5], which has a lower concentration of oxygen than atmospheric air. Importantly, swallowing opens the ET once every minute during the wake hours, but patency slows down (every 5 minutes) during sleep [5]. This suggests that conditions of oxygen limitation prevail in the middle ear. Aerotolerant strains will have an adaptive advantage under these conditions and would be key to preserve community stability. The most prevalent otic Bacteroidetes were members of the family Prevotellaceae, which despite their strictly anaerobic metabolism can adaptively evolve oxygen tolerance under selective pressure [53]. Obligate anaerobes will have a growth disadvantage under conditions of increased aeration. This could explain why anaerobic genera such as *Prevotella, Alloprevotella* and *Fusobacterium* were less abundant in the otic secretions of divers (Fig. 2.8), a group that has the equalization training associated with increased otic ventilation [5]. Furthermore, scuba diving, even if infrequent, can lead to subclinical changes in pulmonary functions [26] that could increase the rates of aerial dispersal into the middle ear and the abundance patterns of otic anaerobes.

Nutritional variables cannot be excluded as selective forces in the middle ear either. Oral Bacteroidetes, for example, also disperse into the digestive tract and proliferate in the strictly anaerobic environment of the colon breaking down dietary complex carbohydrates [54]. Yet, we sequenced a higher proportion of Bacteroidetes phylotypes in the otic samples than typically

detected in the colon (~16%) [54]. The selection of gut Bacteroidetes that can break down complex carbohydrates provides fermentable sugars for Firmicutes but also slows down the growth of Bacteroidetes [54]. Otic Bacteroidetes however could specialize at the degradation of host-derived nutrients such as lipids, proteins and mucin glycoproteins secreted by the mucosal epithelium. Bacteroidetes are well equipped to break down mucin [55] and could support their growth with mucin-derived protein and carbohydrates, which account to 39.5% and 60.5% of the otic mucin, respectively [51]. Some of the simple sugars released during the degradation of the otic mucin could also support the growth of fermentative bacteria and the formation of syntrophic microcolonies. The degradation of mucin and fiber by gut Bacteroidetes supports the fermentative metabolism of strict anaerobes in the class Clostridia, which can account for up to 95% of all the gut Firmicutes [54]. This class was under-represented (~4%) in the otic communities. Instead, otic Firmicutes were represented by *Streptococcus* and *Veillonella*, abundant oral taxa that form metabolically linked co-aggregates during the primary colonization of the tooth surface [30]. The metabolic co-dependence of these two bacteria is established with the fermentation of sugars to lactate by the *Streptococcus* partner and the fermentation of lactate by *Veillonella* to produce propionate, acetate, CO2 and H2 [56,57]. A syntrophic consortium between otic Bacteroidetes, *Streptococcus* and *Veillonella* could promote the degradation and fermentation of mucin sugars into short chain fatty acids critical to mucosal health. The lactate dependency of *Veillonella* may also permit direct syntrophic interactions with Bacteroidetes partners that ferment simple sugars into lactate [58]. The high representation of pathways for carbohydrate and amino acid metabolism and reduced membrane transport predicted for the otic phylotypes (Fig. 2.6) does indeed support a trophic web in the otic mucosa driven by the metabolism of mucins and relying on lactate cross-feeding.

The similarities between the otic and gut trophic webs are not unexpected given the fact that both mucosae are seeded with oral microbes and both sites enrich for anaerobic migrants. A wide range of microbes enter the mouth with air, food, and via host-to-host contact before dispersing into the aerodigestive tract via air and/or saliva [59]. The oral cavity provides a heterogenous landscape (tooth surfaces, tongue, gingival crevices, palate, etc.) that locally selects for the growth of specific taxa, increasing their representation in saliva and their dispersal potential to other parts of the gastrointestinal tract and the lower respiratory airways [38]. Neutral models of community assembly suggest that the majority of microbial sequences recovered from the upper gastrointestinal tract and the lungs in healthy individuals disperse from oral reservoirs [36]. Similarly, oral dispersal had a profound influence in shaping the composition of the communities sequenced from otic secretions. Indeed, we identified in the oropharyngeal and buccal communities most of the core otic taxa (87% of the otic OTUs) (Fig. 2.4b), including many taxa known to disperse through the aerodigestive tract with air and/or saliva. Further, most (~70%) of the shared OTUs were neutrally distributed in a neutral model fit when considering the oropharynx or buccal communities as potential sources of immigration (Fig. 2.4c). ET patency only lasts about 400 milliseconds but occurs frequently (about 1,000 times a day just by swallowing) [60], providing a constant source of oral migrants. The process is analogous to the subclinical micro-aspiration of saliva aerosols that seeds the lower airways and the healthy lungs with oral microbes [52]. But unlike the seeding of the lungs with saliva aerosols carried during inhalation, microbial immigration into the middle ear is via exhaled air drawn from the lungs during ET patency. Not surprisingly, oral microbes commonly carried into the lower respiratory tract via aerosols such as *Prevotella*, *Veillonella*, *Streptococcus*, and *Fusobacterium* [52] were also among the most abundant in the otic secretions (Fig. 2.4). The

adapted insular model of the lung microbiome [61] based on island biogeography theory [62] explains the constant presence of these microbes and their abundance in the lower airways as an equilibrium between the rates of microbial immigration (primarily by micro-aspiration during inhalation) and extinction (exhalation, coughing, etc.) with little contribution from the local growth of its members [61]. A similar model could explain the colonization of the middle ear with oral seeds, though with some notable differences. The middle ear is but a few centimeters away from the richly colonized mucosa of the oropharynx (the lungs are about half a meter), which could significantly increase the rates of microbial immigration. Spatial proximity could also permit the direct migration of oropharyngeal bacteria by swarming, a mode of flagellar motility that is stimulated by mucosal lubricants such as surfactants and mucin [63,64]. Extinction rates in the middle ear would be determined by the efficiency of mucociliary and muscular clearance [7,65]. The enrichment of specific groups in the otic samples suggests that these mechanism for mucus clearance cannot prevent the colonization of the otic mucosa by oral migrants. Furthermore, most of the otic OTUs that deviated from the neutral model were over-represented in the otic communities compared to the oropharyngeal or buccal sources (Fig. 2.4c), suggesting a process of positive selection. Among the oral sequences enriched in the otic environment were strict anaerobes within the Bacteroidetes, Fusobacteria and Firmicutes. Also, over-represented were many Proteobacterial sequences assigned to groups of facultative anaerobes, which could have a competitive advantage for growth with intermittent aeration. Indeed, otic Proteobacteria represented 16% of the sequences identified in the non-divers otic samples and had an even higher representation (~25%) in the more aerated middle ear mucosa of divers. By contrast, many oral Proteobacteria are negatively selected under the strictly anaerobic conditions of the colon, reducing their representation to ~0.1% of the gut phylotypes [54].

Dispersal ability could have also contributed to the over-representation of some oral taxa in the otic communities. More frequent otic ventilation, as predicted for divers, could also increase the rates of micro-aspiration of saliva aerosols from the oropharynx and the dispersal of oral migrants. This could explain the higher representation in divers of facultative anaerobic taxa such as *Streptococcus*, a genus that is most abundant in the buccal communities (Fig. 2.4).

The correlations between otic community structure and aeration cannot rule out the influence of other host variables. Scuba diving can cause small changes in pulmonary function that could increase the rates of aerial dispersal into the middle ear [26]. Anatomy and even body position and posture are known to influence ET function [5]. Thus, ET opening time is shorter when lying down because the increased blood flow to the head and neck causes venous engorgement around the tympanic tube [66,67]. As a result, the mean volume of air passing through the tube's lumen is two thirds lower when in the supine than the prone position [68]. Thus, increased otic ventilation in divers could have resulted from higher levels of physical activity in this group. Further, subtle differences in the anatomy of the ET are not uncommon [5] and could have affected the rates of microbial immigration over extinction and, by extent, the structure of the otic community. Importantly, we selected a homogenous cohort of young adults among the college population, but we cannot exclude those dietary preferences contributed to intra- or inter-group differences. Future investigations could address these variables in larger surveys that select participants based on their dietary and exercise routines. Also important for future studies are insights into the intrinsic and extrinsic factors that lead to the positive or negative selection of taxa in the middle ear, particularly otopathogens. Our study highlighted correlations that point at a critical role for aeration and host-derived nutrients in the assembly of otic biofilms, but other variables such as pressure fluctuations and sound-induced vibrations

could exert selective pressure and permit the diversification of oral taxa into lineages better suited for growth and reproduction in the middle ear mucosa. In support of this, we recovered from the otic samples cultivars that were closely related yet phylogenetically distinct to oral isolates (Fig. 2.5). These otic lineages could, in turn, influence the functionality of the otic community, its interactions with the host mucosa and the outcome of infections.

DECLARATIONS

Ethics approval and consent to participate

The research proposed in this study was approved on May 17 of 2017 by the Institutional Review Board (IRB) at Michigan State University, East Lansing, Michigan, United States of America. The committee found the research project to be appropriate in design, to protect the rights and welfare of human subjects, and to meet the requirements of Michigan State University's Federal Wide Assurance and the Federal Guidelines (45 CFR 46 and 21 CFR Part 50).

Consent for publication

Not applicable.

Competing interests

The authors declare that they have no competing interests.

Acknowledgements

The authors thank the study participants in the otic human study who kindly provided the swab samples and Dr. Lauryn Przeslawski for assistance with sample collection. We are also grateful to Dr. Emily Chrisovan at Michigan State's Research Technology Support Facility for advice with amplicon sequencing, to Hugh McCullough for assistance with 16S rRNA

sequencing of cultivars, and to Drs. Ashley Shade, Patrick Kearns, and Nejc Stopnisek at Michigan State and Dr. Arvind Venkataraman at Procter & Gamble for bioinformatics support.

Funding

This work was supported by award N00014-17-2678 from the Office of Naval Research to G.R. and K.K.

Affiliations

Department of Microbiology and Molecular Genetics, Michigan State University, 567 Wilson Rd., Rm 2215, Biomedical and Physical Sciences building; East Lansing, MI 48824, USA.The research proposed in this study was approved

Contributions

GR conceived the study and planned the sample collection protocol with contributions from KK. The four authors participated in the collection of the samples. J-YL processed samples for Illumina sequencing and analyzed the 16S-V4 data. KJ processed samples for cultivation experiments, J-YL amplified and sequenced the 16S rRNA sequences, and KJ performed the phylogenetic analyses and hemolysis assays. GR wrote the first draft of the manuscript and incorporated contributions from the other authors. All authors read and approved the final version of the manuscript.

APPENDIX

Figure 2.1: Anatomy of the ear, pharynx, and oral cavity. (a) Anatomic structures in the outer, middle, and inner ear (illustration modified from Iain at the English Wikipedia, CC BY-SA 3.0). (b) Lateral cross section of the head showing the oral and nasal cavities, the three pharyngeal regions (naso-, oral-, and laryngo-) and the mucosal folds around the ET orifice and torus tubarius (illustration modified from Sémhur at Wikimedia Commons, CC BY-SA 3.0). (c) Frontal view of the oral cavity (licensed from Biorender and edited to add labels).

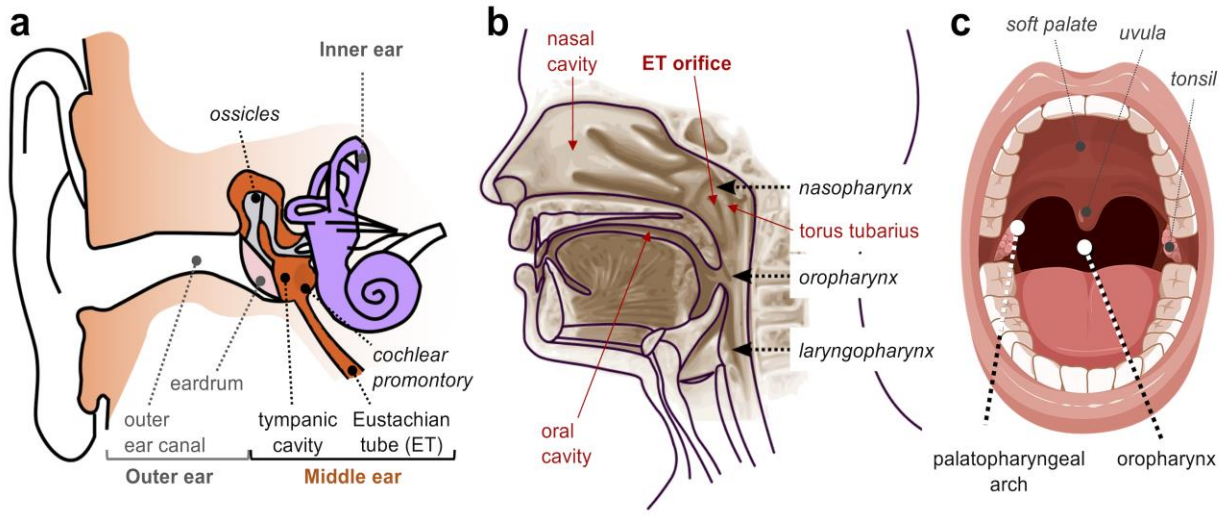

Figure 2.2: Genus diversity in otic secretions. (a) Alpha diversity of the otic (blue), oropharyngeal (gray) and buccal (orange) communities based on richness (observed species), diversity (Shannon index) and evenness (Simpson index). Box plots show 50% of the diversity values in boxes, 25th and 75th percentiles as whiskers, median (line across the boxes), average (cross), outliers (circles outside the boxes) and confidence value from *t*-test comparisons (*, p <0.05; **, $p < 0.01$; ***, $p < 0.001$; exact confidence values in Table 2.4, Additional File 1). Estimation graphics at the bottom show the mean (circle) diversity difference (Δ) of oropharyngeal or buccal samples versus the otic mean diversity (dashed blue line), the complete Δ distribution of values (shaded curve) and the 95% confidence interval of Δ (vertical line). (b) Principal Coordinates Analysis (PCoA) of weighted UniFrac distance in non-divers (circles) and divers (triangles) showing the spatial clustering of otic (blue) and buccal (orange) samples and overlap of these clusters with the central oropharyngeal samples (gray). Axes PC1 and PC2 show the proportion (%) of variance explained.

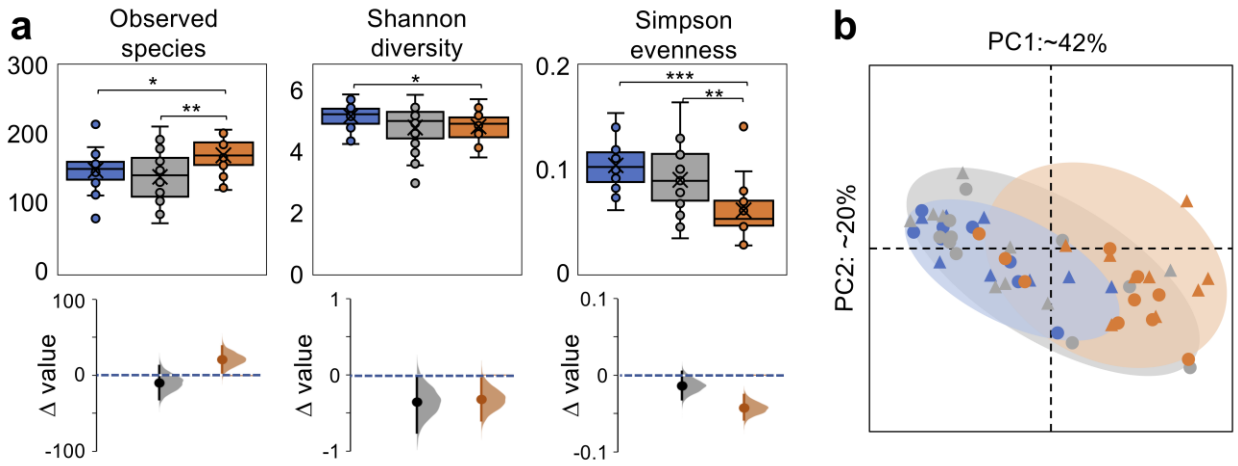

Figure 2.3: Genus-level structure of the otic communities in reference to oropharyngeal and buccal microbiomes. (a) Inter-individual differences and mean relative abundance (%) of genera (color-coded by phylum) at each collection site (b) Distribution of relative abundance values (*top*) and estimation plots (*bottom*) for dominant (>1%) otic genera. Data are color-coded for the otic (blue), oropharyngeal (gray) and buccal (orange) samples. Boxes in the bloxplots contain 50% of the values (horizontal line, median), whiskers the 25th and 75th percentiles, outliers (circles outsides the boxes) and t-test confidence values (*, p<0.05; **, p<0.01; ***, p<0.001). Estimation plots showing the mean difference (Δ, solid circle) between otic (blue line at zero) and oropharyngeal (gray) or buccal (orange) samples, the complete Δ distribution (shaded curve), and 95% confidence interval of Δ (vertical line). Statistic values used to assess significance of the data are shown Supplemental Table 4.

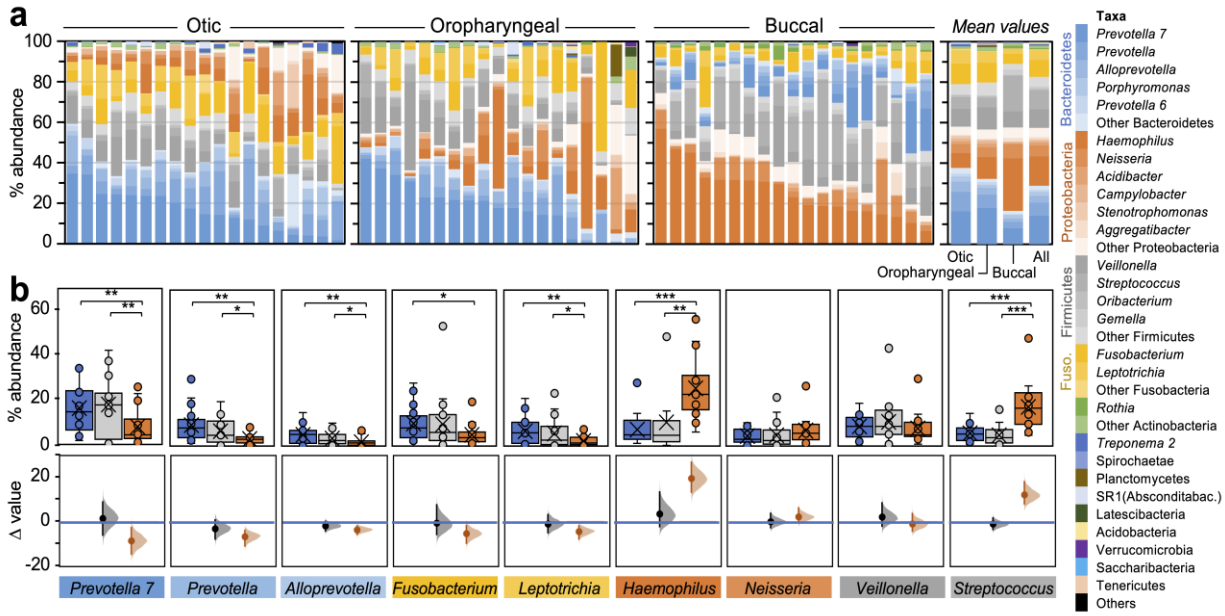

Figure 2.4: Distribution and abundance of otic, oropharyngeal and buccal genera. (a-b) Core membership of genera shared by at least half of non-divers (nD) and divers (D) at each collection site (a) and among all microbiomes (b). (c) Neutral model fit of otic community assembly with the oropharyngeal or buccal communities as potential sources (R^2, goodness of fit). Gray symbols represent neutrally distributed OTUs (within 95% confidence interval around the best-fit). Taxa above (green) or below (red) the confidence interval are more likely to be positively (over-represented) or negatively (under-represented) selected in the middle ear, respectively. (d-e) Heatmaps of individual (d) or average (e) Z-score transformed relative abundance (normalized z-score>-1.0) of the 20 dominant genera (color-coded by phylum: Bacteroidetes, blue; Fusobacteria, yellow; Firmicutes, gray; Proteobacteria, orange; Actinobacteria, green; Spirochaeta, dark blue; SR1, light blue; Planctomycetes, dark gold).

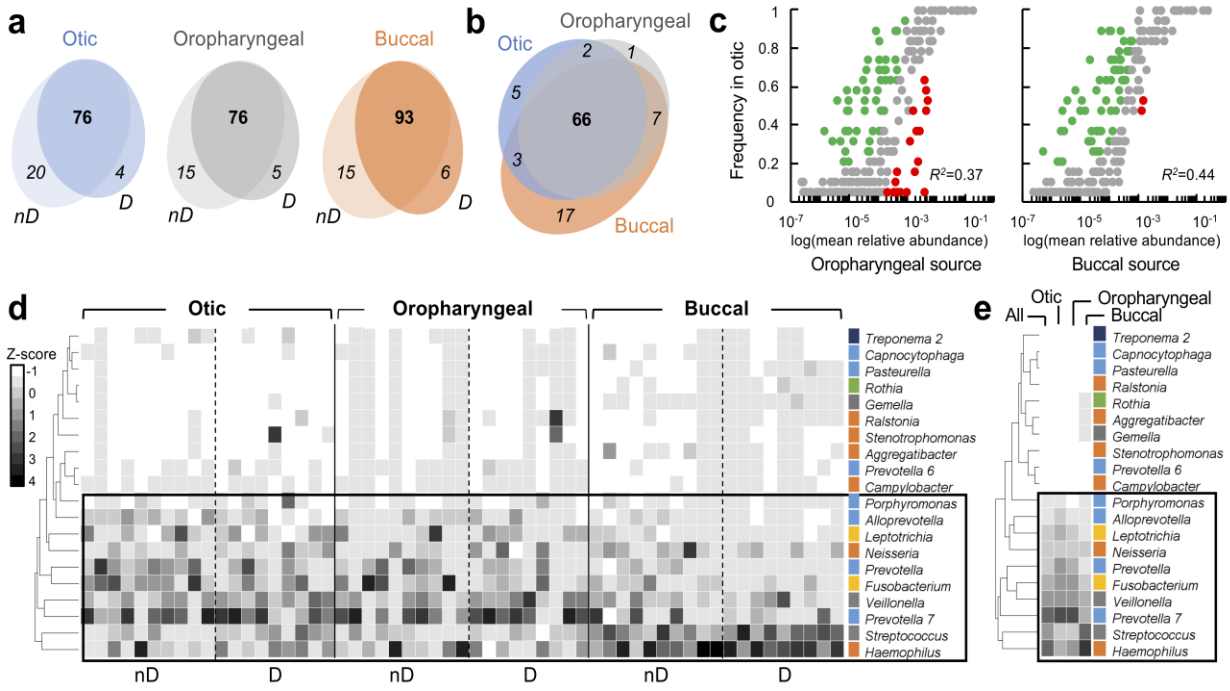

Figure 2.5: Taxonomic and phylogenetic characterization of otic, oropharyngeal and buccal cultivars. The graph shows the number and genus assignment (based on 16S rRNA sequence) of otic, oropharyngeal and buccal isolates. The maximum-likelihood tree built with 16S rRNA sequences shows the phylogenetic placement of the otic ("L" number, in red), oropharyngeal ("C") and buccal ("B") isolates and the closest strains (accession numbers, in parentheses). The scale bar indicates 5% divergence of 16S rRNA sequences filtered to a conservation threshold above 70% using the Living Tree Project (LTP) database.[15, 16] The numbers at each node are bootstrap probabilities by 1,000 replications above 50%.

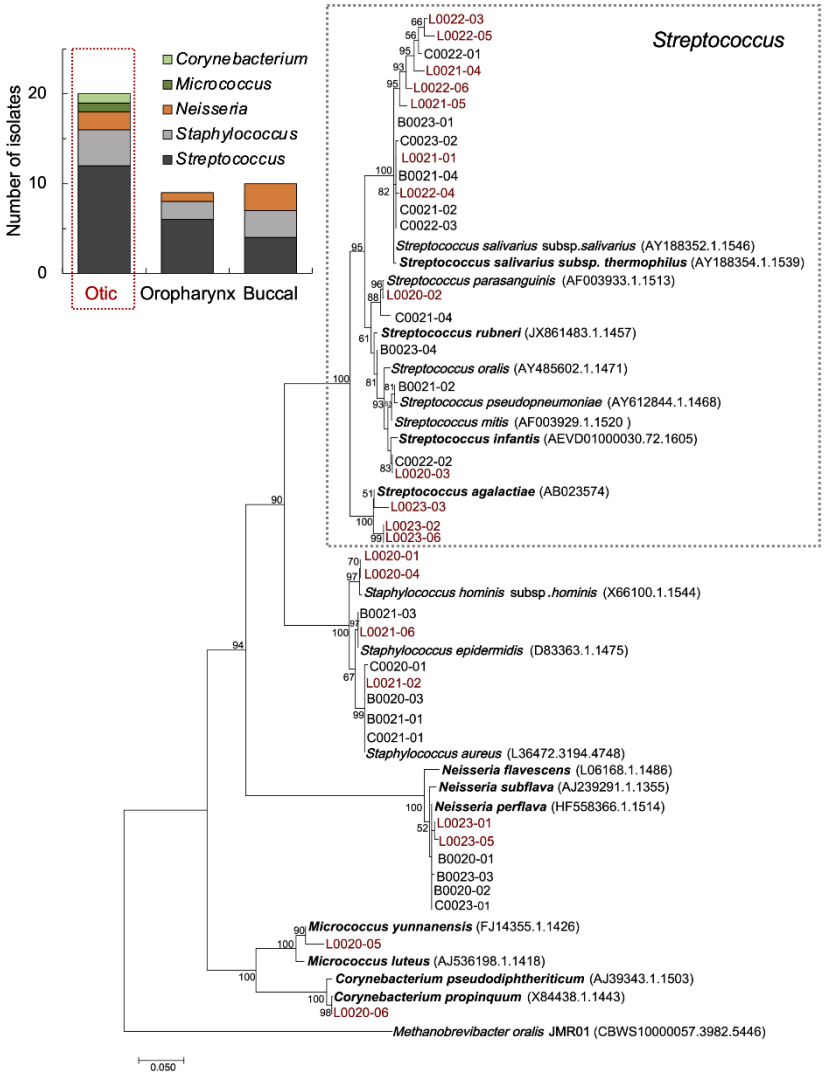

Figure 2.6: Taxonomic-based prediction of dominant metabolic functions. Pairwise comparisons of the abundance of the top 5 metabolic functions represented in the buccal (B) versus otic (O) or oropharyngeal (C; for center of the oropharynx) samples. Data from the statistical analyses is available in Table 2.4.

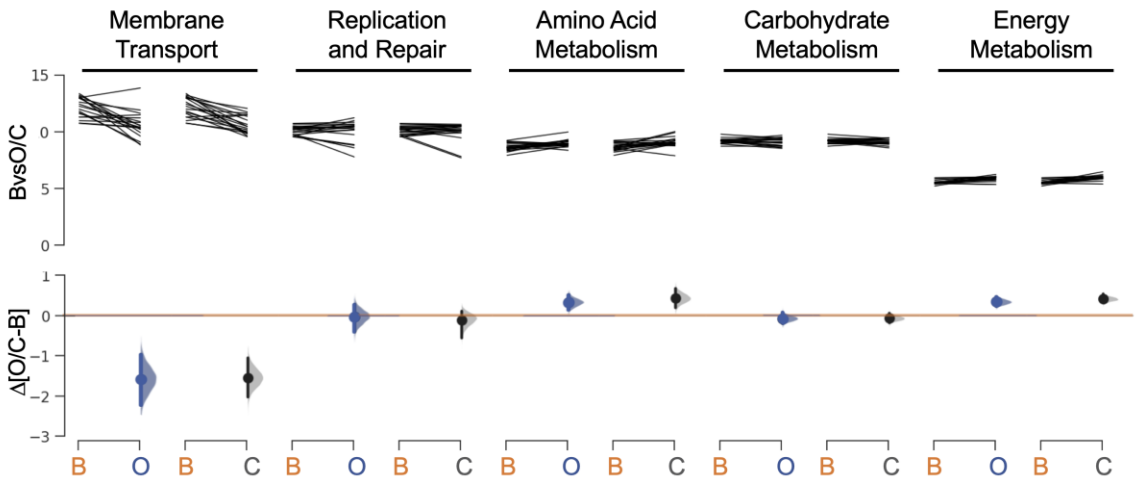

Table 2.1: Age and gender of study participants. Age and gender (female, F; male, M) of study's participants. The table shows the age ranges and, in parenthesis, the mean and standard deviation. The plots at right show the age distribution by gender and diving group. Boxes contain 50% of all values and whiskers represent the 25th and 75th percentiles. The median is shown as a horizontal line across the boxes, average as a cross and outliers as circles outside the boxes.

Group	Total (*n*=19)	Non-diver (*n* = 10)	Diver (*n* = 9)
Age	18-32 (19.9±1.6)	18-21 (18.8±0.6)	18-32 (21.1±2.1)
Gender F:M	11:8	5:5	6:3

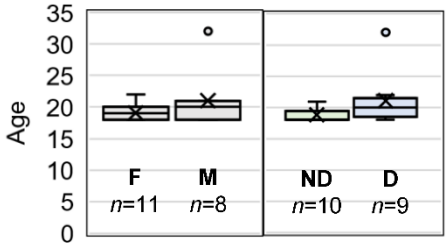

Table 2.2: Diving experience (mean and standard deviation [SD] of total number of dives and diving depth (in ft) reported by the participants in the diver's group (*n*=9). The plots at the bottom show boxes containing 50% of all values and whiskers representing the 25th and 75th percentiles. The median is shown as a horizontal line across the boxes, the average as a cross and the outliers as circles outside the boxes.

No. dives Mean(±SD)	**Depth (ft)** Mean(±SD)
13.8(±7.0)	70(±8.7)

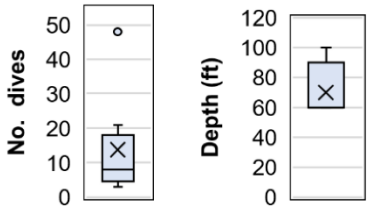

Table 2.3: Mean relative abundance (%, from Figure 3) and standard deviation (in parenthesis) of the 4 most abundant phyla at the three collection sites for all of the participants or each subject cohort (non-divers and divers). The sum of the mean values for the phyla is shown as % of the total.

	Bacteroidetes	Fusobacteria	Proteobacteria	Firmicutes	Actinobacteria	Total
Otic	38 (±6)	17 (±4)	20 (±7)	21 (±4)	1.1 (±0.4)	>98%
Non-divers	40 (±5)	22 (±4)	16 (±6)	19 (±4)	1 (±0.4)	>97%
Divers	35 (±6)	13 (±2)	25 (±8)	24 (±4)	1.4 (±0.4)	>98%
Oropharynx	32 (±7)	16 (±6)	24 (±11)	23 (±6)	1.8 (±0.8)	>97%
Non-divers	31 (±8)	19 (±8)	27 (±12)	20 (±5)	1.7 (±1)	>98%
Divers	34 (±7)	11 (±3)	22 (±10)	27 (±7)	1.8 (±0.6)	>96%
Buccal	16 (±5)	8 (±3)	41 (±8)	31 (±5)	2.7 (±0.9)	>99%
Non-divers	20 (±6)	10 (±4)	41 (±9)	26 (±4)	2.6 (±0.7)	>99%
Divers	13 (±4)	5 (±1)	42 (±6)	37 (±5)	2.9 (±1.2)	>99%

Table 2.4: Summary of statistic values estimated from the data analyses in various figures.

The tables show *p*-values calculated with the Student's *t*-test function in Microsoft Excel (*, $p<0.05$; **, $p<0.01$; ***, $p<0.001$; highlighted in green) and, for data compared in estimation plots, the standardized mean difference (SMD, effect size) and bias corrected and accelerated (BCa) bootstrapped 95% confidence intervals (95%CIs, lower and higher).

Figure 2: (a) Pairwise comparisons of otic, oropharyngeal and buccal alpha diversity indexes				
Index	Comparison	*p*-value	SMD	95%CIs
Observed species	O and C [C-O]	0.424	-9.37	-31.2, 12.7
	O and B [B-O]	0.025*	21.5	4.14, 38.8
	C and B [B-C]	0.007**	30.8	9.16, 50.8
Shannon diversity	O and C [C-O]	0.085	-0.352	-0.760, -0.008
	O and B [B-O]	0.034*	-0.319	-0.597, -0.045
	C and B [B-C]	0.872	0.033	-0.309, 0.461
Simpson evenness	O and C [C-O]	0.152	-0.014	-0.032, 0.004
	O and B [B-O]	1.26E-05***	-0.043	-0.058, -0.026
	C and B [B-C]	0.006**	-0.029	-0.047, -0.009

Figure 3: (a) Box plots comparing 9 most abundant genera in the otic, oropharyngeal and buccal samples (*p*-value)			
Genus	Otic-oropharyngeal	Otic-buccal	Oropharyngeal-buccal
Prevotella 7	0.681	0.008**	0.007**
Prevotella	0.200	0.001**	0.018*
Alloprevotella	0.157	0.002**	0.040*
Fusobacterium	0.902	0.017*	0.131
Leptotrichia	0.611	0.006**	0.048*
Haemophilus	0.372	0.000004***	0.002**
Neisseria	0.861	0.132	0.275
Veillonella	0.423	0.626	0.272
Streptococcus	0.490	0.000025***	0.000009***

Table 2.4 (cont'd)

Figure 3: (b) Estimation plots comparing the 9 most abundant genera between the otic and oropharyngeal or buccal samples				
	Otic vs oropharyngeal		Otic vs buccal	
Genus	SMD	95%CIs	SMD	95%CIs
Prevotella 7	0.0155	-0.0543, 0.0875	-0.0838	-0.1378, -0.0261
Prevotella	-0.0283	-0.0738, 0.0094	-0.0643	-0.1052, -0.0360
Alloprevotella	-0.0161	-0.0376, 0.0042	-0.0330	-0.0529, -0.0155
Fusobacterium	-0.0041	-0.0541, 0.0813	-0.0502	-0.0913, -0.0142
Leptotrichia	-0.0104	-0.0479, 0.0310	-0.0432	-0.0749, -0.0179
Haemophilus	0.0338	-0.0215, 0.1286	0.1866	0.1238, 0.2548
Neisseria	0.0028	-0.0228, 0.0389	0.0241	-0.0002, 0.0614
Streptococcus	-0.0090	-0.0328, 0.0165	0.1190	0.0803, 0.1748
Veillonella	0.0206	-0.0185, 0.0808	-0.0094	-0.0395, 0.0340

Figure 6: (b) Pairwise comparison of 5 most abundant relative proportion of predicted functions in otic, oropharyngeal, and buccal samples				
Predicted functions	Comparison	*p*-value	SMD	95%CIs
Membrane Transport	Buccal-otic	1.32E-04***	-1.592	-2.238, -0.982
	Buccal-oropharyngeal	6.98E-06***	-1.555	-2.036, -1.062
Replication and Repair	Buccal-otic	0.854	-0.033	-0.406, 0.278
	Buccal-oropharyngeal	0.482	-0.116	-0.558, 0.104
Amino Acid Metabolism	Buccal-otic	4.8E-03**	0.324	0.132, 0.507
	Buccal-oropharyngeal	3.0E-03**	0.429	0.188, 0.666
Carbohydrate Metabolism	Buccal-otic	0.277	-0.080	-0.213, 0.063
	Buccal-oropharyngeal	0.272	-0.072	-0.190, 0.055
Energy Metabolism	Buccal-otic	4.54E-05***	0.334	0.222, 0.455
	Buccal-oropharyngeal	2.01E-06***	0.408	0.304, 0.532

Table 2.4 (cont'd)

Supplementary Figure 1: Box plots of dominant otic gand buccal enera in female vs male (*p*-value)				
	Non-divers		Divers	
Genus	Otic	Buccal	Otic	Buccal
Prevotella 7	0.708	0.777	0.703	0.359
Prevotella	0.354	0.335	0.140	0.682
Alloprevotella	0.828	0.245	0.584	0.748
Fusobacterium	0.909	0.688	0.918	0.484
Leptotrichia	0.137	0.495	0.993	0.468
Haemophilus	0.599	0.201	0.038*	0.181
Veillonella	0.619	0.046*	0.983	0.248
Streptococcus	0.194	0.951	0.319	0.463

Figure 2.9: Estimation plots comparing the dominant otic phyla (a) and genera (b) in non-divers vs divers [D-nD]			
Figure S2a:		Otic phyla	
Phylum	*p*-value	SMD	95%CIs
Bacteroidetes	0.2813	-5.772	-16.026, 3.61
Fusobacteria	0.0103*	-8.483	-13.412, -3.02
Proteobacteria	0.1925	8.926	-3.621, 21.14
Firmicutes	0.1388	5.39	-0.57, 12.521
Figure S2b:		Otic genera	
Genus	*p*-value	SMD	95%CIs
Prevotella 7	0.9554	0.0027	-0.0824, 0.0939
Prevotella	0.0838	-0.0588	-0.1193, 0.0002
Alloprevotella	0.0327*	-0.0374	-0.0665, -0.0008
Fusobacterium	0.0476*	-0.0675	-0.1258, -0.0130
Leptotrichia	0.7332	-0.0097	-0.0641, 0.0380
Haemophilus	0.8641	0.0054	-0.0615, 0.0499
Veillonella	0.3531	0.023	-0.0202, 0.0687
Streptococcus	0.0657	0.0323	0.0021, 0.0632

Table 2.4 (cont'd)

Figure 2.12: Pairwise comparison of mean relative proportions of predicted functions in non-divers vs divers (D-nD).						
	41 predicted functions			22 predicted functions		
Comparison	*p*-value	SMD	95%CIs	*p*-value	SMD	95%CIs
Otic	1	4.15E-10	-0.008, 0.012	0.984	1.9E-04	-0.013, 0.023
Oropharyngeal	1	5.61E-10	-0.038, 0.026	0.878	-0.005	-0.075, 0.042
Buccal	1	2.44E-10	-0.030, 0.056	0.949	0.003	-0.054, 0.107

Table 2.5: Phylogenetic (16S rRNA sequence identity) and phenotypic (hemolysis) characterization of otic, oropharyngeal and buccal cultivars.

Strain	Hemolysis	GenBank no.[1]		Reference Strain (Accession #; % identity)[2]
		27F	1492R	
Otic				
L0020-01	α	MH446998	---	*Staphylococcus hominis* subsp. *novobiosepticus* (NR_041323.1; 99.88%)
L0020-02	α	MH447036	MH447037	*Streptococcus parasanguinis* (NR_115241.1; 99.76%)
L0020-03	γ	MH447038	MH447039	*Streptococcus mitis* (NR_115732.1; 99.29%)
L0020-04	α	MH447042	MH447043	*Staphylococcus hominis subsp. novobiosepticus* (NR_041323.1; 99.65%)
L0020-05	γ	MH447028	---	*Micrococcus yunnanensis* (NR_116578.1; 98.0%)
L0020-06	γ	MH447030	MH447031	*Corynebacterium propinquum* (NR_037038.1; 99.89%)
L0021-01	α	MH447000	MH447001	*Streptococcus salivarius* (NR_042776.1; 99.76%)
L0021-02	β	MH447032	MH447033	*Staphylococcus aureus* (NR_115606.1; 100%)
L0021-04	α	MH447016	---	*Streptococcus salivarius* (NR_042776.1; 97.31%)
L0021-05	α	MH447018	---	*Streptococcus salivarius* (NR_042776.1; 97.67%)
L0021-06	γ	MH447044	MH447045	*Staphylococcus epidermidis* (NR_036904.1; 100%)
L0022-03	α	MH447020	---	*Streptococcus salivarius* (NR_042776.1; 97.57%)
L0022-04	α	MH447040	MH447041	*Streptococcus salivarius* (NR_042776.1; 97.53%)
L0022-05	α	MH447022	---	*Streptococcus salivarius* (NR_042776.1; 96.99%)
L0022-06	α	MH447024	---	*Streptococcus salivarius* (NR_042776.1; 98.02%)
L0023-01	β	MH447068	MH447069	*Neisseria perflava* (NR_117694.1; 99.76%)
L0023-02	α	MH447034	MH447035	*Streptococcus agalactiae* (NR_115728.1; 100%)
L0023-03	α	MH447026	---	*Streptococcus agalactiae* (NR_115728.1; 97.45%)

Table 2.5 (cont'd)

L0023-05	γ	MH463670	---	*Neisseria perflava* (NR_117694.1; 99.18%)
L0023-06	γ	MH463668	---	*Streptococcus agalactiae* (NR_115728.1; 99.88%)
Oropharyngeal				
C0020-01	γ	MH447046	MH447047	*Staphylococcus aureus* (NR_115606.1; 99.88%)
C0021-01	β	MH447012	---	*Staphylococcus aureus* (NR_115606.1; 100%)
C0021-02	α	MH447048	MH447049	*Streptococcus salivarius* (NR_042776.1; 100%)
C0021-04	α	MH447050	MH447051	*Streptococcus parasanguinis* (NR_115241.1; 98.24%)
C0022-01	α	MH447014	---	*Streptococcus salivarius* (NR_042776.1; 97.32%)
C0022-02	α	MH463669	---	*Streptococcus mitis* (NR_115732.1; 99.29%)
C0022-03	α	MH447052	MH447053	*Streptococcus salivarius* (NR_042776.1; 99.76%)
C0023-01	α	MH447054	MH447055	*Neisseria perflava* (NR_117694.1; 100%)
C0023-02	α	MH447056	MH447057	*Streptococcus salivarius* (NR_042776.1; 99.41%)
Buccal				
B0020-01	γ	MH447058	MH447059	*Neisseria perflava* (NR_117694.1; 100%)
B0020-02	γ	MH447060	MH447061	*Neisseria perflava* (NR_117694.1; 100%)
B0020-03	γ	MH447062	MH447063	*Staphylococcus aureus* (NR_115606.1; 100%)
B0021-01	β	MH447002	---	*Staphylococcus aureus* (NR_115606.1; 100%)
B0021-02	α	MH447064	MH447065	*Streptococcus mitis* (NR_115732.1; 99.76%)
B0021-03	α	MH447004	---	*Staphylococcus epidermidis* (NR_036904.1; 100%)
B0021-04	α	MH447006	---	*Streptococcus rubneri* (NR_109720.1; 99.06%)
B0023-01	α	MH447008	---	*Streptococcus salivarius* (NR_042776.1; 100%)
B0023-03	α	MH447066	MH447067	*Neisseria perflava* (NR_117694.1; 99.76%)
B0023-04	γ	MH447010	---	*Streptococcus rubneri* (NR_109720.1; 99.06%)

Table 2.5 (cont'd)

[1] Accession numbers of raw sequences obtained after amplification of the cultivar's 16S rRNA with universal 27F or 1492R primers.[2] Closest relative based on % identity of the cultivar's atrial 16S rRNA sequence (850-bp forward amplicon generated after 5' and 3' trimming). Sequences below the species cutoff of 98.65% identity are shaded in gray.

Figure 2.7: Gender distribution of most abundant genera in the otic and buccal communities. Statistically significant differences in the relative abundance of otic and buccal genera were assessed in pairwise comparisons with the *t*-test function of MS Excel (*, $p<0.05$). The calculated *p*-values are shown in Table 2.4.

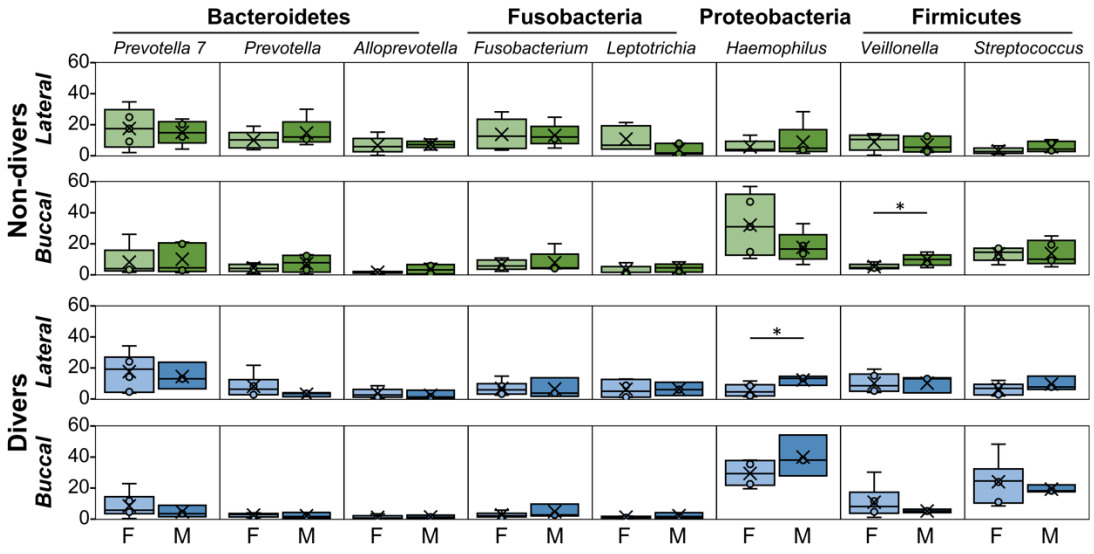

Figure 2.8: Relative abundance of dominant phyla (a) and genera (b) in the otic communities of non-divers and divers. The figures show the distribution of relative abundance values (*top*) and estimation plots (*bottom*) for dominant otic phyla (a) and genera (b) in non-divers (nD) and divers (D). Taxa names are color-coded for phyla (Bacteroidetes, blue; Fusobacteria, yellow; Proteobacteria, orange; Firmicutes, gray). The estimation plots show the mean difference (Δ, solid circle), the complete Δ distribution for divers (shaded curve), and 95% confidence interval of Δ (vertical line). The most significant differences in divers are highlighted in a shaded area. Statistic values used to assess significance of the data are shown Table 2.4.

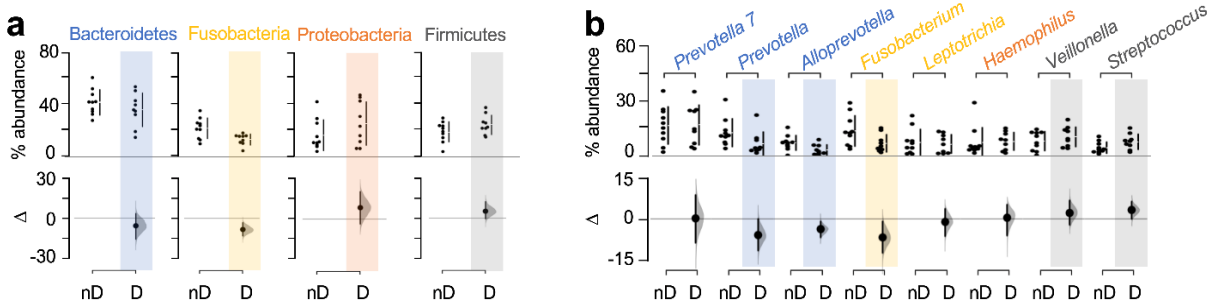

Figure 2.9: Oropharyngeal and/or buccal OTUs over-represented in the otic neutral model. List of OTUs with a relative abundance of >0.1% in the otic communities that fell above the upper bound of the confidence interval in the neutral model fit using the oropharyngeal or buccal communities as sources (as shown in Fig. 4c). The green circles show the relative abundance of the OTUs over-represented in the otic samples (shade of green is approximate, as in the gradient scale) compared to the source communities. Source communities with no circles are sites from which the OTU was neutrally distributed.

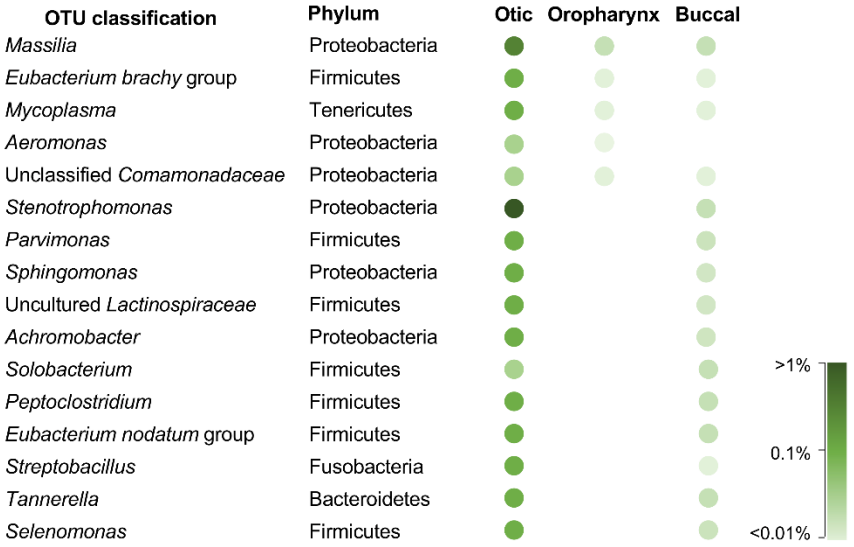

Figure 2.10: **Correlation between the relative abundances (%) of OTUs in otic and potential source (oropharyngeal and buccal) communities.** OTUs with more than 2-fold increases (green) or decreases (red) in otic relative abundance compared to the oropharyngeal communities are colored in both plots (R^2, Pearson's correlation coefficient).

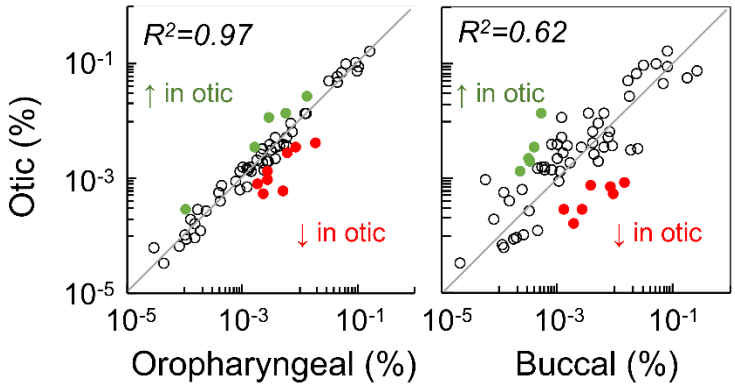

Figure 2.11: Core metabolic structure of the otic communities and neighboring oropharynx and buccal mucosae. Heatmap illustrates normalized relative proportions of 22 abundant functions (KO level 2) with >1% representation in all the samples collected from non-divers (nD) and divers (D). Pairwise comparison of predicted functions within each core functional module is shown in Figure 6.

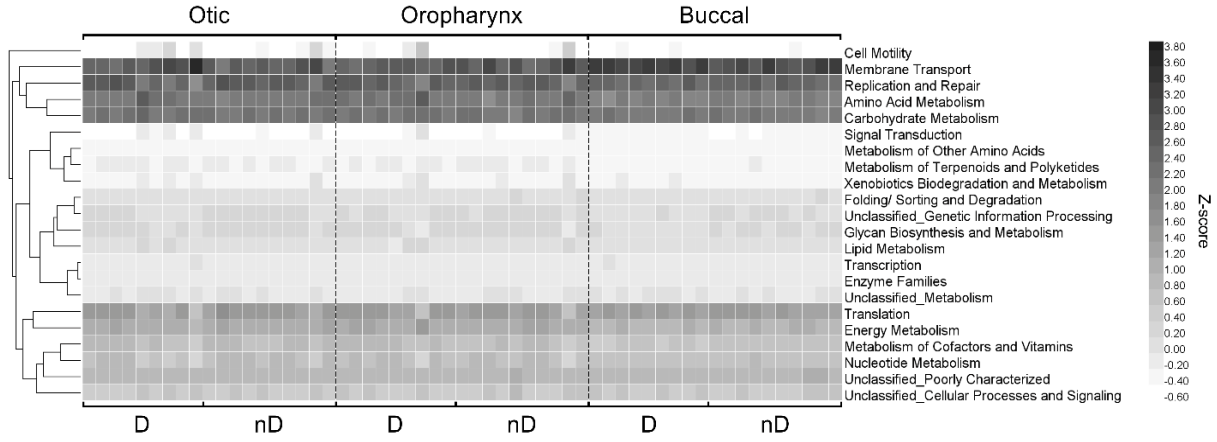

Figure 2.12: Metabolic structure of the otic, oropharyngeal or buccal communities of non-divers (nD; horizontal line) compared to divers (D). The lines connect the mean relative proportions of the 41 predicted functions and the most prevalent 22. The 6 multi-paired estimation plots at the bottom compare the mean relative portions of the 41 and 22 functions for each sample type (oral, oropharyngeal and buccal).

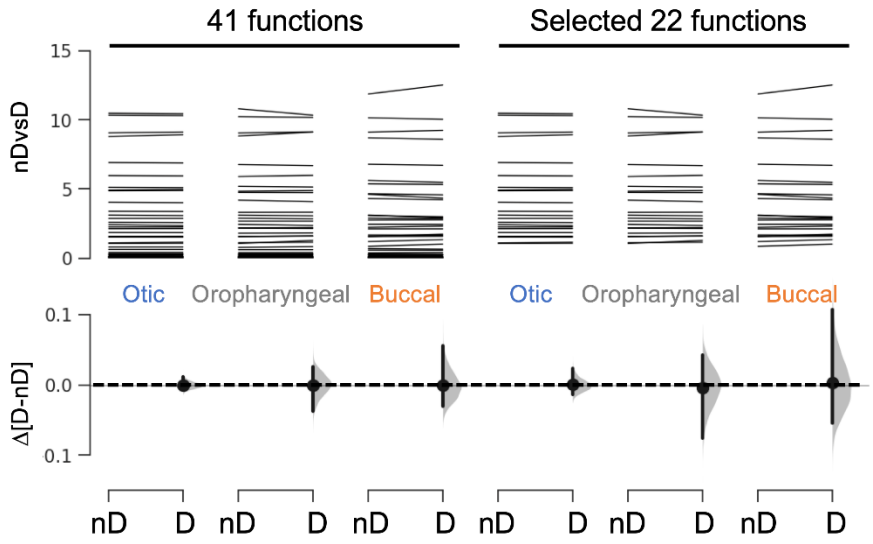

REFERENCES

REFERENCES

1. Dickson RP, Erb-Downward JR, Martinez FJ, Huffnagle GB (2016) The microbiome and the respiratory tract. Annual Review of Physiology 78 (1):481-504. doi:10.1146/annurev-physiol-021115-105238

2. Lim DJ, Chun YM, Lee HY, Moon SK, Chang KH, Li JD, Andalibi A (2001) Cell biology of tubotympanum in relation to pathogenesis of otitis media - a review. Vaccine 19:S17-25. doi:10.1016/s0264-410x(00)00273-5

3. Christensen-Dalsgaard J, Carr CE (2008) Evolution of a sensory novelty: Tympanic ears and the associated neural processing. Brain Res Bull 75 (2-4):365-370. doi:10.1016/j.brainresbull.2007.10.044

4. Keefe DH (2015) Acoustical transmission-line model of the middle-ear cavities and mastoid air cells. J Acoust Soc Am 137 (4):1877-1887. doi:10.1121/1.4916200

5. Bluestone CD (2005) The Eustachian Tube: Structure, function, and role in the middle ear. BC Decker Inc, Hamilton, Ontario

6. Manley GA (2010) An evolutionary perspective on middle ears. Hearing Res 263 (1-2):3-8. doi:10.1016/j.heares.2009.09.004

7. Honjo I, Hayashi M, Ito S, Takahashi H (1985) Pumping and clearance function of the eustachian tube. Am J Otolaryngol 6 (3):241-244. doi:10.1016/S0196-0709(85)80095-8

8. McGuire JF (2002) Surfactant in the middle ear and eustachian tube: a review. Int J Pediatr Otorhinolaryngol 66 (1):1-15. doi:10.1016/S0165-5876(02)00203-3

9. Lopez-Rodriguez E, Perez-Gil J (2014) Structure-function relationships in pulmonary surfactant membranes: from biophysics to therapy. Biochim Biophys Acta 1838 (6):1568-1585. doi:10.1016/j.bbamem.2014.01.028

10. Phelps DS (2001) Surfactant regulation of host defense function in the lung: a question of balance. Pediatr Pathol Mol Med 20 (4):269-292. doi:10.1080/15513810109168822

11. Wu H, Kuzmenko A, Wan S, Schaffer L, Weiss A, Fisher JH, Kim KS, McCormack FX (2003) Surfactant proteins A and D inhibit the growth of Gram-negative bacteria by increasing membrane permeability. J Clin Invest 111 (10):1589-1602. doi:10.1172/JCI16889

12. Sadler-Kimes D, Siegel MI, Todhunter JS (1989) Age-related morphologic differences in the components of the eustachian tube/middle ear system. Ann Otol Rhinol Laryngol 98 (11):854-858. doi:10.1177/000348948909801104

13. Proctor B (1973) Anatomy of the eustachian tube. Arch Otolaryngol 97 (1):2-8. doi:10.1001/archotol.1973.00780010006002

14. Hall-Stoodley L, Hu FZ, Gieseke A, Nistico L, Nguyen D, Hayes J, Forbes M, Greenberg DP, Dice B, Burrows A, Wackym PA, Stoodley P, Post JC, Ehrlich GD, Kerschner JE (2006) Direct detection of bacterial biofilms on the middle-ear mucosa of children with chronic otitis media. JAMA 296 (2):202-211. doi:10.1001/jama.296.2.202

15. Tonnaer EL, Mylanus EA, Mulder JJ, Curfs JH (2009) Detection of bacteria in healthy middle ears during cochlear implantation. Arch Otolaryngol Head Neck Surg 135 (3):232-237. doi:10.1001/archoto.2008.556

16. Minami SB, Mutai H, Suzuki T, Horii A, Oishi N, Wasano K, Katsura M, Tanaka F, Takiguchi T, Fujii M, Kaga K (2017) Microbiomes of the normal middle ear and ears with chronic otitis media. Laryngoscope 127 (10):E371-E377. doi:10.1002/lary.26579

17. Jervis-Bardy J, Leong LEX, Papanicolas LE, Ivey KL, Chawla S, Woods CM, Frauenfelder C, Ooi EH, Rogers GB (2019) Examining the evidence for an adult healthy middle ear microbiome. mSphere 4 (5). doi:10.1128/mSphere.00456-19

18. Luers JC, Huttenbrink KB (2016) Surgical anatomy and pathology of the middle ear. J Anat 228 (2):338-353. doi:10.1111/joa.12389

19. Nguyen CT, Jung W, Kim J, Chaney EJ, Novak M, Stewart CN, Boppart SA (2012) Noninvasive in vivo optical detection of biofilm in the human middle ear. Proc Natl Acad Sci USA 109 (24):9529-9534. doi:10.1073/pnas.1201592109

20. Frank DN, Spiegelman GB, Davis W, Wagner E, Lyons E, Pace NR (2003) Culture-independent molecular analysis of microbial constituents of the healthy human outer ear. J Clin Microbiol 41 (1):295-303. doi:10.1128/jcm.41.1.295-303.2003

21. Grice EA, Kong HH, Conlan S, Deming CB, Davis J, Young AC, Program NCS, Bouffard GG, Blakesley RW, Murray PR, Green ED, Turner ML, Segre JA (2009) Topographical and temporal diversity of the human skin microbiome. Science 324 (5931):1190-1192. doi:10.1126/science.1171700

22. Namin AW, Czerny MS, Antisdel JL (2015) Facial paresis secondary to an aggressive acute bacterial rhinosinusitis. JAMA Otolaryngol Head Neck Surg 141 (9):856-857. doi:10.1001/jamaoto.2015.1086

23. Liktor B, Szekanecz Z, Batta TJ, Sziklai I, Karosi T (2013) Perspectives of pharmacological treatment in otosclerosis. Eur Arch Otorhinolaryngol 270 (3):793-804. doi:10.1007/s00405-012-2126-0

24. Liu J, Li Y, Yuan X, Lin Z (2009) Bell's palsy may have relations to bacterial infection. Med Hypotheses 72 (2):169-170. doi:10.1016/j.mehy.2008.09.023

25. Sziklai I, Batta TJ, Karosi T (2009) Otosclerosis: an organ-specific inflammatory disease with sensorineural hearing loss. Eur Arch Otorhinolaryngol 266 (11):1711-1718. doi:10.1007/s00405-009-0967-y

26. Tetzlaff K, Thomas PS (2017) Short- and long-term effects of diving on pulmonary function. Eur Respir Rev 26 (143). doi:10.1183/16000617.0097-2016

27. Welch JLM, Dewhirst FE, Borisy GG (2019) Biogeography of the oral microbiome: The site-specialist hypothesis. Annu Rev Microbiol. doi:10.1146/annurev-micro-090817-062503

28. Haig SJ, Quince C, Davies RL, Dorea CC, Collins G (2015) The relationship between microbial community evenness and function in slow sand filters. mBio 6 (5):e00729-00715. doi:10.1128/mBio.00729-15

29. Gao L, Xu T, Huang G, Jiang S, Gu Y, Chen F (2018) Oral microbiomes: more and more importance in oral cavity and whole body. Protein Cell 9 (5):488-500. doi:10.1007/s13238-018-0548-1

30. Palmer RJ, Diaz PI, Kolenbrander PE (2006) Rapid succession within the *Veillonella* population of developing human oral biofilm in situ. J Bacteriol 188 (11):4117. doi:10.1128/JB.01958-05

31. Ravva SV, Sarreal CZ, Mandrell RE (2011) Bacterial communities in aerosols and manure samples from two different dairies in central and Sonoma valleys of California. PloS one 6 (2):e17281. doi:10.1371/journal.pone.0017281

32. Murphy EC, Frick IM (2013) Gram-positive anaerobic cocci--commensals and opportunistic pathogens. FEMS Microbiol Rev 37 (4):520-553. doi:10.1111/1574-6976.12005

33. Holdeman LV, Cato EP, Burmeister JA, Moore WEC (1980) Descriptions of *Eubacterium timidum* sp. nov., *Eubacterium brachy* sp. nov., and *Eubacterium nodatum* sp. nov. isolated from human periodontitis. Int J Syst Evol Microbiol 30 (1):163-169. doi:10.1099/00207713-30-1-163

34. Eisenberg T, Fawzy A, Nicklas W, Semmler T, Ewers C (2016) Phylogenetic and comparative genomics of the family Leptotrichiaceae and introduction of a novel fingerprinting MLVA for *Streptobacillus moniliformis*. BMC Genomics 17 (1):864. doi:10.1186/s12864-016-3206-0

35. Sloan WT, Lunn M, Woodcock S, Head IM, Nee S, Curtis TP (2006) Quantifying the roles of immigration and chance in shaping prokaryote community structure. Environ Microbiol 8 (4):732-740. doi:10.1111/j.1462-2920.2005.00956.x

36. Venkataraman A, Bassis CM, Beck JM, Young VB, Curtis JL, Huffnagle GB, Schmidt TM (2015) Application of a neutral community model to assess structuring of the human lung microbiome. mBio 6 (1). doi:10.1128/mBio.02284-14

37. Liu G, Tang CM, Exley RM (2015) Non-pathogenic *Neisseria*: members of an abundant, multi-habitat, diverse genus. Microbiology 161 (7):1297-1312. doi:10.1099/mic.0.000086

38. Bassis CM, Erb-Downward JR, Dickson RP, Freeman CM, Schmidt TM, Young VB, Beck JM, Curtis JL, Huffnagle GB (2015) Analysis of the upper respiratory tract microbiotas as

the source of the lung and gastric microbiotas in healthy individuals. mBio 6 (2):e00037-00015. doi:10.1128/mBio.00037-15

39. Stackebrandt E, Ebers J (2006) Taxonomic parameters revisited: tarnished gold standards. Microbiol Today 33 (4):152–155

40. Munoz R, Yarza P, Ludwig W, Euzeby J, Amann R, Schleifer KH, Glockner FO, Rossello-Mora R (2011) Release LTPs104 of the All-Species Living Tree. Syst Appl Microbiol 34 (3):169-170. doi:10.1016/j.syapm.2011.03.001

41. Yarza P, Richter M, Peplies J, Euzeby J, Amann R, Schleifer KH, Ludwig W, Glockner FO, Rossello-Mora R (2008) The All-Species Living Tree project: A 16S rRNA-based phylogenetic tree of all sequenced type strains. Syst Appl Microbiol 31 (4):241-250. doi:10.1016/j.syapm.2008.07.001

42. Facklam R (2002) What happened to the streptococci: Overview of taxonomic and nomenclature changes. Clin Microbiol Rev 15 (4):613-+. doi:10.1128/Cmr.15.4.613-630.2002

43. Huch M, De Bruyne K, Cleenwerck I, Bub A, Cho GS, Watzl B, Snauwaert I, Franz CM, Vandamme P (2013) *Streptococcus* rubneri sp. nov., isolated from the human throat. Int J Syst Evol Microbiol 63 (Pt 11):4026-4032. doi:10.1099/ijs.0.048538-0

44. Rossi-Tamisier M, Benamar S, Raoult D, Fournier PE (2015) Cautionary tale of using 16S rRNA gene sequence similarity values in identification of human-associated bacterial species. Int J Syst Evol Microbiol 65:1929-1934. doi:10.1099/ijs.0.000161

45. Ruoff KL (2002) Miscellaneous catalase-negative, gram-positive cocci: emerging opportunists. J Clin Microbiol 40 (4):1129-1133. doi:10.1128/jcm.40.4.1129-1133.2002

46. Tsao RY, Lutwick L (2017) Non-hemolytic group B *Streptococcus* as a cause of chemotherapy port infection. IDCases 10:53-54. doi:10.1016/j.idcr.2017.08.007

47. Bomar L, Brugger SD, Lemon KP (2018) Bacterial microbiota of the nasal passages across the span of human life. Curr Opin Microbiol 41:8-14. doi:10.1016/j.mib.2017.10.023

48. Ohara-Nemoto Y, Haraga H, Kimura S, Nemoto TK (2008) Occurrence of staphylococci in the oral cavities of healthy adults and nasal oral trafficking of the bacteria. J Med Microbiol 57 (Pt 1):95-99. doi:10.1099/jmm.0.47561-0

49. McCormack MG, Smith AJ, Akram AN, Jackson M, Robertson D, Edwards G (2015) *Staphylococcus aureus* and the oral cavity: an overlooked source of carriage and infection? Am J Infect Control 43 (1):35-37. doi:10.1016/j.ajic.2014.09.015

50. Koskinen K, Reichert JL, Hoier S, Schachenreiter J, Duller S, Moissl-Eichinger C, Schopf V (2018) The nasal microbiome mirrors and potentially shapes olfactory function. Sci Rep 8 (1):1296. doi:10.1038/s41598-018-19438-3

51. Reddy MS, Murphy TF, Faden HS, Bernstein JM (1997) Middle ear mucin glycoprotein: Purification and interaction with nontypable *Haemophilus influenzae* and Moraxella catarrhalis. Otolaryngol Head Neck Surg 116 (2):175-180. doi:10.1016/S0194-59989770321-8

52. Huffnagle GB, Dickson RP, Lukacs NW (2017) The respiratory tract microbiome and lung inflammation: a two-way street. Mucosal Immunol 10 (2):299-306. doi:10.1038/mi.2016.108

53. Silva VL, Carvalho MA, Nicoli JR, Farias LM (2003) Aerotolerance of human clinical isolates of Prevotella spp. J Appl Microbiol 94 (4):701-707. doi:10.1046/j.1365-2672.2003.01902.x

54. Eckburg PB, Bik EM, Bernstein CN, Purdom E, Dethlefsen L, Sargent M, Gill SR, Nelson KE, Relman DA (2005) Diversity of the human intestinal microbial flora. Science 308 (5728):1635-1638. doi:10.1126/science.1110591

55. Tailford LE, Crost EH, Kavanaugh D, Juge N (2015) Mucin glycan foraging in the human gut microbiome. Front Genet 6:81. doi:10.3389/fgene.2015.00081

56. Cotter PD, Hill C (2003) Surviving the acid test: responses of gram-positive bacteria to low pH. Microbiol Mol Biol Rev 67 (3):429-453. doi:10.1128/mmbr.67.3.429-453.2003

57. Delwiche EA, Pestka JJ, Tortorello ML (1985) The *Veillonella*e: gram-negative cocci with a unique physiology. Annu Rev Microbiol 39:175-193. doi:10.1146/annurev.mi.39.100185.001135

58. Rios-Covian D, Salazar N, Gueimonde M, de los Reyes-Gavilan CG (2017) Shaping the metabolism of intestinal Bacteroides population through diet to improve human health. Front Microbiol 8. doi:10.3389/fmicb.2017.00376

59. Proctor DM, Shelef KM, Gonzalez A, Davis CL, Dethlefsen L, Burns AR, Loomer PM, Armitage GC, Ryder MI, Millman ME, Knight R, Holmes SP, Relman DA (2020) Microbial biogeography and ecology of the mouth and implications for periodontal diseases. Periodontol 2000 82 (1):26-41. doi:10.1111/prd.12268

60. Cinamon U (2004) Passive and dynamic properties of the eustachian tube: quantitative studies in a model. Otol Neurotol 25 (6):1031-1033. doi:10.1097/00129492-200411000-00030

61. Dickson RP, Erb-Downward JR, Huffnagle GB (2014) Towards an ecology of the lung: new conceptual models of pulmonary microbiology and pneumonia pathogenesis. Lancet Respir Med 2 (3):238-246. doi:10.1016/S2213-2600(14)70028-1

62. MacArthur RH, Wilson EO (1963) An equilibrium theory of insular zoogeography. Evolution 17 (4):373-387. doi:10.2307/2407089

63. Yeung AT, Parayno A, Hancock RE (2012) Mucin promotes rapid surface motility in Pseudomonas aeruginosa. mBio 3 (3). doi:10.1128/mBio.00073-12

64. Xu J, Platt TG, Fuqua C (2012) Regulatory linkages between flagella and surfactant during swarming behavior: lubricating the flagellar propeller? J Bacteriol 194 (6):1283-1286. doi:10.1128/JB.00019-12

65. Sade J (1971) Mucociliary flow in the middle ear. Ann Otol Rhinol Laryngol 80 (3):336-341. doi:10.1177/000348947108000306

66. Jonson B, Rundcrantz H (1969) Posture and pressure within the internal jugular vein. Acta Otolaryngol 68 (3):271-275. doi:10.3109/00016486909121565

67. Leclerc JE, Doyle WJ, Karnavas W (1987) Physiological modulation of eustachian tube function. Acta Otolaryngol 104 (5-6):500-510

68. Ingelstedt S, Ivarsson, Jonson B (1967) Mechanics of the human middle ear: Pressure regulation in aviation and diving, a non-traumatic method. Acta Otolaryngol 228:1-58

69. Kozich JJ, Westcott SL, Baxter NT, Highlander SK, Schloss PD (2013) Development of a dual-index sequencing strategy and curation pipeline for analyzing amplicon sequence data on the MiSeq Illumina sequencing platform. Appl Environ Microbiol 79 (17):5112-5120. doi:10.1128/AEM.01043-13

70. Edgar RC (2018) Updating the 97% identity threshold for 16S ribosomal RNA OTUs. Bioinformatics. doi:10.1093/bioinformatics/bty113

71. Edgar RC (2013) UPARSE: highly accurate OTU sequences from microbial amplicon reads. Nat Methods 10 (10):996-998. doi:10.1038/nmeth.2604

72. Quast C, Pruesse E, Yilmaz P, Gerken J, Schweer T, Yarza P, Peplies J, Glockner FO (2013) The SILVA ribosomal RNA gene database project: improved data processing and web-based tools. Nucleic Acids Res 41 (Database issue):D590-596. doi:10.1093/nar/gks1219

73. Lee SH, Sorensen JW, Grady KL, Tobin TC, Shade A (2017) Divergent extremes but convergent recovery of bacterial and archaeal soil communities to an ongoing subterranean coal mine fire. ISME J 11 (6):1447-1459. doi:10.1038/ismej.2017.1

74. Rideout JR, He Y, Navas-Molina JA, Walters WA, Ursell LK, Gibbons SM, Chase J, McDonald D, Gonzalez A, Robbins-Pianka A, Clemente JC, Gilbert JA, Huse SM, Zhou HW, Knight R, Caporaso JG (2014) Subsampled open-reference clustering creates consistent, comprehensive OTU definitions and scales to billions of sequences. PeerJ 2:e545. doi:10.7717/peerj.545

75. Caporaso JG, Kuczynski J, Stombaugh J, Bittinger K, Bushman FD, Costello EK, Fierer N, Pena AG, Goodrich JK, Gordon JI, Huttley GA, Kelley ST, Knights D, Koenig JE, Ley RE, Lozupone CA, McDonald D, Muegge BD, Pirrung M, Reeder J, Sevinsky JR, Turnbaugh

PJ, Walters WA, Widmann J, Yatsunenko T, Zaneveld J, Knight R (2010) QIIME allows analysis of high-throughput community sequencing data. Nat Methods 7 (5):335-336. doi:10.1038/nmeth.f.303

76. Lozupone C, Knight R (2005) UniFrac: a new phylogenetic method for comparing microbial communities. Appl Environ Microbiol 71 (12):8228-8235. doi:10.1128/AEM.71.12.8228-8235.2005

77. Heberle H, Meirelles GV, da Silva FR, Telles GP, Minghim R (2015) InteractiVenn: a web-based tool for the analysis of sets through Venn diagrams. BMC Bioinformatics 16:169. doi:10.1186/s12859-015-0611-3

78. Claridge-Chang A, Assam PN (2016) Estimation statistics should replace significance testing. Nat Methods 13 (2):108-109. doi:10.1038/nmeth.3729

79. Ho J, Tumkaya T, Aryal S, Choi H, Claridge-Chang A (2019) Moving beyond P values: data analysis with estimation graphics. Nat Methods 16 (7):565-566. doi:10.1038/s41592-019-0470-3

80. Langille MGI, Zaneveld J, Caporaso JG, McDonald D, Knights D, Reyes JA, Clemente JC, Burkepile DE, Vega Thurber RL, Knight R, Beiko RG, Huttenhower C (2013) Predictive functional profiling of microbial communities using 16S rRNA marker gene sequences. Nature Biotechnol 31:814. doi:10.1038/nbt.2676

81. Kanehisa M, Goto S, Sato Y, Furumichi M, Tanabe M (2011) KEGG for integration and interpretation of large-scale molecular data sets. Nucleic Acids Res 40 (D1):D109-D114. doi:10.1093/nar/gkr988

82. Weber N, Liou D, Dommer J, MacMenamin P, Quiñones M, Misner I, Oler AJ, Wan J, Kim L, Coakley McCarthy M, Ezeji S, Noble K, Hurt DE (2017) Nephele: a cloud platform for simplified, standardized and reproducible microbiome data analysis. Bioinformatics 34 (8):1411-1413. doi:10.1093/bioinformatics/btx617

83. Deng W, Wang Y, Liu Z, Cheng H, Xue Y (2014) HemI: a toolkit for illustrating heatmaps. PloS one 9 (11):e111988. doi:10.1371/journal.pone.0111988

84. Lane DJ (1991) 16S/23S rRNA sequencing. In: Stackebrandt E, Goodfellow M (eds) Nucleic acid techniques in bacterial systematics. John Wiley & Sons, New York, pp 115-175. doi:10.1002/jobm.3620310616

85. Kim M, Oh HS, Park SC, Chun J (2014) Towards a taxonomic coherence between average nucleotide identity and 16S rRNA gene sequence similarity for species demarcation of prokaryotes. Int J Syst Evol Microbiol 64 (2):346-351. doi:10.1099/ijs.0.059774-0

86. Edgar RC (2004) MUSCLE: a multiple sequence alignment method with reduced time and space complexity. BMC Bioinformatics 5:113. doi:10.1186/1471-2105-5-113

87. Edgar RC (2004) MUSCLE: multiple sequence alignment with high accuracy and high throughput. Nucleic Acids Res 32 (5):1792-1797. doi:10.1093/nar/gkh340

88. Kumar S, Stecher G, Li M, Knyaz C, Tamura K (2018) MEGA X: Molecular Evolutionary Genetics Analysis across computing platforms. Mol Biol Evol 35 (6):1547-1549. doi:10.1093/molbev/msy096

CHAPTER 3

COMPETATIVE ADVANTAGE OF ORAL STREPTOCOCCI FOR COLONIZATION OF THE MIDDLE EAR MUCOSA

PUBLICATION NOTICE

The following chapter was published in "*Jacob, K. and Reguera, G. 2022. Competitive advantage of oral streptococci for colonization of the middle ear. Biofilm. 100067* https://doi.org/10.1016/j.bioflm.2022.100067" and reprint permission was granted for use in this dissertation.

ABSTRACT

The identification of a diverse microbiome in otic secretions from healthy young adults challenged the entrenched dogma of middle ear sterility and underscored previously unknown roles for oral commensals in the seeding of otic biofilms. We gained insights into the selective forces that enrich for specific groups of oral migrants in the middle ear mucosa by investigating the phylogeny and physiology of 19 strains isolated previously from otic secretions and representing otic commensals (*Streptococcus*) or transient migrants (*Staphylococcus*, *Neisseria* and actinobacterial *Micrococcus* and *Corynebacterium*). Phylogenetic analyses of full length 16S rRNA sequences recovered from partially sequenced genomes resolved close relationships between the isolates and oral commensals. Physiological functions that facilitate mucosal colonization (swarming motility, surfactant production) and nutrition (mucin and protein degradation) were also widespread among the cultivars, as was their ability to grow in the presence or absence of oxygen. Yet, streptococci stood out for their enhanced biofilm-forming abilities under oxic and anoxic conditions and ability to ferment host-derived mucosal substrates into lactate, a key metabolic intermediate in the otic trophic webs. Additionally, the otic streptococci inhibited the growth of common otopathogens, an antagonistic interaction that could exclude competitors and protect the middle ear mucosa from infections. These adaptive traits allow streptococcal migrants to colonize the otic mucosa and grow microcolonies with syntrophic anaerobic partners, establishing trophic interactions with other commensals that mirror those formed by the oral ancestors in buccal biofilms.

INTRODUCTION

The oral cavity provides a heterogenous landscape of surfaces and microenvironments (teeth, gingiva, tongue, cheek, hard and soft palate, etc.) for the growth of microbial communities [17]. The availability of dietary substrates supports the growth and diversification of oral commensals and makes these communities some of the richest and most diverse in the human body [18]. Many of these microbes readily disperse via saliva and saliva aerosols into perioral regions [17] and, from there, to other parts of the aerodigestive tract [19]. The saliva aerosols also enter the middle ear when the tubal extension of the tympanic cavity (the tympanic or Eustachian tube, Fig. 3.1) opens [20]. The tube is passively collapsed at rest to sound proof the tympanic cavity and minimize microbial entry, yet it opens when we swallow or yawn to draw in air from the lower airways (Fig. 3.1) [20]. The cycles of aperture and collapse of the Eustachian tube promote the intermittent aeration of the tympanic cavity, relieve negative pressure across the eardrum and drain into the nasopharynx excess mucus and fluids [20].

The episodic ventilation of the middle ear reduces oxygen availability to the otic mucosa and establishes redox conditions that favor the growth of anaerobes [21]. In support of this, strict anaerobic genera in the Bacteroidetes (*Prevotella* and *Alloprevotella*), Fusobacteria (*Fusobacterium* and *Leptotrichia*) and Firmicutes (*Veillonella*) are more abundant in otic secretions collected at the nasopharyngeal orifice of the Eustachian tube than in oral samples [21]. The genus *Streptococcus*, which includes mostly facultative anaerobes [22], is also enriched in otic secretions [21]. The co-enrichment of streptococci with Bacteroidetes and *Veillonella* spp. in otic secretions suggests that these groups are part of syntrophic consortia (Fig. 3.1) similar to those described in oral biofilms [21]. This model (Fig. 3.1) is based on the metabolic co-dependency of Bacteroidetes to break down mucin glycoproteins and other mucosal proteins into sugars and

peptides, which some streptococci ferment into lactate [23] to sustain propionate and acetate production by *Veillonella* [24, 25]. The lactate dependency of *Veillonella* spp. may also favor direct metabolic interactions with lactate producing Bacteroidetes partners [26]. Through their collective activities, Bacteroidetes, streptococci and *Veillonella* are predicted to degrade and ferment host-derived nutrients (mucins and proteins) into short chain fatty acids that contribute to mucosal health in other body sites [27].

Although oral-like consortia are predicted to colonize the middle ear in health [21], the physiological traits that facilitate mucosal colonization remain largely unknown. The presence of bacterial microcolonies in biopsy specimens of the mucosal lining of the tympanic cavity [28, 29] points at biofilm formation as a critical selective factor for the growth of otic commensals. Microcolonies protect mucosal colonizers against immunoattack and clearance [30]. The latter is particularly vigorous closer and within the Eustachian tube, due to the higher density of cilial cells in these regions and the pumping force exerted by the periodic contraction and relaxation of muscles around the Eustachian tube (muscular clearance) [31, 32]. Additionally, microcolonies protect anaerobic commensals from oxygen intrusions when the Eustachian tube opens [20]. The aggregative nature of many oral streptococci is expected to facilitate firm attachment of colonizers to the otic epithelium and the formation of microcolonies with anoxic niches for anaerobic syntrophic partners [33]. To test this, we investigated the colonization potential of streptococcal commensals and transient migrants (*Staphylococcus, Neisseria* and actinobacterial *Micrococcus* and *Corynebacterium*) previously recovered from otic secretions [21]. Streptococcal and staphylococcal species are, for example, among the most prominent members in the oral and nasal microbiomes, respectively [9, 19]. Both groups disperse in the aerodigestive tract and enter the middle ear during the intermittent openings of the Eustachian tube. Yet, while streptococci are

abundant in otic secretions from healthy individuals, staphylococcal-like sequences are seldom detected [21]. This suggests that streptococcal migrants have a competitive advantage over the transient staphylococcal species during the colonization of the middle ear mucosa. Hence, we sequenced and partially assembled the genomes of otic streptococcal and non-streptococcal cultivars (19 in all) [21] and used the full length 16S rRNA sequences to identify their closest relatives. We then screened the cultivars for adaptive traits predicted to be important for mucosal colonization (e.g., motility in mucus, microcolony formation) and for growth under conditions (redox, nutritional) relevant to the middle ear microenvironment. Our study revealed similar adaptive traits for mucosal growth by the isolates but aggregative and metabolic properties of streptococci critical for successful colonization of the middle ear mucosa. These same properties are retained from their closest oral ancestors, with whom they share the ability to establish trophic webs with anaerobes and antagonize competitors. These findings provide novel insights into the adaptive responses that sustain the growth and functionality of otic communities and influence the outcome of infections.

MATERIALS AND METHODS

Bacterial strains and culture conditions

The bacterial strains used in this study include 19 cultivars isolated from otic secretions [44]. Briefly, the samples were collected with a single swab from the left and right nasopharyngeal openings of the Eustachian tube in 4 young (19-32 years old), healthy adults recruited as part of a larger study approved by the Michigan State University Biomedical and Physical Health Review Board (IRB # 17-502). The cultivars were isolated as single colonies on Tryptic Soy Agar (TSA) plates (30g/L of Tryptic Soy Broth from Sigma Aldrich and 15g/L of Bacto Agar from BD) grown at 37oC. The isolates were routinely grown overnight in 5 ml of

Tryptic Soy Broth (TSB) at 37ºC with gentle agitation. For growth studies, we transferred mid-log phase (OD600 ~0.5) TSB cultures twice (initial OD600 of 0.1) to prepare a stationary phase (~0.9-1.0 OD600) inoculum for growth assays in Corning® 96-well clear round bottom TC-treated microplate (Corning 3799). Growth was initiated with the addition of 18 µl of the inoculum to 162 µl of TSB per well and monitored spectrophotometrically every 30 min (OD630 readings after 0.1 sec of gentle agitation) while incubating the plates at 37°C inside a PowerWave HT (BioTek) plate reader. Each microtiter plate contained a control well with TSB medium (no cells) to use as a blank. To test for growth in anoxic medium, we introduced the inoculated plates in an 855-ABC Portable Anaerobic Chamber (Plas Labs, Inc.) containing a headspace of N2:CO2 (80:20), removed the lid several times to disperse the air, and allowed the media to equilibrate in the anoxic atmosphere for 10 min. We then placed the plate in the plate reader (PowerWave HT, BioTek) housed inside the anaerobic chamber. Microplate OD readings were every 30 min after 0.1 sec of agitation. We used the ANOVA (Analysis of Variance) test in the Microsoft Excel® software to determine the significance of the difference between the means of aerobic and anaerobic growth (generation times) for each taxonomic group.

Eligible participants (*n*=23) were asked to rinse their mouth with a sterile saline solution to remove food debris and to follow a series of deep inhalation and yawn cycles that forced the opening the tympanic tube (they had to hear a "pop") and the drainage of the middle ear fluids. They were then asked to swallow to naturally open the ET one more time and to open their mouth to initiate sample collection. We used a sterile tongue depressor to improve access to the back of the mouth and prevent oral and/or tonsil contamination. Sample collection was with FLOQSwabs™ (Copan) and storage was in collection tubes filled with eNAT™ (DNA sequencing; 19 participants) or ESwab™ (cultivation; 4 participants) collection tubes (Copan).

We first collected in a single swab the left and right otic secretions, using an ascending motion to swab the mucosal channels that laterally drain the otic fluids behind the palatopharyngeal arch. The physician then used separate swabs to collect control samples from the central region of the oropharynx and from the inner lining of the cheeks and upper gingiva and palate (buccal samples). To preserve the anonymity of the participants, we barcoded the swab samples and all the forms and questionnaire collected for each individual. All samples were stored in the collection tubes at 4^{o}C for 8-24 h before transport to the lab for immediate processing.

DNA sequencing and phylogenetic analyses

For taxonomic and phylogenetic analyses, we grew 19 otic isolates (Table 3.1) in 2 ml of TSB at 37°C for 24 h and harvested the cells by centrifugation (25,000 x g for 5 min) in an Eppendorf 5417R refrigerated centrifuge prior to extracting the genomic DNA with a FastDNATM Spin kit (MP Biomedicals). Library preparation with an Illumina Nextera kit and whole genome sequencing in an Illumina NextSeq 550 platform were at the Microbial Genome Sequencing Center (MiGS; Pittsburgh, PA). We used the FastQC tool from the Babraham Institute (https://www.bioinformatics.babraham.ac.uk/projects/fastqc/) for sequence quality control and Trimmomatics [7] for cleaning/trimming of the Illumina short reads. After assembling the genomes de novo with the Spades assembler [1], we identified the 16S rRNA gene sequences in the contigs with the BAsic Rapid Ribosomal RNA Predictor (Barnap) (https://github.com/tseemann/barrnap). The 16S rRNA gene sequences were deposited in the GenBank database under individual accession numbers (Table 3.1). We used the full-length 16S rRNA sequences to identify the closest species (% identity) in the GenBank database using the nucleotide Basic Local Alignment Search Tool (BLAST) at the U.S. National Center of Biological Information (NCBI) using a species identity cutoff value of 98.7% [70]. We retrieved

the 16S rRNA gene sequences from the closest type strains listed in the SILVA rRNA database (https://www.arb-silva.de) and aligned them to the otic sequences with the MUSCLE program in the MEGA X software [43]. We used the alignment to build a maximum-likelihood phylogenetic tree and calculate bootstrap confidence values for each node using 1,000 replications. The tree shows bootstrap values above 50% [27].

Catalase assay

Frozen stocks of the otic isolates were directly streaked on 1.5% (w/v) TSA plates to grow individual colonies at 37oC overnight. We spread each colony onto a microscope slide and added a drop of freshly prepared 3% hydrogen peroxide. Catalase-positive strains breakdown the hydrogen peroxide into water and oxygen gas, which generates bubbles. Lack or weak production of bubbles is used to designate a strain as catalase negative.

Swarming motility and surfactant detection assays

We screened each otic isolate for their ability to move on soft (0.5% and, when indicated, 0.4% w/v agar) TSA plates, as a modification of a previously described assay [57]. For these assays, we first grew each isolate and the positive control (*P. aeruginosa* PA01) in TSB at 37oC overnight (OD600 ~1) and prepared a diluted TSB inoculum (OD600 0.1). We pipetted a 5-µl drop of the diluted culture onto the surface of the soft agar plates and allowed it to absorb until completely dry (~30 min). We then incubated the plates at 37˚C and photographed the areas of growth at 18, 42 and 62 h against a ruler using a dissecting scope (Leica MZ6) at a magnification of 0.8X and 1X. The photographs were then analyzed with the ImageJ software [66] to measure the colony diameter over time and calculate the area expansion (swarming distance) from the initial inoculation spot.

We also screened the ability of the otic isolates to produce surfactants with a previously described atomized oil assay [10]. For this, we plated a 5-µl drop of the diluted TSB culture (OD600 of 0.1) on agar-solidified (1.5% w/v) TSA medium, allowed the inoculum to absorb for ~30 min, and incubated the plates at 37°C for 24 h. Using an airbrush (type H; Paasche Airbrush Co., Chicago, IL), we applied a fine mist of mineral oil onto the plate surface. Surfactant-producing colonies readily display a halo of mineral oil dispersal whose size provides a semiquantitative measure of surfactant secretion [10]. Photography and halo diameter visualization was as described above for swarming assays, except that we measured the size of the oil dispersal zone from the colony edge. All strains were tested in three independent swarming and surfactant assays plates to calculate the average and standard deviation values.

Protease and mucinase plate assays

We used TSA plates containing 5% lactose-free, skim milk (Fairlife, LLC) or 0.5% Type II porcine gastric mucin (Sigma Aldrich) to screen the otic isolates for mucinase and protease secretion, respectively, using *P. aeruginosa* PA01 as a positive control. For these assays, we spot-plated 5 µl of overnight TSB cultures and incubated at 37oC for 24 h, as described earlier for the surfactant assays. Strains that secrete proteases to the medium degrade the milk's casein and produce a clear halo around the area of growth after 24 h of incubation. Mucinase producers have zones of mucin lysis around or under the colony that show as zones of discoloration after staining with 7ml of 0.1% amido black for 30 min and destaining with 14 ml of 2.5 M acetic acid for 30 min. When indicated, plates were incubated for 48 h to confirm emerging phenotypes. Each strain was tested in triplicate and photographed on a lightboard (A4 LED Light Box 9x12 Inch Light Pad, ME456) with an iPhone 11 at 2.4x magnification.

Organic acid detection in culture supernatant fluids

We grew triplicate stationary phase cultures of the otic isolates in oxic and anoxic TSB medium at 37oC and harvested the culture supernatant fluids by centrifugation (14,000 rpm, 10 min). We measured the pH of the supernatant fluids (5 ml) with a pH probe (Thermo ScientificTM OrionTM 720A+ benchtop pH meter) and stored 1 ml of the samples at –20^{o}C for chemical analyses by high performance liquid chromatography (HPLC). Once thawed, we filter-sterilized 250 µl of the supernatant fluid into 1-ml HPLC vials and measured their organic acid content in a Shimadzu 20A HPLC equipped with an Aminex HPX-87H column and a Micro-Guard cation H+ guard column (Bio-Rad, Hercules, CA) at 55°C, as previously described [20]. As controls, we included samples with TSB medium and standard solutions of acetate, lactate, and pyruvate (provided at 1, 2, 5, 10 or 20 mM).

Biofilm assays

We used a previously described assay [50] to test the ability of the otic cultivars to form biofilms in Corning® 96-well clear round bottom TC-treated microplates (Corning 3799). We first grew overnight cultures in TSB with gentle agitation (~200 rpm) and used them to prepare a diluted cell suspension (OD600 ~0.1) for inoculation (18 µl) into TSB medium (162 µl per well). Each isolate was tested in 8 replicate wells. After incubating the plates at 37°C for 24 h, we removed the planktonic culture, washed the wells with ddH2O and stained the surface-attached cells with 0.1% (w/v) crystal violet. We then rinsed the wells with water and let the stained biofilms to dry overnight at room temperature before solubilizing the biofilm-associated crystal violet with 180 µl of 30% glacial acetic acid and measured the crystal violet in the solution spectrophotometrically at 550 nm [50]. Correlations between aerobic biofilm formation and culture acidification were statistically analyzed and visualized with the K-mean clustering R

functions (https://www.rdocumentation.org/packages/stats/versions/3.6.2/topics/kmeans) available in the RStudio software (version 4.0.4). Clustering visualization in R-Studio by plotting k-mean cluster results against desired averaged datasets (oxic-anoxic biofilm formation, aerobic pH, or aerobic doubling time).

Growth inhibition plate assays

We screened the otic streptococcal isolates for their ability to inhibit the growth of bacterial species (*S. pneumoniae, M. catarrhalis,* and *non-typeable H influenzae*) commonly associated with infections of the middle ear [64]. As test strains, we used *S. pneumoniae* ATCC 6303 and *M. catarrhalis* ATCC 25238 (from the laboratory strain collection of Dr. Martha Mulks, Department of Microbiology and Molecular Genetics, Michigan State University) and a non-typeable *H. influenzae* (NTHi) strain isolated by Dr. Poorna Viswanathan in the teaching lab of the Department of Microbiology and Molecular Genetics (Michigan State University). The NTHi strain was confirmed prior to experimental use by multiplex PCR confirmation, as described previously [81]. We also included for testing the laboratory strain *S. aureus* JE2, which was kindly provided by Dr. Neal Hammer (Department of Microbiology and Molecular Genetics, Michigan State University). The otic streptococci and *S. aureus* JE2 were routinely grown in 5 ml TSB at 37°C with gentle agitation to prepare overnight cultures for the plate assays. *S. pneumoniae* and *M. catarrhalis* were grown at 37°C overnight in 5 mL of brain heart infusion (BHI) broth (Sigma-Aldrich) without agitation. The NTHi reference strain of *H. influenzae* was also grown statically at 37°C but in supplemented BHI (sBHI) [55], which contains (per L): 30 g BHI, 0.01 mg hemin (Bovine, Sigma Aldrich), and 0.002 mg β-Nicotinamide adenine dinucleotide sodium salt (Sigma Aldrich). All incubations were in a 37oC incubator with a 5% CO2 atmosphere except for *S. aureus*, which were in air.

We used the spot-on-lawn method [65] to investigate antagonistic interactions between the otic streptococci and test strains. We first spotted 5 µl of a diluted (OD600 0.1) overnight culture of each streptococcal strain onto a 1.5% (w/v agar) TSA plate and allowed it to dry for 30 min at room temperature before incubating at 37°C for 24 h to grow the colonies. We then overlayed the plates with a warm (55oC) 8-ml layer of soft-agar (0.75%, w/v, final concentration) medium (TSA, BHI or sBHI) containing the test strain (OD600 0.1). The general procedure to make 0.75% agar overlays was to autoclave 6 ml of 1% agar-solidified growth medium, cool down the melted agar in a 55oC water bath, add 2 ml of the test strain culture to a final OD600 of 0.1, and mix by inversion before pouring over the TSA plate surface with the otic colonies. To make sBHI overlays, we added the chemical supplements to 6 ml of warm (55oC), melted 1% (w/v) agar BHI before mixing with 2 ml of an overnight NTHi culture to a final OD600 of 0.1. The overlays were allowed to solidify at room temperature before incubating for an additional 24 h at 37°C in an incubator with or without (*S. aureus* overlay) 5% CO2. These culture conditions promoted the growth of the test strains as a turbid lawn in the overlays after 24 h, except for areas of growth inhibition (halos or clear zones) on top and around colonies of antagonistic streptococci growing underneath. At the end of the incubation period, we photographed the overlayed plates with a dissecting scope (0.63x objective) against a ruler and used the ImageJ program (4) to measure the size of the growth inhibition zone from the streptococcal colony edge underneath in triplicate biological replicates.

Availability of data and materials

The 16S rRNA gene sequences retrieved from Illumina sequences were deposited in the GenBank database under individual accession numbers (Table 3.3.1).

RESULTS

Phylogenetic analysis supports the oral ancestry otic streptococcal commensals

A previous study of the microbiology of the middle ear [21] recovered from healthy young adults 19 cultivars representing otic *Streptococcus* commensals and transient or low abundant groups (*Staphylococcus, Neisseria,* and the actinobacterial genera *Micrococcus* and *Corynebacterium*). Phylogenetic analysis of partial 16S rDNA amplicons sequenced from the isolates revealed close relationships with oral (oropharyngeal and buccal) strains recovered from the same host [21]. To reach the resolution needed for species-level demarcation, we sequenced and partially assembled the genomes of the otic cultivars and retrieved full-length 16S rDNA sequences for each of the isolates. A species sequence identity cutoff of >98.7% [3] matched each otic isolate to more than one species within each genus (Table 3.1 shows the top identity hit for each strain). Phylogenetic inference methods resolved, however, close evolutionary ties with oral commensals or species that disperse from perioral regions (Fig. 3.2).

The nearest neighbor to most of the *Streptococcus* sequences (7 of them) was *Streptococcus salivarius* (subspecies *salivarius* and *thermophilus*) (Fig. 3.2). Genomic divergence (size and gene content) for species and subspecies within the Salivarius group is high [34]. As a result, strains of *S. salivarius* can have very different metabolic and physiological characteristics or even habitat/host preferences despite high 16S rRNA sequence identity [34, 35]. Thus, the physiology of otic and oral strains in the *S. salivarius* subclade may differ substantially. The remaining streptococcal sequences clustered separately with oral relatives within the Mitis group (L0020-02 and *Streptococcus parasanguinis*), Viridans group (L0023-02 and *Streptococcus pseudopneumoniae*) and the Lancefield's group B *Streptococcus* or GBS (L0023-01 and L0023-

03 and *Streptococcus agalactiae*) [5, 35] (Fig. 3.2). Hence, 16S rRNA phylogeny supports the oral ancestry of all the streptococcal cultivars [21].

The 16S rRNA sequence identity of the non-streptococcal strains also produced more than one match to species of *Staphylococcus, Neisseria*, *Micrococcus* and *Corynebacterium* (Table 3.1). A catalase negative test confirmed the classification of the three staphylococcal isolates as *Staphylococcus* spp. (Fig. 3.2). The closest neighbors to the otic staphylococci were species (*Staphylococcus hominis, Staphylococcus aureus*, and *Staphylococcus epidermidis*) that are highly represented in the nasal passages [9]. Their nasal abundance facilitates dispersal in the contiguous oral cavity [10] and their transient detection in perioral regions [10, 11]. On the other hand, the three *Neisseria* isolates were closely related to oropharyngeal commensals [12, 36] (*Neisseria perflava, Neisseria subflava* and *Neisseria flavescens*; Fig. 3.2) that transiently disperse in the aerodigestive tract and the middle ear [21] via saliva aerosols [13]. The otic isolates also included two actinobacterial *Micrococcus* and *Corynebacterium* strains (Table 3.1). The *Micrococcus* isolate was catalase-positive, a general phenotypic trait of the genus [37], and branched closely to *Micrococcus yunnanensis* (Fig. 3.2). This is a soil *Micrococcus* species [38] that, like other environmental micrococci, enters in the human aerodigestive tract with air [39]. The second actinobacterial isolate was closely related to *Corynebacterium pseudodiphtericum* (Fig. 3.2). *Corynebacterium* commensals are prominent members of the nasal microbiomes and antagonists of nasal pathobionts, including some of the most important otopathogens [40]. Their abundance in the nasal microflora explains their detection in oral and perioral regions [14]. However, actinobacteria only account for ~1% of the operational taxonomic units (OTUs) in otic secretions, suggesting they are negatively selected for growth and reproduction in the middle ear mucosa [21].

Surfactant-mediated swarming motility is widespread among the otic cultivars

Successful colonization of respiratory mucosae requires bacterial migrants to move rapidly across the mucus layer in order to avoid immune attack and clearance [30]. Some flagellated bacteria can reach the underlying epithelial lining by rapidly swarming in groups through the viscous mucoid layer, a process that is stimulated by the lubricating effect of surfactants and mucin glycoproteins [41]. Swarming (flagellated) and swarming-like (non-flagellated) behaviors can be identified in laboratory plate assays that test the expansion of microcolonies on a soft agar (0.4-0.5%) surface [41]. Thus, we tested the ability of the 19 otic isolates to swarm on the surface of 0.5% tryptone soy agar (TSA) plates in reference to the robust swarmer *Pseudomonas aeruginosa* PA01 [42]. Figure 3A shows the average expansion of triplicate colonies over time (Table 3.2). Although *P. aeruginosa* showed large zones of swarming expansion already at 18 h, we only detected swarming activity in the otic isolates after 42 or 62 h of colony growth (Fig. 3.3A). Lag phases are not unusual prior to swarming on agar plates as cells reprogram their physiology to be able to grow on the agar-solidified medium [41]. Consistent with this, the strains that grew faster on the semisolid TSA plates (three staphylococcal and the two actinobacterial isolates) produced visible zones of swarming expansion at 42 h, while the slowest growers (*N. perflava* (L0023-05 and L0023-06) required 62 h of incubation (Table 3.2). Notably, most of the streptococci grew well in tryptone soy broth (TSB), yet they aggregated strongly when growing on the surface of the soft-agar plates (Fig. 3.3B) and delayed swarming (Table 3.2). We partially rescued the swarming delay by lowering the agar concentration from 0.5 to 0.4% (Fig. 3.3B). For example, the streptococcal strain L0022-03 did not swarm on 0.5% TSA plates until after 62 h (Table 3.2) but expanded 0.28 cm away from the edge of the colony after 42 h of growth on 0.4% TSA plates (Fig. 3.3B). This is because lowering the agar concentration facilitates water movement to the surface

and immerses the cells in a layer of liquid that reduces frictionally forces between the cell and the surface and stimulates swarming [41].

The need for some bacteria to express cellular components (flagella, exopolysaccharide, surfactants, etc.) mediating swarming on semisolid agar can also delay the appearance of expansion zones [41]. Secretion of surfactants is particularly important to reduce frictional resistance between the surface of swarming cells and the underlying substratum [41]. As a result, the concentration and diffusion rates of secreted surfactants in soft-agar medium often correlate well with the extent of swarming expansion [43]. Therefore, we also screened for surfactant production by colonies grown on hard agar plates (1.5% TSA) for 24 h and airbrushed with a fine mist of mineral oil droplets. This atomized oil assay instantaneously reveals halos of oil droplet dispersal around surfactant-producing strains and provides a semiquantitative estimation of surfactant production, even at concentrations too low to be detected by traditional methods such as the water drop collapse assay [43]. The assay detected haloes of oil dispersal around 9 of the isolates (Table 3.2) and identified positive correlations between surfactant production and the onset of swarming on 0.5% TSA for most strains (Fig. 3.3A). For example, the actinobacterial isolates, which were robust swarmers, produced the highest levels of surfactant (Table 3.2). By contrast, temperate swarmers such as the streptococcal isolates produced low or undetectable levels of surfactants under the experimental conditions. As an exception, the staphylococcal isolates swarmed robustly on the soft agar plates (Fig. 3.3) although they did not produce detectable halos of mineral oil dispersion (Table 3.2). Although staphylococcal cells lack flagellar locomotion, they can passively ‘spread’ on soft agar surfaces [44] through the coordinated synthesis of lubricating peptides known as phenol-soluble modulins (PSMs) [45]. PSM surfactants accumulate very close

to the colony edge [46]. Hence, they are unlikely to produce a halo of oil dispersal in the atomized assay used for testing.

Redox and nutritional advantage of otic streptococci in the middle ear mucosa

Successful colonizers of the middle ear mucosa face sharp redox fluctuations due to the brief (400 milliseconds) yet infrequent (approximately every minute when we swallow) openings of the Eustachian tube [20]. For this reason, we tested the ability of the otic cultivars to grow under aerobic or anaerobic conditions (Fig. 3.3.3.4A). All the isolates grew well in oxic and anoxic liquid medium, except for two *Neisseria* strains (L0023-05 and L0023-06) that grew slowly in the oxic broth. These two strains flocculated extensively in the oxic medium, an aggregative behavior exhibited by microaerophiles in response to elevated (and toxic) concentrations of oxygen [47]. Pairwise comparisons (two-tailed t-test) also identified significant differences in the redox preference of most of the streptococcal and staphylococcal strains (Table 3.3). Despite these differences, the streptococcal and staphylococcal strains grew faster aerobically and anaerobically (0.56±0.23 and 0.50±0.12 doubling times, respectively) than most other strains, suggestive of a competitive advantage for growth and reproduction under sharp redox fluctuations. The actinobacterial strains also grew in the presence or absence of oxygen but show a more pronounced redox preference (Table 3.3). For example, both isolates doubled approximately every 0.5 h under anoxic conditions but slower (*Micrococcus* L0020-05, ~0.74 h doubling time) or faster (*Corynebacterium* L0020-06, 0.17 h average generation time) in oxic media (Table 3.3). The aerobic preference of the *Corynebacterium* L0020-06 strain matches well with the enrichment of this genus in the aerated nasal passages [9] and the reduced abundance of this group in otic secretions [21].

In addition to redox fluctuations, bacteria colonizing the otic mucosa must cope with a scarcity of nutrients. The limited carriage of dietary substrates in saliva aerosols reduces nutrient availability in the middle ear and is predicted to select for commensals that can use host-derived nutrients such as mucosal proteins and mucin glycoproteins to grow [21]. A screening for the secretion of proteases and mucinases by the otic isolates supported this prediction (Table 3.3). For these experiments, we spot-plated the cultivars onto TSA plates supplemented with 5% lactose-free skim milk (protease assay) or 0.5% porcine gastric mucin (mucinase assay) for 24 h to identify zones of substrate degradation around the colonies. Figure 4B shows typical results for representative otic strains and the positive control *P. aeruginosa* PA01. All the isolates were able to degrade mucin under these conditions, although some strains required additional incubation (48 h) to produce a clear halo (Table 3.3). As an example of delayed hydrolysis, three aggregative strains of *S. salivarius* (L0021-01, L0022-03 and L0022-04) produced only faint mucin clearings after 24 h (+/– in Table 3.3) but the zone of degradation expanded after incubating for 48 h. While mucinase activity was widespread, protease activity was only detected in the streptococcal and staphylococcal groups (Table 3.3). It is unlikely that the casein substrate used in the assays produced false negatives, because extracellular proteases have low substrate selectivity and cleave a wide range of substrates [48]. This is particularly advantageous in the middle ear mucosa, where colonizers must scavenge nitrogen sources by breaking downs mucosal proteins and the protein backbone of mucins [49]. In addition to providing a metabolic advantage, proteases facilitate mucosal penetration, control mucus viscosity, modulate host immune responses, and antagonize competitors [50]. Hence, protease secretion confers on staphylococci and streptococci a competitive advantage for otic colonization.

Metabolic advantage of streptococci for syntrophic growth in biofilms

The presence of bacterial microcolonies on the epithelial surface of biopsy specimens collected from the tympanic cavity of healthy individuals [29] motivated us to investigate the biofilm-forming abilities of the otic isolates. For these assays, we stained 24-h biofilms with crystal violet and measured the absorbance of the biofilm-associated dye to estimate the biofilm biomass (Fig. 3.5A). All but two streptococcal strains (*S. pseudopneumoniae* L0023-02 and *S. agalactiae* L0023-03) formed robust biofilms under aerobic conditions (Fig. 3.5A). The group of *S. salivarius* L0021-04 and L0021-05, *S. parasanguinis* L0020-02, and *S. agalactiae* L0023-01 clustered separately with a staphylococcal isolate (*S. aureus* L0021-02) for their ability to form robust biofilms in both oxic and anoxic media (Fig. 3.5A). A group comprised of *S. salivarius* L0021-01, L0022-03, L0022-04, L0022-05 and L0022-06 had a biofilm growth advantage in oxic medium only (Fig. 3.5A). The enhanced biofilm abilities of these isolates correlated well with the pH drops measured in the culture broth at 24 h (Fig. 3.5B). Indeed, K-means clustering analyses partitioned the best biofilm formers (9 streptococci and *S. aureus* L0021-02 with an average biofilm biomass A_{550}~2.2) separately from all other strains based on the low pH (average pH~4.8) of the medium. The culture pH also partitioned the low biofilm formers (average biofilm biomass $A_{550}\leq 0.1$) in two clusters: one with the two actinobacterial strains (average pH~7.7) and another with the remaining strains (average pH~5.6). Collectively, the clustering of strain phenotypes in three separate groups explained 91.3% of the data variance.

The pH measurements correlated well with lactate levels in the culture broth (p=0.03) and entry in stationary phase (Fig. 3.3.3.5C). Thus, the best biofilm formers produced more lactate than any other strain and entered stationary phase (0.62±0.05 OD_{600}) once the pH dropped below 5. This response is similar to that described for oral streptococcal commensals, which also produce

lactic acid as the main fermentation byproduct [51] and stop growing once the pH drops to inhibitory levels, usually at or below 5 [52]. To prevent growth inhibition, commensal oral streptococci co-aggregate with lactate-utilizing bacteria such as *Veillonella* [53]. A similar metabolic dependence via lactate helps explain the co-enrichment of *Streptococcus* and *Veillonella* sequences in otic secretions [21].

Antagonistic interactions of otic streptococci with common otopathogens

Commensal oral streptococci mediate intra- and interspecies antagonistic interactions in oral biofilms that are critical to dental and mucosal health [33]. Given their oral ancestry, we screened the otic streptococci for their ability to inhibit the growth of known otopathogens (*Streptococcus pneumoniae, Moraxella catarrhalis*, and non-typeable *Haemophilus influenzae*). For these assays, we followed the same protocol as in other plate assays and spot-plated overnight cultures on TSA plates before incubating them at 37^{o}C. After allowing the colonies to grow for 24h, we covered them with a soft (0.75%) agar overlay containing a diluted cell suspension of each otopathogen in a growth medium suitable for their growth. Incubation of the overlayed plates for an additional 24 h revealed clear zones of growth inhibition on top and around some of the underlying streptococcal colonies. Fig. 3.3.3.6 shows representative plate assays for all the otic strains against each otopathogen and the zones of growth inhibition, which reveal antagonistic interactions due to nutrient competition, secretion of growth inhibitors by the streptococci, or both. The zones of growth inhibition are particularly large against *S. pneumoniae* and *M. catarrhalis*, consistent with the secretion of a diffusible inhibitory compound. By contrast, antagonistic effects against *H. influenzae* were less pronounced and strain-specific (Fig. 3.6).

We also used the plate assay to screen for potential antagonism of the otic streptococci towards the nasopharyngeal staphylococci. As a test strain, we used *S. aureus* subsp. *aureus* JE2

[54], a plasmid-cured derivative of the epidemic community-associated methicillin-resistant *S. aureus* (CA-MRSA) isolate USA300 [55]. We observed antagonism by all the non-Salivarius isolates (Fig. 3.6), indicative of a species-specific mechanism for growth inhibition by these streptococcal groups (*S. pseudopneumoniae*, *S. parasanguinis* and *S. agalactiae*). The ability of non-Salivarius streptococci to inhibit the growth of *S. aureus* is not uncommon. Despite being catalase positive, *S. aureus* is sensitive to hydrogen peroxide produced by *S. pneumoniae* in the nasal mucosa [56]. This is because hydrogen peroxide is converted into a highly toxic hydroxyl radical ($^{\bullet}OH$) that rapidly kills *S. aureus* [57]. However, non-Salivarius otic streptococci release hydrogen peroxide as a byproduct of their metabolism [58-60] and use catalase-independent mechanisms for anti-oxidative stress resistance [61]. These phenotypic traits confer on the streptococcal isolates a competitive advantage during the colonization of the middle ear mucosa and help explain why *Staphylococcus* sequences are seldom detected in otic secretions [21].

DISCUSSION

The recovery from otic secretions of close relatives of oral bacteria (Fig. 3.2) highlights the role that saliva aerosols play in the dispersal of bacteria through the aerodigestive tract. Human saliva carries bacteria shed from oral surfaces such as teeth and gums and spreads them to distant mucosae [62, 63]. The constant flux of saliva to the oropharynx (back of the throat) facilitates the formation of aerosols and oral bacterial carriage to the middle ear every time the Eustachian tube opens [21]. In support of this, phylogenetic analysis of full-length 16S rRNA sequences resolved close evolutionary relationships between the otic cultivars and species that reside or transiently disperse in the oral cavity (Fig. 3.2). Particularly important were the ancestral ties between the otic streptococci and pioneer species of oral biofilms. Most of the otic streptococci were closely related to *S. salivarius*, one of the first colonizers of the human oral cavity after birth and an abundant

commensal throughout the life of the host [64]. This bacterium disperses as aggregates that survive stomach passage [65] and seed the mucosa of the small intestine [66]. *S. salivarius* aggregates may also disperse in saliva aerosols, a dispersal path that provides the primary mechanism for seeding of the otic mucosa [21]. Aggregation facilitates immunoescape and the formation of microcolonies on the mucosal epithelium. It also promotes coaggregation with anaerobic syntrophic partners and supports trophic interactions (Fig. 3.1) that mirror those described in oral biofilms. Additionally, oral *S. salivarius* strains mediate antagonistic interactions with virulent streptococci that prevent tooth decay, periodontal disease, and the spread of respiratory pathogens such as the otopathogen *S. pneumoniae* [67, 68]. We observed similar interspecies interference of otic *S. salivarius* strains towards common otopathogens (Fig. 3.6), suggesting similar roles for these middle ear residents in disease prevention.

The non-Salivarius otic streptococci were also close relatives of oral species (Fig. 3.2). For example, one of the isolates (L0020-02) was closely related to *S. parasanguinis*, a bacterium that groups with species in the Mitis group based on 16S rRNA gene sequence analysis and that shares with them many phenotypic characteristics [35]. Like *S. salivarius*, *S. parasanguinis* is one of the early colonizers of the oral cavity [33] and disperses in saliva [69]. It produces fimbriae to firmly attach to and co-disperse within syntrophic oral aggregates [70]. The otic streptococci also included strains closely related to *S. pseudopneumoniae* (L0023-02; Viridans group) and *S. agalactiae* (L0023-01 and L0023-03; GBS group), which are oral streptococci linked to infective processes in the aerodigestive tract and other body sites [71, 72]. Yet, the otic relatives readily inhibited the growth of the three most common otopathogens (*S. pneumoniae, M. catarrhalis,* and non-typeable *H. influenzae*) and were the only otic streptococci that interfered with the growth of *S. aureus* (Fig. 3.6). Antagonism towards *S. aureus* may involve the production of hydrogen

peroxide as a metabolic byproduct, as noted for related oral streptococcal species [58-60]. Hydrogen peroxide also functions as a signaling molecule for the co-aggregation of non-salivarius streptococci in syntrophic biofilms [59]. Future studies will need to evaluate the role of these streptococcal lineages in producing hydrogen peroxide as a signal for intra and interspecies co-aggregation and as an antagonist of bacterial competitors in the middle ear mucosa.

The results presented in this study also identified physiological traits of streptococci that could facilitate the colonization of the middle ear mucosa and the formation of syntrophic biofilms. The otic streptococci were all temperate swarmers on soft agar plates (Fig. 3.3) and only some secreted surfactants (Table 3.2). Endogenous surfactants stimulate swarming on semisolid agar surfaces but may not be needed for efficient swarming through the native mucus layers [41]. This is particularly true for bacteria colonizing the middle ear mucosa, which is rich in host surfactants [73]. Furthermore, surfactant production by bacterial colonizers may be undesirable in the middle ear mucosa, where surfactant-induced changes in the mucus rheology could interfere with critical mucosal functions such as antimicrobial activity, immunomodulation and Eustachian tube mechanics [73]. Indeed, careful control of host surfactants regulates the viscosity and surface tension of the tympanic mucus layer [74] and keeps the surface tension of the mucus sufficiently low (58 mN/m) to facilitate the opening of the collapsed Eustachian tube [73]. Disruption of surfactant homeostasis increases the pressure needed to open the Eustachian tube, risking barotrauma and making the middle ear mucosa more vulnerable to infections [73].

An important finding of our study was the identification of phenotypic traits in streptococcal and staphylococcal cultivars that could give both groups a competitive advantage during the colonization of the middle ear. For example, the streptococcal and staphylococcal isolates grew well with and without oxygen (Fig. 3.4A) and secreted mucins and proteases (Table

3.3), which are adaptive responses for growth and reproduction under otic redox fluctuations using the available mucosal nutrients. Moreover, both groups produced lactate as the main fermentation byproduct (Fig. 3.5C), a key metabolic intermediate in the syntrophic otic communities [21]. By contrast, the otic *Neisseria* strains L0020-05 and L0020-06 grew poorly and flocculated extensively in oxic broth (Fig. 3.4A). Furthermore, the strains did not form robust biofilms (Fig. 3.5A), nor did they produce lactate fermentatively (Fig. 3.5C). These two *Neisseria* species formed a separate clade with species in the family *Neisseriaceae* that populate the tongue dorsum [75]. And although these species readily disperse via saliva into the oropharynx [12], they are not positively selected in the middle ear [21]. Additionally, the *Neisseria* cultivars were, along with the actinobacterial isolates (*Micrococcus* spp. L0020-05 and *Corynebacterium* spp. L0020-06) the only strains that did not secrete proteases on casein plates (Table 3.3). Not surprisingly, despite their abundance in the oral and perioral regions [14], these groups are not enriched in otic secretions [21].

The most notable difference between the staphylococcal and streptococcal isolates was arguably the aggregative properties of most *Streptococcus* (Fig. 3.3B). Aggregation allows oral streptococci to recognize and recruit other bacteria to biofilms [53]. For example, oral streptococci coaggregate with actinomyces to colonize the tooth surface and recruit other bacteria during the formation of the dental plaque [33, 76]. Lactate exchange between streptococcal and *Veillonella* strains is critical for coaggregation during the early stages of biofilm formation on oral surfaces [53]. Fusobacteria also mediate early coaggregation in oral biofilms, forming physical bridges across the microcolonies that facilitate the attachment of non-coaggregating bacteria [33, 76]. Thus, aggregative behaviors drive syntrophic interactions that sustain the growth of the dental plaque throughout all dentition stages and during the formation of subgingival biofilms in the

predentate and postdentate states [63]. The widespread presence and abundance of syntrophic co-aggregates in the oral cavity promotes their co-dispersal in saliva [77] and affords immunoprotection in non-oral mucosae [78].

The fact that the otic streptococci, like the oral ancestors, were highly aggregative (Fig. 3.4), formed robust biofilms (Fig. 3.5A) and produced lactate (Fig. 3.4C) suggests that they are the primary colonizers of the middle ear mucosa. These adaptive traits allow streptococci to grow and reproduce in the middle ear mucosa with obligate anaerobic, syntrophic partners such as *Prevotella, Fusobacterium* and *Veillonella* [21]. The syntrophic microcolonies metabolize and ferment host mucins and proteins in the otic mucosa (Fig. 3.1), indirectly controlling the viscoelastic properties of the mucus layer and Eustachian tube functionality [73]. The detection of a differential gradient of mucin gene expression along the tympanic cavity and Eustachian tube [73] suggests a high degree of spatial heterogeneity in bacterial colonization as well. Shaped like an inverted flask [20], the posterior region of the Eustachian tube is more readily seeded with saliva aerosols during the cycles of tubal aperture. Concentration of streptococcal aggregates in this region closer to the nasopharyngeal opening of the Eustachian tube could provide increased protection against otopathogens, which typically reside in nasal reservoirs. Future research should therefore consider the mechanisms that allow otic streptococci to co-aggregate with syntrophic partners, their spatial distribution in the otic mucosa and antagonistic interactions with transient migrants. This knowledge is important to understand the functionality of the otic communities and how they influence host functions and the outcome of infections.

DECLARATIONS

Ethics approval and consent to participate

The isolates used in this study were recovered from human mucosal samples using a protocol approved on May 17 of 2017 by the Institutional Review Board (IRB) at Michigan State University, East Lansing, Michigan, United States of America. The committee found the research project to be appropriate in design, to protect the rights and welfare of human subjects, and to meet the requirements of Michigan State University's Federal Wide Assurance and the Federal Guidelines (45 CFR 46 and 21 CFR Part 50).

Consent for publication

Not applicable.

Competing interests

The authors declare that they have no competing interests.

Acknowledgements

The authors would like to thank Dr. Michaela TerAvest and Nicholas Tefft at Michigan State University for assistance with the HPLC analyses and Drs. Batsirai Mabvakure and Heather Blankenship at the Michigan Department of Health and Human Services Bureau of Laboratory for guidance on Illumina short read assembly and contig gene analysis. We are also thankful to Drs. Martha Mulks, Poorna Viswanathan and Neal Hammer for providing the test strains used in the growth inhibition plate assays.

Funding

This research was funded by grants N00014-17-2678 and N00014-20-1-2471 from the Microbiome program at the Office of Naval Research (ONR) to GR. KJ acknowledges support from a summer 2020 G. D. Edith Hsiung and Margaret Everett Kimball Endowed fellowship from

the department of Microbiology and Molecular Genetics at Michigan State University. The funders had no role in study design, data collection and analysis, decision to publish or preparation of manuscript.

Affiliations

Department of Microbiology and Molecular Genetics, Michigan State University, 567 Wilson Rd., Rm 6190, Biomedical and Physical Sciences building; East Lansing, MI 48824, USA.

Contributions

Kristin M. Jacob: Formal analysis, processed samples for cultivation experiments, sequenced and partially assembled the genomes of otic cultivars to retrieve 16S rRNA sequences, performed the taxonomic and phylogenetic analyses and all the physiological characterization assays. All authors read and approved the final version of the manuscript. Gemma Reguera: conceived the study and planned and interpreted the experiments with KJ, Writing – original draft, wrote the first draft of the manuscript and incorporated contributions from KJ. All authors read and approved the final version of the manuscript.

APPENDIX

Table 3.1: **Taxonomic classification (reference strain) of otic strains based on the % identity (ID) of their full-length 16S rRNA sequence.**

Strain	GenBank no.	Reference Strain (Accession; % ID)
Streptococcus		
L0020-02	MW866489	*Streptococcus parasanguinis* (NR_024842.1; 99.47)
L0021-01	MW866494	*Streptococcus salivarius* (NR_042776.1; 99.81)
L0021-04	MW866496	*Streptococcus salivarius* (NR_042776.1; 99.81)
L0021-05	MW866497	*Streptococcus salivarius* (NR_042776.1; 99.81)
L0022-03	MW866499	*Streptococcus salivarius* (NR_042776.1; 99.81)
L0022-04	MW866500	*Streptococcus salivarius* (NR_042776.1; 99.81)
L0022-05	MW866501	*Streptococcus salivarius* (NR_042776.1; 99.81)
L0022-06	MW866502	*Streptococcus salivarius* (NR_042776.1; 99.81)
L0023-01	MW866503	*Streptococcus agalactiae* (NR_040821.1; 100)
L0023-02	MW866504	*Streptococcus oralis* (NR_117719.1; 99.47)
L0023-03	MW866505	*Streptococcus agalactiae* (NR_040821.1; 100)
Staphylococcus		
L0020-04	MW866491	*Staphylococcus hominis* (NR_036956.1; 99.61)
L0021-02	MW866495	*Staphylococcus aureus* (NR_037007.2; 99.87)
L0021-06	MW866498	*Staphylococcus saccharolyticus* (NR_113405.1; 99.4)
Micrococcus		
L0020-05	MW866492	*Micrococcus luteus* (NR_075062.2, 99.61)
Corynebacterium		
L0020-06	MW866493	*Corynebacterium pseudodiphtericum* (NR_042137.1; 99.47)
Neisseria		
L0020-03	MW866490	*Neisseria perflava* (NR_114694; 99.93)
L0023-05	MW866507	*Neisseria perflava* NR_117694.1; 99.74*)*
L0023-06	MW866506	*Neisseria perflava* NR_117694.1; 99.74*)*

Table 3.2: **Coaggregation, swarming motility and surfactant production of otic isolates in reference to positive control (*P. aeruginosa* PA01).**

Species/closest relative	Strain	Aggregation[a]	Surfactant[b]	Swarming[c]		
				18 h	42 h	62 h
Streptococcus						
S. parasanguinis	L0020-02	+	–	–	–	0.07 (0.10)
S. salivarius	L0021-01	+	0.23 (0.19)	–	–	0.16 (0.05)
S. salivarius	L0021-04	+	0.46 (0.09)	–	–	0.05 (0.13)
S. salivarius	L0021-05	+	–	–	–	0.05 (0.07)
S. salivarius	L0022-03	+	0.28 (0.19)	–	–	0.19 (0.004)
S. salivarius	L0022-04	+	–	–	–	0.20 (0.08)
S. salivarius	L0022-05	+	0.18 (0.12)	–	–	0.20 (0.03)
S. salivarius	L0022-06	+	0.09 (0.06)	–	–	0.18 (0.02)
S. agalactiae	L0023-01	+	–	–	0.21 (0.02)	0.23 (0.02)
S. pseudopneumoniae	L0023-02	+	–	–	–	0.07 (0.10)
S. agalactiae	L0023-03	+	0.31 (0.11)	–	0.19 (0.01)	0.20 (0.06)
Staphylococcus						
S. hominis	L0020-04	–	–	–	0.37 (0.004)	0.66 (0.08)
S. aureus	L0021-02	–	–	–	0.53 (0.002)	0.79 (0.001)
S. epidermidis	L0021-06	–	–	–	0.46 (0.03)	0.64 (0.02)
Actinobacteria						
M. yunnanensis	L0020-05	–	0.86 (0.13)	–	0.54 (0.05)	0.75 (0.04)
C. pseudodiphtericum	L0020-06	–	2.64 (0.05)	–	0.41 (0.06)	0.72 (0.03)
Neisseria						
N. perflava	L0020-03	–	–	–	0.44 (0.03)	0.68 (0.001)

Table 3.2 (cont'd)

N. flavescens	L0023-05	+	–	–	–	0.23 (0.32)
N. flavescens	L0023-06	+	–	–	–	0.25 (0.35)
P. aeruginosa	PA01	–	1.37 (0.06)	1.24 (0.35)	1.58 (0.53)	2.18 (0.47)

[a] Aggregative (+) or uniform (–) growth of cultures spotted on 0.5% TSA plates.

[b] Average (and standard deviation) of triplicate surfactant haloes (cm) measured as the zone of mineral oil dispersion around colonies grown at 37ºC on 1.5% TSA plates. (–, not detected).

[c] Average (and standard deviation) of triplicate swarming expansion zones (cm) around colonies grown at 37ºC on soft agar (0.5%) TSA plates for 18, 42 and 62 h. (–, not detected).

Table 3.3: Growth (aerobic and anaerobic doubling times) and extracellular enzymatic activity (protease and mucinase) of otic isolates. Doubling times are in hours (standard deviation of triplicate cultures in parenthesis; nt, not tested). Protease and mucinase activities were determined by the presence (+) or absence (–) of a halo of degradation in TSA plates supplemented with skim milk (protease assay) or mucin (mucinase assay) after 24 h of growth in reference to positive control (*P. aeruginosa* PA01). The presence of a faint halo is indicated with "+/–".

		Doubling time (h)[a]		Extracellular enzymes	
Species/closest relative	Strain	Aerobic	Anaerobic	Protease	Mucinase
Streptococcus					
S. parasanguinis	L0020-02	0.629 (0.011)	0.558 (0.026)*	–	+
S. salivarius	L0021-01	0.389 (0.008)**	0.431 (0.006)	–	+/–
S. salivarius	L0021-04	0.376 (0.018)*	0.419 (0.012)	+	+
S. salivarius	L0021-05	0.407 (0.054)	0.375 (0.041)	+	+
S. salivarius	L0022-03	0.419 (0.008)	0.367 (0.004)**	+	+/–
S. salivarius	L0022-04	0.451 (0.003)	0.352 (0.009)**	+	+/–
S. salivarius	L0022-05	0.459 (0.042)	0.381 (0.041)	+	+
S. salivarius	L0022-06	0.487 (0.037)*	0.661 (0.021)	+	+
S. agalactiae	L0023-01	0.561 (0.071)	0.583 (0.009)	+	+
S. pseudopneumoniae	L0023-02	1.026 (0.404)	0.682 (0.058)	–	+
S. agalactiae	L0023-03	0.918 (0.026)	0.614 (0.022)***	+	+
Staphylococcus					
S. hominis	L0020-04	0.907 (0.073)	0.621 (0.091)*	+	+
S. aureus	L0021-02	0.406 (0.006)	0.446 (0.037)	+	+
S. epidermidis	L0021-06	0.406 (0.013)**	0.498 (0.012)	+	+

Table 3.3 (cont'd)

Actinobacterial species					
M. yunnanensis	L0020-05	1. 048 (0.060)	0.495 (0.026)*	–	+
C. pseudodiphtericum	L0020-06	0.173 (0.042)***	0.546 (0.127)	–	+
Neisseria					
N. perflava	L0020-03	0.885 (0.008)*	1.008 (0.026)	–	+
N. flavescens	L0023-05	9.089 (5.068)	1.307 (0.305)	–	+
N. flavescens	L0023-06	2.273 (0.967)	1.680 (0.593)	–	+
P. aeruginosa	PA01	nt	nt	+	+

[a] Two-tailed t-test significance identifying fastest growth conditions (aerobic or anaerobic): $p<0.05$*, $p<0.005$**, $p<0.0005$***

Figure 3.1: Illustration of the human ear anatomy (*left*) and trophic webs within bacterial microcolonies in the middle ear mucosa (*right*). The human ear is divided in three compartments (outer, middle, and inner). The eardrum separates the outer ear canal from the tympanic cavity of the middle ear, which extends as a tube (tympanic or Eustachian tube) into the nasopharynx to draw in air and drain otic secretions. The microbiome sequenced from otic secretions of healthy young adults [21] supports the establishment of a trophic web (inset) for the degradation of host mucins and proteins by Bacteroidetes into substrates (sugars and peptides) that *Streptococcus* and *Veillonella* cooperatively ferment into short chain fatty acids (SCFs) via lactate.

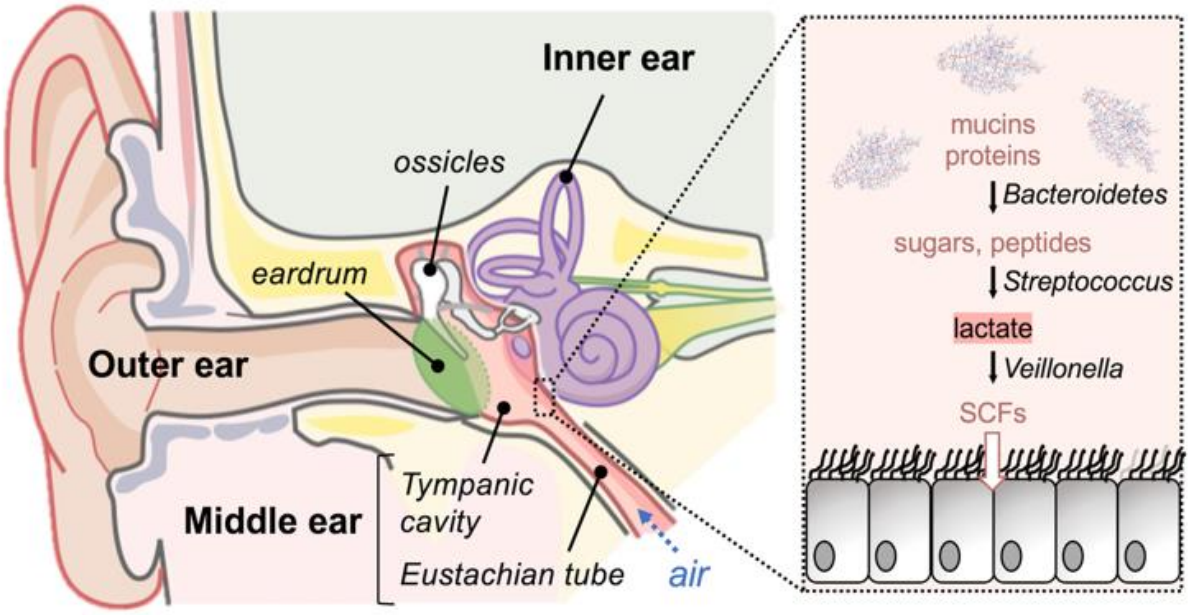

Figure 3.2: 16S rRNA gene phylogeny of otic cultivars. Maximum-likelihood tree constructed with full-length 16S rRNA sequences from the otic isolates and the closest reference strains (accession number in parentheses). The scale bar indicates 5% sequence divergence filtered to a conservation threshold above 79% using the Living Tree Database [15, 16]. Bootstrap probabilities by 1000 replicates at or above 50% are denoted by numbers at each node. The circles identify catalase-positive isolates.

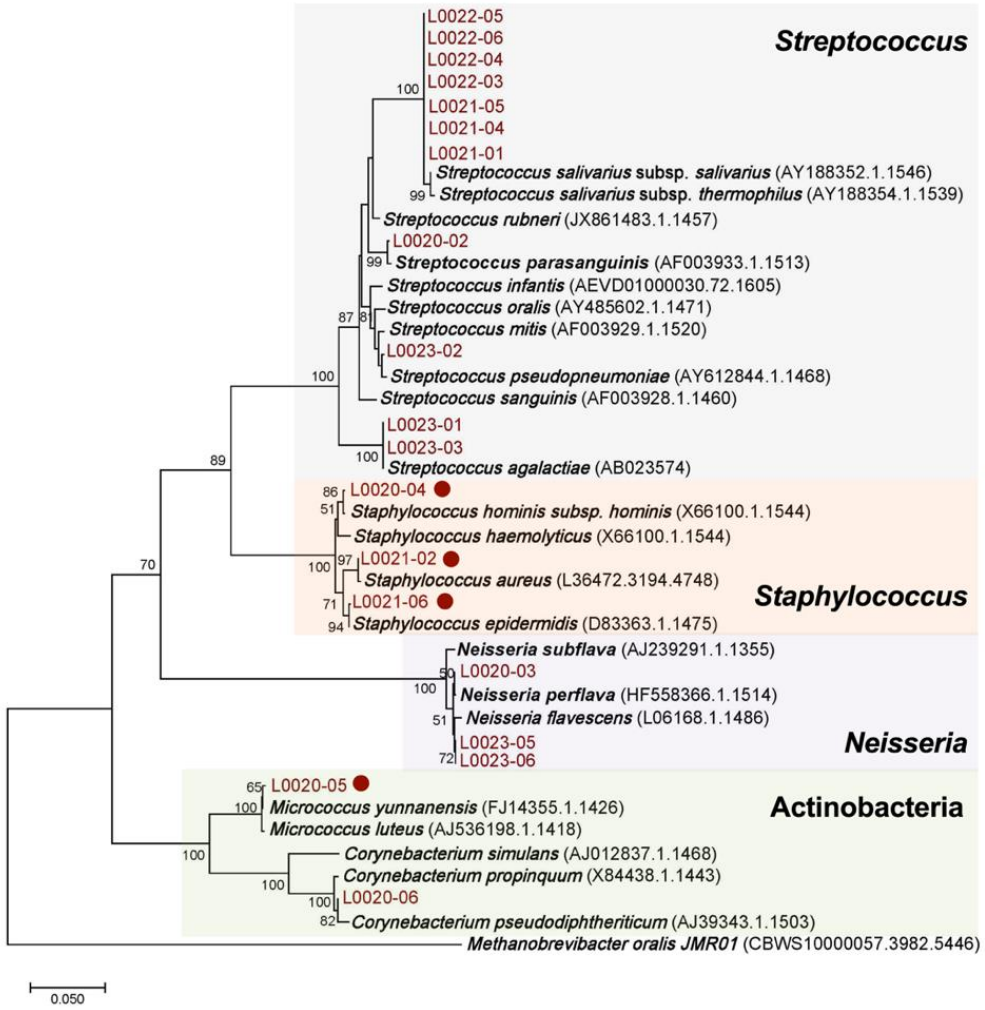

Figure 3.3: Swarming motility and surfactant production by otic cultivars in reference to *Pseudomonas aeruginosa* PA01. (A) Average surfactant production (halo of mineral oil dispersal around 24h colonies grown on 1.5% TSA), and size of swarming expansion (0.5% TSA plates at 18, 42 and 62 h) measured in triplicate replicates of the otic isolates (*Streptococcus*, gray circles; *Staphylococcus*, orange triangles; *Neisseria*, purple squares; actinobacterial strains of *Corynebacterium* and *Micrococcus*, green diamonds) and the positive control (*P. aeruginosa* PA01, white circles). (B) Representative images of swarming (0.4% TSA, 42 h) and surfactant (1.5% TSA, 24 h) plate assays for *P. aeruginosa* PA01 (positive control, boxed) and otic strains of *Streptococcus*, *Corynebacterium*, and *Micrococcus* (scale bars, 0.5 cm). The edge of the surfactant halo is highlighted with a dashed white line. The orange box identifies approximate areas of the colony edge and surfactant dispersion zone enlarged in the bottom images.

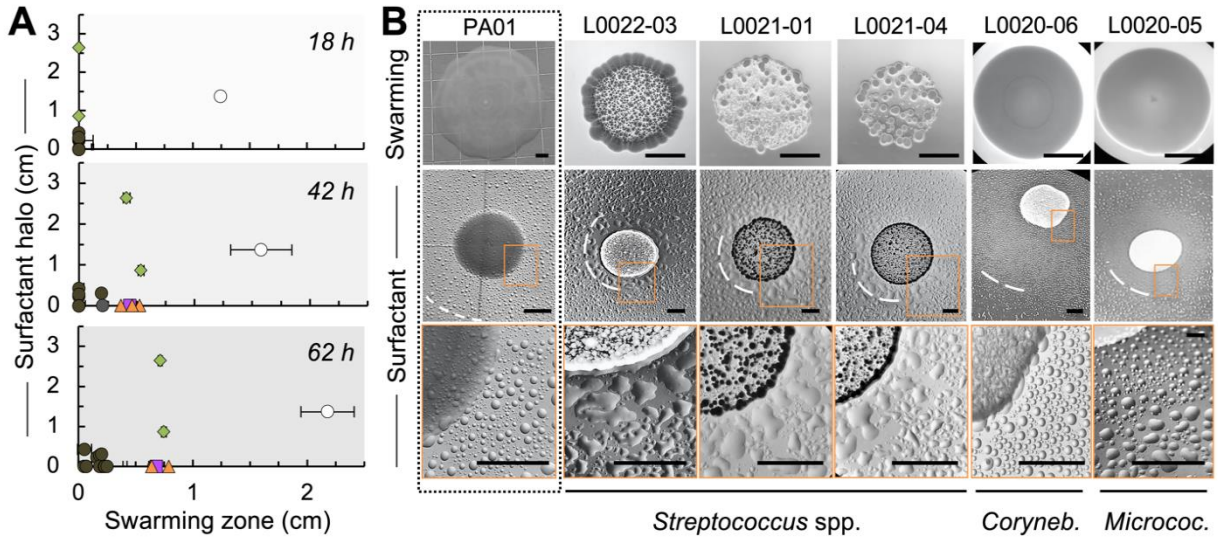

Figure 3.4: Growth of otic isolates as a function of oxygen availability and host nutrients (protein and mucin). (A) Average doubling times of otic isolates growing in at least triplicate TSB cultures aerobically or anaerobically at 37ºC. Symbols: *Streptococcus* (gray circles), *Staphylococcus* (orange triangles), *Neisseria* (purple squares) and actinobacterial genera *Micrococcus* and *Corynebacterium* (green diamonds). The flocculating strains of *Neisseria* are labeled. The raw data plotted in this graph and significant differences between aerobic and anaerobic generations times for each strain are shown in Table 3.3. (B) Protease and mucinase activity (haloes of milk casein or porcine gastric mucin degradation, respectively) of representative otic isolates and *P. aeruginosa* PA01 (positive control, boxed). The milk casein plates were photographed without staining after 24 h of incubation at 37ºC. The mucin plates were incubated for 48 h and stained with 0.1% amido black prior to photography. Scale bars, 0.5 cm.

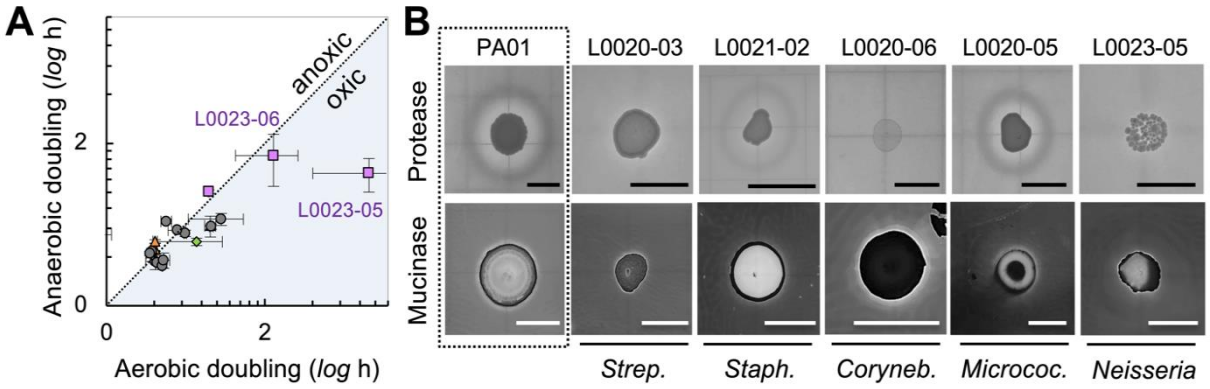

Figure 3.5: Adaptive responses promoting the establishment of otic trophic webs. (A) Biofilm biomass (crystal violet staining, measured as absorbance at 550 nm, A_{550}) of otic isolates in oxic (blue) and anoxic (white) cultures. The dashed circles identify two separate clusters of isolates with highest biofilm-forming abilities. (B) Correlation between biofilm formation and pH in oxic cultures. The circle highlights a cluster of strains with highest biofilm-forming activities and lowest pH. (C) Lactate and acetate production (mM) in stationary-phase cultures grown in oxic (black) and anoxic (white) media. The asterisks show significant differences (*$p \leq 0.05$, **$p \leq 0.01$, ***$p \leq 0.001$) between oxic and anoxic values in a two-tailed t-test analysis with the Microsoft Excel® software. All data points in A-C are average values of three independent biological experiments and are color-coded for *Streptococcus* (gray), *Staphylococcus*(orange), *Neisseria* (purple) and actinobacterial genera *Micrococcus* and *Corynebacterium* (green).

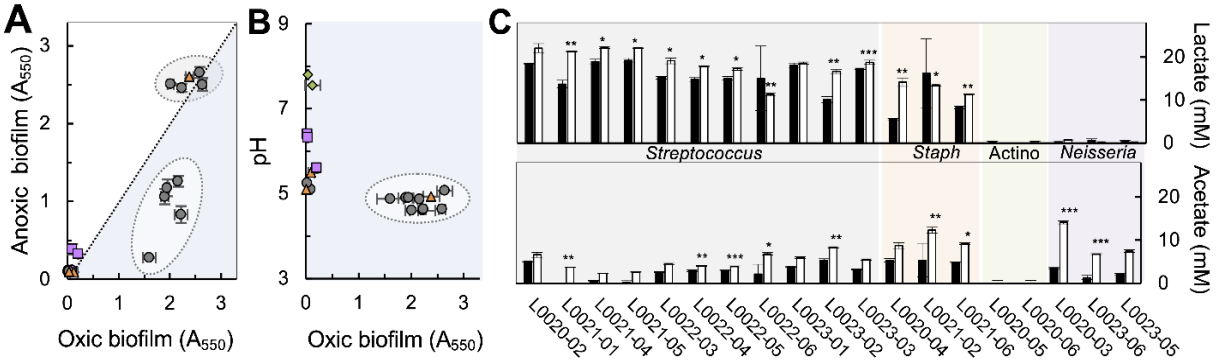

Figure 3.6: Growth inhibition of common otopathogens by otic streptococci. TSA plates containing 24-h colonies of the otic streptococci were incubated for 24h with soft-agar overlays of the otopathogens *Streptococcus pneumoniae, Moraxella catarrhalis, Haemophilus influenzae* and *Staphylococcus aureus*. All incubations were at 37^{o}C in atmospheric air. The plates show clear areas of growth inhibition of the otopathogen on top and/or around antagonistic streptococcal colonies underneath (scale bar, 0.5 cm). The symbols indicate average size of the growth inhibition halo around the underlying streptococcal colony in triplicate plate assays (+, <0.4; ++, >0.4; +/-, ~0.1 but not always reproducible).

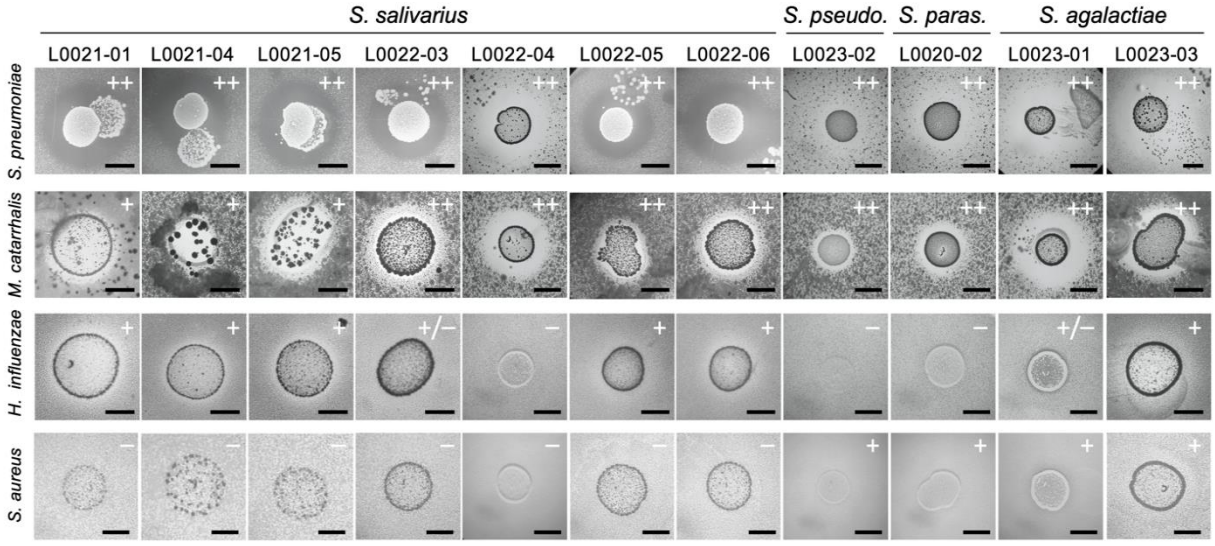

REFERENCES

REFERENCES

1. Bankevich A, Nurk S, Antipov D, Gurevich AA, Dvorkin M, Kulikov AS, Lesin VM, Nikolenko SI, Pham S, Prjibelski AD, Pyshkin AV, Sirotkin AV, Vyahhi N, Tesler G, Alekseyev MA, Pevzner PA (2012) SPAdes: a new genome assembly algorithm and its applications to single-cell sequencing. J Comput Biol 19 (5):455-477. doi:10.1089/cmb.2012.0021

2. Bassis CM, Erb-Downward JR, Dickson RP, Freeman CM, Schmidt TM, Young VB, Beck JM, Curtis JL, Huffnagle GB (2015) Analysis of the upper respiratory tract microbiotas as the source of the lung and gastric microbiotas in healthy individuals. mBio 6 (2):e00037-00015. doi:10.1128/mBio.00037-15

3. Belstrom D (2020) The salivary microbiota in health and disease. J Oral Microbiol 12 (1):1723975. doi:10.1080/20002297.2020.1723975

4. Bible AN, Khalsa-Moyers GK, Mukherjee T, Green CS, Mishra P, Purcell A, Aksenova A, Hurst GB, Alexandre G (2015) Metabolic adaptations of Azospirillum brasilense to oxygen stress by cell-to-cell clumping and flocculation. Appl Environ Microbiol 81 (24):8346-8357. doi:10.1128/aem.02782-15

5. Blaak EE, Canfora EE, Theis S, Frost G, Groen AK, Mithieux G, Nauta A, Scott K, Stahl B, van Harsselaar J, van Tol R, Vaughan EE, Verbeke K (2020) Short chain fatty acids in human gut and metabolic health. Benef Microbes 11 (5):411-455. doi:10.3920/BM2020.0057

6. Bluestone CD (2005) The Eustachian Tube: Structure, function, and role in the middle ear. BC Decker Inc, Hamilton, Ontario

7. Bolger AM, Lohse M, Usadel B (2014) Trimmomatic: a flexible trimmer for Illumina sequence data. Bioinformatics 30 (15):2114-2120. doi:10.1093/bioinformatics/btu170

8. Bomar L, Brugger SD, Lemon KP (2018) Bacterial microbiota of the nasal passages across the span of human life. Curr Opin Microbiol 41:8-14. doi:10.1016/j.mib.2017.10.023

9. Brugger SD, Bomar L, Lemon KP (2016) Commensal–pathogen interactions along the human nasal passages. PLOS Pathogens 12 (7):e1005633. doi:10.1371/journal.ppat.1005633

10. Burch AY, Shimada BK, Browne PJ, Lindow SE (2010) Novel high-throughput detection method to assess bacterial surfactant production. Appl Environ Microbiol 76 (16):5363-5372. doi:10.1128/AEM.00592-10

11. Chen Z, Wang X, Yang F, Hu Q, Tong H, Dong X (2017) Molecular insights into hydrogen peroxide-sensing mechanism of the metalloregulator MntR in controlling bacterial resistance to oxidative stresses. J Biol Chem 292 (13):5519-5531. doi:10.1074/jbc.M116.764126

12. Cotter PD, Hill C (2003) Surviving the acid test: responses of gram-positive bacteria to low pH. Microbiol Mol Biol Rev 67 (3):429-453. doi:10.1128/mmbr.67.3.429-453.2003

13. Crielaard W, Zaura E, Schuller AA, Huse SM, Montijn RC, Keijser BJ (2011) Exploring the oral microbiota of children at various developmental stages of their dentition in the relation to their oral health. BMC Med Genomics 4:22. doi:10.1186/1755-8794-4-22

14. Delorme C, Abraham AL, Renault P, Guédon E (2015) Genomics of *Streptococcus* salivarius, a major human commensal. Infect Genet Evol 33:381-392. doi:10.1016/j.meegid.2014.10.001

15. Delwiche EA, Pestka JJ, Tortorello ML (1985) The *Veillonella*e: Gram-negative cocci with a unique physiology. Annu Rev Microbiol 39:175-193. doi:10.1146/annurev.mi.39.100185.001135

16. Dewhirst FE, Chen T, Izard J, Paster BJ, Tanner AC, Yu WH, Lakshmanan A, Wade WG (2010) The human oral microbiome. J Bacteriol 192 (19):5002-5017. doi:10.1128/JB.00542-10

17. Diep BA, Gill SR, Chang RF, Phan TH, Chen JH, Davidson MG, Lin F, Lin J, Carleton HA, Mongodin EF, Sensabaugh GF, Perdreau-Remington F (2006) Complete genome sequence of USA300, an epidemic clone of community-acquired meticillin-resistant *Staphylococcus aureus*. Lancet 367 (9512):731-739. doi:10.1016/s0140-6736(06)68231-7

18. Donati C, Zolfo M, Albanese D, Tin Truong D, Asnicar F, Iebba V, Cavalieri D, Jousson O, De Filippo C, Huttenhower C, Segata N (2016) Uncovering oral *Neisseria* tropism and persistence using metagenomic sequencing. Nature Microbiol 1 (7):16070. doi:10.1038/nmicrobiol.2016.70

19. Duan D, Scoffield JA, Zhou X, Wu H (2016) Fine-tuned production of hydrogen peroxide promotes biofilm formation of *Streptococcus* parasanguinis by a pathogenic cohabitant Aggregatibacter actinomycetemcomitans. Environ Microbiol 18 (11):4023-4036. doi:10.1111/1462-2920.13425

20. Duhl KL, Tefft NM, TerAvest MA (2018) Shewanella oneidensis MR-1 utilizes both sodium- and proton-pumping NADH dehydrogenases during aerobic growth. Appl Environ Microbiol 84 (12):e00415-00418. doi:10.1128/aem.00415-18

21. Facklam R (2002) What happened to the streptococci: Overview of taxonomic and nomenclature changes. Clin Microbiol Rev 15 (4):613-+. doi:10.1128/Cmr.15.4.613-630.2002

22. Fey PD, Endres JL, Yajjala VK, Widhelm TJ, Boissy RJ, Bose JL, Bayles KW (2013) A genetic resource for rapid and comprehensive phenotype screening of nonessential *Staphylococcus aureus* genes. mBio 4 (1):e00537-00512. doi:10.1128/mBio.00537-12

23. Gao L, Xu T, Huang G, Jiang S, Gu Y, Chen F (2018) Oral microbiomes: more and more importance in oral cavity and whole body. Protein Cell 9 (5):488-500. doi:10.1007/s13238-018-0548-1

24. Garnett JA, Simpson PJ, Taylor J, Benjamin SV, Tagliaferri C, Cota E, Chen Y-YM, Wu H, Matthews S (2012) Structural insight into the role of *Streptococcus* parasanguinis Fap1 within oral biofilm formation. Biochem Biophys Res Commun 417 (1):421-426. doi:10.1016/j.bbrc.2011.11.131

25. Ghadiali SN, Banks J, Swarts JD (2002) Effect of surface tension and surfactant administration on Eustachian tube mechanics. J Appl Phys 93 (3):1007-1014. doi:10.1152/japplphysiol.01123.2001

26. Hakalehto E, Vilpponen-Salmela T, Kinnunen K, von Wright A (2011) Lactic acid bacteria enriched from human gastric biopsies. ISRN Gastroenterol 2011:109183. doi:10.5402/2011/109183

27. Hall BG (2018) Phylogenetic trees made easy: a how-to manual. Fifth edition. edn. Sinauer Associates is imprint of Oxford University Press, New York

28. Hall-Stoodley L, Hu FZ, Gieseke A, Nistico L, Nguyen D, Hayes J, Forbes M, Greenberg DP, Dice B, Burrows A, Wackym PA, Stoodley P, Post JC, Ehrlich GD, Kerschner JE (2006) Direct detection of bacterial biofilms on the middle-ear mucosa of children with chronic otitis media. JAMA 296 (2):202-211. doi:10.1001/jama.296.2.202

29. Honjo I, Hayashi M, Ito S, Takahashi H (1985) Pumping and clearance function of the eustachian tube. Am J Otolaryngol 6 (3):241-244. doi:10.1016/S0196-0709(85)80095-8

30. Huch M, De Bruyne K, Cleenwerck I, Bub A, Cho GS, Watzl B, Snauwaert I, Franz CM, Vandamme P (2013) *Streptococcus* rubneri sp. nov., isolated from the human throat. Int J Syst Evol Microbiol 63 (Pt 11):4026-4032. doi:10.1099/ijs.0.048538-0

31. Kaci G, Goudercourt D, Dennin V, Pot B, Doré J, Ehrlich SD, Renault P, Blottière HM, Daniel C, Delorme C (2014) Anti-Inflammatory properties of *Streptococcus* salivarius, a commensal bacterium of the oral cavity and digestive tract. Appl Environ Microbiol 80 (3):928-934. doi:10.1128/aem.03133-13

32. Kaito C, Sekimizu K (2007) Colony spreading in *Staphylococcus aureus*. J Bacteriol 189 (6):2553-2557. doi:10.1128/jb.01635-06

33. Kandler O (1983) Carbohydrate metabolism in lactic acid bacteria. Antonie van Leeuwenhoek 49 (3):209-224. doi:10.1007/bf00399499

34. Keith ER, Podmore RG, Anderson TP, Murdoch DR (2006) Characteristics of *Streptococcus pseudopneumoniae* isolated from purulent sputum samples. J Clin Microbiol 44 (3):923-927. doi:10.1128/jcm.44.3.923-927.2006

35. Khan R, Petersen FC, Shekhar S (2019) Commensal bacteria: An emerging player in defense against respiratory pathogens. Front Immunol 10 (1203). doi:10.3389/fimmu.2019.01203

36. Knapp JS, Hook EW, 3rd (1988) Prevalence and persistence of *Neisseria* cinerea and other *Neisseria* spp. in adults. J Clin Microbiol 26 (5):896-900. doi:10.1128/JCM.26.5.896-900.1988

37. Kocur M, Kloos WE, SCHLEIFER K-H (2006) The genus *Micrococcus*. In: Dworkin M, Falkow S, Rosenberg E, Schleifer K-H, Stackebrandt E (eds) The Prokaryotes: Volume 3: Archaea. Bacteria: Firmicutes, Actinomycetes. Springer New York, New York, NY, pp 961-971. doi:10.1007/0-387-30743-5_37

38. Köhler T, Curty LK, Barja F, van Delden C, Pechère J-C (2000) Swarming of *Pseudomonas aeruginosa* is dependent on cell-to-cell signaling and requires flagella and pili. J Bacteriol 182 (21):5990-5996. doi:10.1128/jb.182.21.5990-5996.2000

39. Kolenbrander PE (2000) Oral microbial communities: biofilms, interactions, and genetic systems. Annu Rev Microbiol 54:413-437. doi:10.1146/annurev.micro.54.1.413

40. Kooken JM, Fox KF, Fox A (2012) Characterization of *Micrococcus* strains isolated from indoor air. Mol Cell Probes 26 (1):1-5. doi:10.1016/j.mcp.2011.09.003

41.`Koskinen K, Reichert JL, Hoier S, Schachenreiter J, Duller S, Moissl-Eichinger C, Schopf V (2018) The nasal microbiome mirrors and potentially shapes olfactory function. Sci Rep 8 (1):1296. doi:10.1038/s41598-018-19438-3

42. Kriebel K, Hieke C, Müller-Hilke B, Nakata M, Kreikemeyer B (2018) Oral biofilms from symbiotic to pathogenic interactions and associated disease – Connection of periodontitis and rheumatic arthritis by peptidylarginine deiminase. Front Microbiol 9 (53). doi:10.3389/fmicb.2018.00053

43. Kumar S, Stecher G, Li M, Knyaz C, Tamura K (2018) MEGA X: Molecular Evolutionary Genetics Analysis across computing platforms. Mol Biol Evol 35 (6):1547-1549. doi:10.1093/molbev/msy096

44. Lee J-Y, Jacob KM, Kashefi K, Reguera G (2021) Oral seeding and niche-adaptation of middle ear biofilms in health. Biofilm 3:100041. doi:10.1016/j.bioflm.2020.100041

45. Liu G, Tang CM, Exley RM (2015) Non-pathogenic *Neisseria*: Members of an abundant, multi-habitat, diverse genus. Microbiology 161 (7):1297-1312. doi:10.1099/mic.0.000086

46. Mashima I, Nakazawa F (2015) Interaction between *Streptococcus* spp. and *Veillonella tobetsuensis* in the early stages of oral biofilm formation. J Bacteriol 197 (13):2104-2111. doi:10.1128/jb.02512-14

47. Mason MR, Chambers S, Dabdoub SM, Thikkurissy S, Kumar PS (2018) Characterizing oral microbial communities across dentition states and colonization niches. Microbiome 6 (1):67. doi:10.1186/s40168-018-0443-2

48. McCormack MG, Smith AJ, Akram AN, Jackson M, Robertson D, Edwards G (2015) *Staphylococcus aureus* and the oral cavity: an overlooked source of carriage and infection? Am J Infect Control 43 (1):35-37. doi:10.1016/j.ajic.2014.09.015

49. McGuire JF (2002) Surfactant in the middle ear and eustachian tube: a review. Int J Pediatr Otorhinolaryngol 66 (1):1-15. doi:10.1016/s0165-5876(02)00203-3

50. Merritt JH, Kadouri DE, O'Toole GA (2005) Growing and analyzing static biofilms. Current protocols in microbiology Chapter 1:Unit 1B 1. doi:10.1002/9780471729259.mc01b01s00

51. Munoz R, Yarza P, Ludwig W, Euzeby J, Amann R, Schleifer KH, Glockner FO, Rossello-Mora R (2011) Release LTPs104 of the All-Species Living Tree. Syst Appl Microbiol 34 (3):169-170. doi:10.1016/j.syapm.2011.03.001

52. Ohara-Nemoto Y, Haraga H, Kimura S, Nemoto TK (2008) Occurrence of staphylococci in the oral cavities of healthy adults and nasal oral trafficking of the bacteria. J Med Microbiol 57 (Pt 1):95-99. doi:10.1099/jmm.0.47561-0

53. Partridge JD, Harshey RM (2013) Swarming: Flexible roaming plans. J Bacteriol 195 (5):909-918. doi:10.1128/jb.02063-12

54. Patterson MJ (1996) *Streptococcus*. In: Baron S (ed) Medical Microbiology. Fourth edn., Galveston (TX),

55. Poje G, Redfield RJ (2003) General methods for culturing *Haemophilus influenzae*. Methods Mol Med 71:51-56. doi:10.1385/1-59259-321-6:51

56. Pollitt EJG, Diggle SP (2017) Defining motility in the Staphylococci. Cell Mol Life Sci 74 (16):2943-2958. doi:10.1007/s00018-017-2507-z

57. Quinones B, Dulla G, Lindow SE (2005) Quorum sensing regulates exopolysaccharide production, motility, and virulence in *Pseudomonas syringae*. Mol Plant Microbe Interact 18 (7):682-693. doi:10.1094/MPMI-18-0682

58. Raabe VN, Shane AL (2019) Group B *Streptococcus* (*Streptococcus agalactiae*). Microbiol Spectr 7 (2):10.1128/microbiolspec.GPP1123-0007-2018. doi:10.1128/microbiolspec.GPP3-0007-2018

59. Redanz S, Cheng X, Giacaman RA, Pfeifer CS, Merritt J, Kreth J (2018) Live and let die: Hydrogen peroxide production by the commensal flora and its role in maintaining a symbiotic microbiome. Mol Oral Microbiol 33 (5):337-352. doi:10.1111/omi.12231

60. Reddy MS, Murphy TF, Faden HS, Bernstein JM (1997) Middle ear mucin glycoprotein: Purification and interaction with non-typable *Haemophilus influenzae* and *Moraxella*

catarrhalis. Otolaryngol Head Neck Surg 116 (2):175-180. doi:10.1016/S0194-59989770321-8

61. Regev-Yochay G, Trzcinski K, Thompson CM, Malley R, Lipsitch M (2006) Interference between *Streptococcus pneumoniae* and *Staphylococcus aureus*: In vitro hydrogen peroxide-mediated killing by *Streptococcus pneumoniae*. J Bacteriol 188 (13):4996-5001. doi:10.1128/JB.00317-06

62. Rios-Covian D, Salazar N, Gueimonde M, de los Reyes-Gavilan CG (2017) Shaping the metabolism of intestinal Bacteroides population through diet to improve human health. Front Microbiol 8. doi:10.3389/fmicb.2017.00376

63. Sade J (1971) Mucociliary flow in the middle ear. Ann Otol Rhinol Laryngol 80 (3):336-341. doi:10.1177/000348947108000306

64. Schilder AG, Chonmaitree T, Cripps AW, Rosenfeld RM, Casselbrant ML, Haggard MP, Venekamp RP (2016) Otitis media. Nat Rev Dis Primers 2 (1):16063. doi:10.1038/nrdp.2016.63

65. Schillinger U, Lücke FK (1989) Antibacterial activity of *Lactobacillus* sake isolated from meat. Appl Environ Microbiol 55 (8):1901-1906. doi:10.1128/aem.55.8.1901-1906.1989

66. Schneider CA, Rasband WS, Eliceiri KW (2012) NIH Image to ImageJ: 25 years of image analysis. Nat Methods 9 (7):671-675. doi:10.1038/nmeth.2089

67. Sheng J, Marquis RE (2006) Enhanced acid resistance of oral streptococci at lethal pH values associated with acid-tolerant catabolism and with ATP synthase activity. FEMS Microbiology Lett 262 (1):93-98. doi:10.1111/j.1574-6968.2006.00374.x

68. Siegel SJ, Weiser JN (2015) Mechanisms of bacterial colonization of the respiratory tract. Annu Rev Microbiol 69:425-444. doi:10.1146/annurev-micro-091014-104209

69. Smith PA, Sherman JM (1942) The lactic acid fermentation of streptococci. J Bacteriol 43 (6):725-731. doi:10.1128/JB.43.6.725-731.1942

70. Stackebrandt E, Ebers J (2006) Taxonomic parameters revisited: tarnished gold standards. Microbiol Today 33 (4):152–155

71. Tonnaer EL, Mylanus EA, Mulder JJ, Curfs JH (2009) Detection of bacteria in healthy middle ears during cochlear implantation. Arch Otolaryngol Head Neck Surg 135 (3):232-237. doi:10.1001/archoto.2008.556

72. Trunk T, Khalil HS, Leo JC (2018) Bacterial autoaggregation. AIMS Microbiol 4 (1):140-164. doi:10.3934/microbiol.2018.1.140

73. Tsompanidou E, Denham EL, Becher D, de Jong A, Buist G, van Oosten M, Manson WL, Back JW, van Dijl JM, Dreisbach A (2013) Distinct roles of phenol-soluble modulins in

spreading of *Staphylococcus aureus* on wet surfaces. Appl Environ Microbiol 79 (3):886-895. doi:10.1128/aem.03157-12

74. Van Hoogmoed CG, Geertsema-doornbusch GI, Teughels W, Quirynen M, Busscher HJ, Van der Mei HC (2008) Reduction of periodontal pathogens adhesion by antagonistic strains. Oral Microbiol Immunol 23 (1):43-48. doi:10.1111/j.1399-302X.2007.00388.x

75. Van Hoogmoed CG, Geertsema-Doornbusch GI, Teughels W, Quirynen M, Busscher HJ, Van der Mei HC (2008) Reduction of periodontal pathogens adhesion by antagonistic strains. Oral Microbiol Immunol 23 (1):43-48. doi:10.1111/j.1399-302X.2007.00388.x

76. Wandersman C (1989) Secretion, processing and activation of bacterial extracellular proteases. Mol Microbiol 3 (12):1825-1831. doi:10.1111/j.1365-2958.1989.tb00169.x

77. Wang K, Lu W, Tu Q, Ge Y, He J, Zhou Y, Gou Y, Van Nostrand JD, Qin Y, Li J, Zhou J, Li Y, Xiao L, Zhou X (2016) Preliminary analysis of salivary microbiome and their potential roles in oral lichen planus. Sci Rep 6:22943. doi:10.1038/srep22943

78. Wang M, Ahrné S, Jeppsson B, Molin G (2005) Comparison of bacterial diversity along the human intestinal tract by direct cloning and sequencing of 16S rRNA genes. FEMS Microbiol Ecol 54 (2):219-231. doi:10.1016/j.femsec.2005.03.012

79. Welch JLM, Dewhirst FE, Borisy GG (2019) Biogeography of the oral microbiome: The site-specialist hypothesis. Annu Rev Microbiol. doi:10.1146/annurev-micro-090817-062503

80. Wilson CB, Weaver WM (1985) Comparative susceptibility of group B streptococci and *Staphylococcus aureus* to killing by oxygen metabolites. J Infect Dis 152 (2):323-329. doi:10.1093/infdis/152.2.323

81. World Health O, Centers for Disease C, Prevention (2011) Laboratory methods for the diagnosis of meningitis caused by *Neisseria meningitidis*, *Streptococcus pneumoniae*, and *Haemophilus influenzae*: WHO manual. 2nd ed edn. World Health Organization, Geneva

82. Wu X, Gordon O, Jiang W, Antezana BS, Angulo-Zamudio UA, Del Rio C, Moller A, Brissac T, Tierney ARP, Warncke K, Orihuela CJ, Read TD, Vidal JE (2019) Interaction between *Streptococcus pneumoniae* and *Staphylococcus aureus* generates ·OH radicals that rapidly kill *Staphylococcus aureus* strains. J Bacteriol 201 (21). doi:10.1128/jb.00474-19

83. Yarza P, Richter M, Peplies J, Euzeby J, Amann R, Schleifer KH, Ludwig W, Glockner FO, Rossello-Mora R (2008) The All-Species Living Tree project: A 16S rRNA-based phylogenetic tree of all sequenced type strains. Syst Appl Microbiol 31 (4):241-250. doi:10.1016/j.syapm.2008.07.001

84. Zhao G-Z, Li J, Qin S, Zhang Y-Q, Zhu W-Y, Jiang C-L, Xu L-H, Li W-J (2009) *Micrococcus yunnanensis* sp. nov., a novel actinobacterium isolated from surface-sterilized *Polyspora axillaris* roots. Int J Syst Evol Microbiol 59 (10):2383-2387. doi:10.1099/ijs.0.010256-0

CHAPTER 4

CONTRIBUTION OF MUCINS TO THE RAPID SPREADING OF NASOPHARYNGEAL STAPHYLOCOCCI ON VISCOUS SURFACES

ABSTRACT

Nasopharyngeal carriage of *Staphylococcus aureus* and *Staphylococcus epidermidis* disperses these strains in perioral regions and, from there, to the middle ear space, increasing the risk of otic infections. Yet, the mechanisms that allow nasopharyngeal staphylococci to invade the middle ear mucosa and infect are not fully understood. Here we show that clinical isolates of *S. aureus* and *S. epidermidis* rapidly spread and formed dendritic branches on semisolid agar media in the presence of mucin glycoproteins. Spreading and dendritic expansion correlated well with the ability of the strains to use mucin as a growth substrate, though not always. Mucin glycosylation, on the other hand, influenced the wettability of the medium and the ability of the strains to move rapidly on the surface. These results point at the lubricating and hydrating properties of gel-forming mucins as the main contributor to staphylococcal surface motility. Mucin also stimulated colony spreading and dendrite formation by laboratory strains of *S. aureus* and *S. epidermidis*. While mucin-induced colony spreading was not regulated by the *agr* quorum sensing in *S. aureus* JE2, dendritic expansion from the colony edge required the endogenous secretion of surfactant-active phenol-soluble modulins (PSMs). This motile response was exacerbated by the addition of PSM-containing supernatants from the most robust clinical spreaders. These results suggest that staphylococcal invasive behaviors are enhanced by the lubricating properties of mucins, providing a plausible mechanism for the rapid spreading of the nasopharyngeal strains to the middle ear during otological conditions that lead to mucus hypersecretion and increase the risk infections.

INTRODUCTION

Staphylococci are common residents of the nasal flora [1] and readily disperse into the neighboring oral cavity via the pharynx [2]. As a result, they are frequently isolated from oral and perioral regions [2, 3]. Staphylococcal strains can also be isolated from otic secretions draining through the nasopharyngeal orifice of the Eustachian tube [4] when the tube opens to periodically ventilate the middle ear cavity [5]. Though isolated from otic secretions, *Staphylococcus*-like sequences are not always detected in these samples [4], suggesting they are transient migrants [6]. Furthermore, otic streptococcal commensals readily inhibit the growth of staphylococcal strains, consistent with a protective role for the natural otic microbiota in health [6]. Yet, pediatric patients with acute otitis media often carry multi-drug resistant strains of *Staphylococcus aureus* [7] and both *S. aureus* and *Staphylococcus epidermidis* strains can be isolated at high frequency from the effusions of patients with chronic otitis media [8]. Given the role that the hyperproduction of otic mucin glycoproteins has in the onset and persistence of otitis media [9], staphylococcal intrusion may be facilitated by changes in the rheological properties of the otic mucus layer caused by the mucins.

Despite being non-flagellated, *Staphylococcus aureus* spreads rapidly (100 μm/min) on wet surfaces when inoculated at high cell densities [10]. This mode of surface movement, named "colony spreading", is a passive form of growth expansion facilitated by the hydration of the underlying medium (0.24% w/v agar plates) [10]. Increasing the agar concentration to 0.3%, as typically used to test for flagellar-mediated swimming, reduces *S. aureus* surface spreading but was reported to promote the movement of cells from the colony edge in slimeless trails ("comets") that can eventually grow into dendrite-like branches [11]. Colony spreading and dendritic expansion are triggered at high cell densities through the activation of the quorum

sensing Agr two-component system (AgrC histidine kinase and AgrA response regulator) [12]. The phosphorylation of the AgrA response regulator leads to the secretion of phenol-soluble modulins (PSMs) [10, 12, 13], including two surfactant-active PSMs (PSMa3 and PSMg) that are the major facilitators of colony spreading and dendritic expansion [14]. A close relative of *S. aureus*, *Staphylococcus epidermidis*, can also spread on wet surfaces, albeit at much lower speeds (6 μm/min), via a mechanism called "darting" [15]. While *S. aureus* colony spreading requires lubrication to reduce frictional forces between the cells and the underlying surface, *S. epidermidis* darting results from "the ejection of cells from a capsulated aggregate" [15]. *S. aureus* aggregates can also detach and roll away from microcolonies as if darting but only under high fluid shear forces [16].

It is perhaps not coincidental that the two staphylococcal species with known modes of surface translocation (*S. aureus* and *S. epidermidis*) are also abundant in the mucoid effluents of chronic otitis media patients [8]. This otological condition is associated with the persistent hyperproduction of gel-forming (MUC5B) and lubricating (MUC4) mucins in the middle ear [17], which may facilitate staphylococcal spreading. By controlling the hydration and lubrication of the mucus layer [18], mucins can promote the translocation (or "surfing") of flagellated bacteria on swarming plates [19, 20]. Surfing motility in *Pseudomonas aeruginosa* is regulated by quorum sensing but not in other flagellated bacteria, consistent with a convergent adaptive response for mucosal colonization facilated by mucin lubrication [21]. Thus, we tested for a similar effect of mucin on staphylococcal surface movement. Here we show that mucin induces colony spreading and rapid dendritic expansion of clinical and laboratory strains of *S. aureus* and *S. epidermidis* in a process that requires the expression of PSMs via the *agr*-quorum sensing

system. This, and the ability of most strains to degrade and grow with mucin, confer on these staphylococci a competitive advantage for mucosal colonization.

MATERIALS AND METHODS

Bacterial strains and culture conditions

The bacterial strains used in this study are 9 staphylococcal strains previously isolated from buccal, oropharyngeal, and otic secretions collected from 4 healthy young adults (19-32 years old) as a part of a larger study approved by the Michigan State University Biomedical and Physical Health Review Board (IRB # 17-502) [23]. The isolates were routinely grown in liquid or agar-solidified tryptic soy medium (TSB and TSA plates, respectively), as previously described [22]. Closely related laboratory strains used in the study included *S. aureus* JE2, *S. aureus* LAC, *S. epidermidis* RP62a, *S. lugdunensis* N920143, and *S. haemolyticus* NRS9. *S. aureus* JE2 mutants were from the Nebraska TN Library (https://www.unmc.edu/pathology/csr/research/library.html) and carried the following transposon insertions: *agrA::*T*n erm* NE1532, *agrB::*T*n erm* NE95, *agrC::*T*n erm* NE873, *sarA::*T*n erm* NE1193 and *rot::*T*n erm* NE386. When indicated, we also included in the study *S. aureus* LAC USA300 strain [51] and the protease-deficient deletion mutant *S. aureus* LAC strain AH1919 ("ΔESPN") [52]. All the laboratory strains and mutants were kindly provided by Dr. Neal Hammer (Department of Microbiology and Molecular Genetics; Michigan State University). The clinical and laboratory strains were grown overnight in 5 mL of TSB with gentle agitation at 37˚C.

DNA sequencing and phylogenetics analysis

Table 4.1 lists the NCBI accession number for the 16S rRNA full length sequences retrieved from Illumina contigs for each of the clinical strains. Three of the sequences were

reported elsewhere [6]. The remaining strains were grown in 2 ml of TSB at 37°C for 24 h with gentle agitation before harvesting the cells by centrifugation and extracting their genomic DNA for sequencing. DNA sequencing, 16S rRNA identification, and phylogenetic analysis were as previously described [22]. NCBI accession numbers can be found in table 4.1.

Mucin planktonic growth and biofilm assays

All the clinical and laboratory strains used in this study were grown from frozen stocks overnight in 5 ml TSB at 37˚C with gentle agitation (~200 rpm). Overnight cultures (500 µl) were diluted in 5 ml of TSB and grown to mid-exponential phase (OD600 ~0.5-0.6) before a new transfer (500µl inoculum) to 5 ml of TSB. The culture was then grown to stationary phase (OD600 ~0.9-1.0) and diluted in TSB (500 µl in 5 ml). Approximately 18 µl of this cell suspension were added to the wells of a Corning® 96-well clear round bottom TC-treated plate (Corning 3799) and mixed with 162 µl of TSB, 50% TSB (TSB with half the concentration of the tryptic soy) or 50% TSB with 0.4% (w/v) Type II, porcine stomach mucin (Sigma Aldrich, M2378). Growth curves for each strain included 3 biological replicates, each containing 8 replicate wells. Plate incubation was at 37oC in a BioTek PowerWave HT plate reader. Growth was monitored spectrophotometrically every 30 min (OD630 after gentle agitation for 0.1 s). Each plate included an uninoculated well with the appropriate medium (TSB, 50% TSB or 50% TSB + 0.4% mucin) to use as a blank. After 18 h of incubation to reach stationary phase in the cultures, the liquid culture was discarded and the biofilms were stained with 0.1% (w/v) crystal violet staining, as previously described [53].

Motility plate assays

Clinical isolates and laboratory strains were screened for surface translocation on motility TSA plates (0.3% w/v agar) with or without 0.4% (w/v) mucin, provided as pure porcine gastric

mucin, commercial porcine stomach mucin (Sigma Aldrich, type II, M2378), or commercial bovine submaxillary mucin (Sigma Aldrich, M3895), as a modification of a previously described assay (79). Pure porcine gastric mucin was kindly donated by Dr. Andrew VanAlst (Dr. Victor DiRita's laboratory at Michigan State University), who purified the mucin from pig intestines using a previously described protocol [54]. When indicated, experiments also included control plates with 0.5% (w/v) TSA (swarming). The protocol to culture cells for inoculation on semisolid agar plates is as described elsewhere [22]. Briefly, the strains were grown overnight in 5 mL TSB at 37°C with gentle agitation, then back diluted in 1 mL of TSB to a starting OD of 0.1 to prepare the inoculum for the plate assay. A drop (1 µl) of the cell suspension was spot plated on the agar surface and allowed to absorb at room temperature until dry. The plates were incubated at 37°C up to 62 hours and imaged periodically using an iPhone 11 at 2.4x zoom. When indicated, the extent of colony expansion was calculated by subtracting the average diameter of the central colony from the average diameter of the dendritic expansion zone (cm) using the measuring tools of ImageJ [55]. The extent of dendritic expansion was also estimated as the perimeter of the colony with the ImageJ stock toolkit. For these measurements, we first converted the image to 8-bit type, enhanced the contrast, and converted the image to binary. We then used the "find edges" function in the ImageJ toolbar options to outline the colony edge and manually traced any area, as needed, with the "wand tracing" tool before measuring the perimeter.

Isolation of PSM-containing supernatants and chemical complementation assays

The isolation of PSM-containing supernatants and plate assays to test their effect on staphylococcal colony spreading and dendritic expansion followed previously described protocols [22]. Where indicated, supernatants were obtained 10 ml overnight cultures (OD_{600} of

~1, stationary phase) of *S. aureus* JE2, *S. aureus* L0021-02, or *S. epidermidis* L0021-06. The cells were pelleted down by centrifugation (Eppendorf 5810R, 3220 g, 10 min) and the culture supernatant fluids were collected, and filter sterilized prior to the plate assays. Test strains were grown at 37^{o}C overnight in 5 ml of TSB, diluted in fresh TSB to an OD_{600} of 0.1, and harvested by centrifugation (Eppendorf 5417, 20817 g, 5 min). Cell resuspension was in equal volumes (1 mL) of filter sterilized supernatant and fresh TSB. The cell suspension was then spot plated on 0.3% (w/v) TSA plates with or without 0.4% (w/v) porcine stomach mucin and incubated at 37^{o}C for 8, 18, 42 and 62h before photographing the colonies.

Surfactant detection plate

Surfactant production of laboratory strains and clinical isolates were assessed with a previously described atomized oil assay (40) essentially as described [22]. In short, isolates were inoculated in 5 mL TSB and incubated at 37°C with gentle agitation. Five milliliters of overnight cultures were spot plated on TSA plates and allowed to dry at room temperature. Plates were placed at 37°C for 24 h, after which an airbrush was used to apply mineral oil to plate surface. Presence of halo around colony indicated presence of secreted surfactants.

Mucin degradation assay

Mucin degradation ability was screened in laboratory and clinical isolates by spot plating 5 µl of overnight cultures on solidified (1.5% w/v) TSA plates containing 0.5% porcine stomach mucin (Type II, Sigma Aldrich). The culture drop was allowed to absorb for ~30 min at room temperature before incubating the plates overnight at 37˚C for 24 h. Images were taken with iPhone 11 for qualitative analysis.

RESULTS

Mucin induces surface expansion and dendritic behavior in clinical staphylococcal strains

We used soft agar plate assays (Fig. 4.1A) to investigate the effect of mucin on the spreading of 9 staphylococcal strains previously isolated from the oral cavity and perioral regions of 4 healthy young adults [22, 23]. Phylogenetic analysis of full-length 16S rRNA sequences placed the strains as close relatives (bootstrap support >90%) of *S. aureus, S. epidermidis,* or *Staphylococcus hominis* (Fig. 4.6). None of the isolates spread significantly or formed dendrites on soft agar surfaces typically used to study swarming motility (0.5% agar [24]) (Fig. 4.1A). Reducing the agar concentration to 0.3% to increase the hydration of the medium did not stimulate spreading either (Fig. 4.1A). Although this agar concentration (0.3% w/v) can reportedly promote the movement of some *S. aureus* strains in comets and dendrites [11], we did not observe any trails or branched structures emerging from the periphery of any of the colonies either (Fig. 4.1A). However, addition of mucin (0.4% pure porcine gastric mucin) stimulated the rapid expansion of some colonies on the plate surface after 18 h of incubation at 37°C (Fig. 4.1A). The *S. epidermidis* and *S. aureus* clinical strains spread more rapidly on the mucin plates than any other strain and all but one (B0021-03) displayed dendritic behavior at the colony edge (Fig. 4.1A). By contrast, clinical strains of *S. hominis* did not show a mucin-dependent response at 18 h. Longer incubation times (≥42 h) stimulated further expansion of the robust spreaders (*S. epidermidis* and *S. aureus*) but had only modest effects on the spreading of the *S. hominis* colonies (Fig. 4.1B). Therefore, mucin promotes surface motility and dendritic expansion in a species-specific manner, with clinical strains of *S. aureus* and *S. epidermidis* showing the most robust response.

Mucin-induced expansion correlates with the ability of clinical strains to use mucin as a growth substrate

Commercial porcine stomach mucin (Type II) also induced the spreading and dendritic expansion of the clinical isolates of *S. aureus* and *S. epidermidis* (Fig. 4.2A), though not as strongly as with pure mucin (Fig. 4.1B). This is likely due to the lower purity of the commercial mucin substrate, which decreases the actual concentration of mucin in the plates. Using the commercial substrate, we also examined if the clinical strains could grow with mucin as a carbon and energy source in liquid cultures (Fig. 4.2B). In general, there was a positive correspondence between the ability of the strains to translocate on the mucin plates and use mucin for growth. For example, mucin promoted the expansion of *S. epidermidis* L0021-06 colonies (Fig. 4.2A) and supported high growth yields in planktonic cultures (Fig. 4.2B) and the secretion of mucinolytic enzymes (Fig. 4.2C). Reversely, *S. hominis* L0020-04 did not spread on mucin plates nor did it use mucin as a growth substrate (Fig. 4.2B) or secrete mucinases (Fig. 4.2C). Notably, all the *S. aureus* strains spread on soft-agar plates and grew planktonically with mucin, in some cases showing clear diauxic growth phases as cells transitioned from growing with the tryptic soy nutrients in the broth to mucin-based growth (Fig. 4.2B, arrows). Additionally, all but one (L0021-02) strain of *S. aureus* had detectable levels of mucinase activity (Fig. 4.2C). The positive correlation between surface translocation and mucin growth suggests that the two processes are linked. This behavior could be analogous to the translocation of flagellated bacteria on semisolid (0.5% agar) surfaces (swarming) [25], whereby cells use motility to disperse to nutrient-rich areas. Once there, the cells stop moving and grow on the available substrates before expanding again to scavenge for more nutrients. This sequential motile-growth behavior produces rings of expansion and, in some organisms, in social behaviors or swarms that expand

the colony periphery into dendritic-like trails such as those induced by mucin on 0.3% agar plates (Fig. 4.1A).

The hydration of the mucin hydrogels modulates staphylococcal colony spreading and dendritic expansion

We also evaluated if laboratory relatives of the staphylococcal clinical isolates retained the ability to translocate rapidly in the presence of mucin. For these experiments, we used as test strains *S. aureus* JE2, *S. epidermidis* RP62a, *S. lugdunensis* N920143, and *S. haemolyticus* NRS9. The latter two are close relatives of the *S. hominis* clinical isolates used in our studies (Fig. 4.6). We reproduced in the laboratory strains similar colony spreading and dendritic expansion phenotypes with mucin (Fig. 4.3A). Yet, unlike the clinical strains, surface motility did not always correlate with the ability of the laboratory strains to grow with mucin (Fig. 4.3B). For example, mucin-induced spreading was modest in the laboratory strain of *S. epidermidis* although the strain secreted mucinases (Fig. 4.3A) and grew to high yields with mucin (Fig. 4.3B). Furthermore, the spreading phenotype was not as strong as the one observed in the clinical strain L0021-06, possibly due to laboratory domestication. *S. lugdunensis* and *S. haemolyticus*, on the other hand, shared with the clinical *S. hominis* relatives their inability to spread on mucin surfaces (Fig. 4.3A), to produce mucinase (Fig. 4.3A), or to grow with mucin (Fig. 4.3B). Mucin did promote the rapid spreading and dendritic expansion of *S. aureus* JE2 (Fig. 4.3A), as observed with the clinical isolates (Fig. 4.2). However, the laboratory strain did not have high mucinase activity (Fig. 4.3A) nor did it grow with mucin as sole carbon and energy source (Fig. 4.3B). Thus, the rapid surface expansion of *S. aureus* JE2 in the presence of mucin is independent of mucin growth. This suggests that mucin lubrication rather than assimilation

facilitates the rapid spreading and dendritic expansion of staphylococcal colonies on 0.3% (w/v) agar plates.

As mucin glycosylation can affect the hydration and lubricating properties of mucin hydrogels [18], we compared the surface translocation of the laboratory strains in the presence of porcine stomach and bovine submaxillary mucins (Fig. 4.3C). These two mucins are similar in size and structural conformation in aqueous solutions [26] but have different concentrations of sialic acid (9-24% in bovine submaxillary mucin and ≤1.2% in porcine stomach mucin). Therefore, the net negative charge of the submaxillary mucin is greater than the gastric type. The distribution of the sialic acid moieties is also different in the two mucins, which affects the exposure of hydrophobic regions in the glycoprotein. Thus, the hydrophobic pockets are buried in the gastric mucin, which increases the hydration of the mucin gel [26]. This is expected to facilitate water movement through the semisolid agar, reducing frictional forces between the cells and the agar surface and stimulating staphylococcal motility. Consistent with this, the more glycosylated gastric mucin stimulated staphylococcal spreading while the less glycosylated, submaxillary type did not (Fig. 4.3C). Spreading of the *S. epidermidis* and *S. aureus* colonies in the presence of porcine stomach mucin increased with prolonged incubation and was significantly greater than the passive growth expansion of the colonies on non-mucin control plates ($p \leq 0.05$, pairwise t-test analysis). The more glycosylated mucin promoted some colony spreading of *S. haemolyticus*, albeit only after 62 h growth ($p \leq 0.05$), and had no effect on *S. haemolyticus* colonies (Fig. 4.3C). The less glycosylated bovine submaxillary mucin, on the other hand, did not stimulate surface movement of any strain even after extended incubated (Fig. 4.3C). Furthermore, colony spreading was significantly reduced compared to the non-mucin control plates, consistent with an inability of the strains to acquire nutrients and grow on the

semisolid agar plates (Fig. 4.3C). This is consistent with the reduced hydration of hydrogels of submaxiliary mucin [26]. Thus, although these plates have the same concentration (w/v) of mucin as in the gastric mucin plates, water carriage through the hydrogels is reduced. This, in turn, reduces nutrient mobilization and lubrication of cells spreading from the central colony.

Mucin-induced dendritic expansion is regulated by quorum sensing

We gained insights into the molecular mechanisms controlling mucin-induced surface movement by evaluating the colony spreading and dendritic expansion phenotypes of mutants of *S. aureus* JE2 inactivated in key components of the agr quorum sensing system (Tn::agrA, Tn::agrB, Tn::agrC, Tn::sarA, and the agr-sarA regulated transcriptional regulator rot; Fig A2.2). The dendrites observed in 18-h WT colonies grown on mucin plates (Fig. 4.3A) grew with prolonged incubation and consolidated after 42h to form colonies with undulated edges (Fig. 4.4A). As a result, the perimeter of the mucin-grown WT colonies increases significantly at 42 h compared to the non-mucin controls (Fig. 4.4B). Inactivation of the agr quorum sensing system prevented dendritic expansion of the spreading colonies and, consequently, the colonies had smooth edges and smaller perimeters than the WT (Fig. 4.4A and B, respectively). For example, deletion of the gene encoding the AgrB transporter (Fig. 4.7) prevented dendritic expansion (Fig. 4.4A) and reduced the perimeter of the mucin-grown colonies 1.4-fold ($p \leq 0.005$) (Fig. 4.4B). This is because this strain cannot synthesize the AgrB endopeptidase and chaperone protein needed for the maturation and export of the agr autoinducer peptide [27-29]. Similarly, inactivation of the quorum sensing histidine kinase (AgrC) or the response regulator (AgrA) prevented dendritic expansion and reduced colony perimeters compared to the WT (Fig. 4.4). Insertional inactivation of the transcriptional enhancer of the agrACDB and RNAIII/hld operons in a Tn::sarA mutant produced colonies with slightly undulated edges and greater perimeters

than the AgrB- or AgrC-defective mutants ($p \leq 0.005$). Still, the sarA mutant had reduced dendritic expansion compared to the WT (1.2-fold average perimeter reduction; $p \leq 0.05$) (Fig. 4.4). Inactivation of SarA reduces the levels of secreted PSMs in an agr-dependent manner and increases the production of extracellular proteases [30]. It is unlikely that protease hyperproduction contributed to the motility phenotype because a Tn::rot mutant, which has increased levels of proteases [31] but WT levels of secreted PSMs [32], restored dendritic expansion (Fig. 4A). Furthermore, a protease-deficient mutant of *S. aureus* LAC also showed mucin-induced dendrite formation (Fig. 4.8). This points at secreted PSMs as major facilitators of mucin-induced dendritic expansion in *S. aureus*.

Further confirming the role of PSM secretion in staphylococcal motility, an aerosolized mineral oil assay [33] only detected surfactant activity around mutants with active quorum sensing signaling networks and endogenous production of PSMs (WT, Tn::sarA and Tn::rot) (Fig. 4.9A). The sensitivity of the atomized oil assay also helped detect reduced surfactant activity in the Tn::sarA strain (Fig. 4.9A), consistent with the lower levels of PSMs secreted by this strain [34]. By contrast, inactivation of pathways needed to produce, sense or respond to the autoinducer peptide (Tn::agrA, Tn::agrB, Tn::agrC; Fig. 4.7), which prevents PSM secretion [35], produced surfactant-deficient colonies (Fig. 4.9A). As the WT strain, none of the mutants grew with mucin (Fig. 4.9B) even though one of them (Tn::sarA) had high levels of mucinase activity (Fig. 4.9A). Therefore, PSM-mediated surfactant activity in the mutants is independent on mucin growth. As PSM secretion also induces biofilm dispersal [36], we also measured biofilm formation in the presence or absence of mucin in the WT and mutant strains (Fig. 4.9C). Consistent with their inability to produce PSMs, the agr-defective mutants formed robust biofilms (Fig. 4.9). Notably, the biofilms were not as robust in the presence of mucin (Fig. 4.9).

These results provide additional evidence for the lubricating effects that mucins have in processes controlled by the surfactant activity of secreted PSMs. Given the need of staphylococcal dendrites to produce PSM surfactants in order to move in the presence of mucin, PSMs and mucins may act synergistically to facilitate the rapid dispersal of the cells.

Effect of PSM-containing supernatants from clinical strains on staphylococcal dendritic expansion

S. aureus secretes PSMs in planktonic tryptic soy broth (TSB), reaching maximum levels in stationary phase [14]. The presence of PSMs in these supernatants can induce partial dendritic expansion of agr mutants and other non-motile strains on wet surfaces (0.24% agar) [14]. We therefore adapted this supernatant assay to evaluate the effect of PSMs secreted by clinical and laboratory strains to mucin-induced translocation by test strains. *S. aureus* JE2 supernatants collected from stationary phase cultures contain 8 PSMs, including the surfactant-active peptides (PSMα3 and PSMγ) that stimulate dendritic spreading on 0.24% TSA plates [14]. However, JE2 supernatant fluids did not rescue the surface motility defect of quorum sensing mutants on mucin plates (0.3% TSA) (Fig. 4.10). The JE2 supernatant did not rescue the motility defect of the Tn::sarA mutant either, although this strain produces some low levels of surfactant-active PSMs (Fig. 4.9B). This indicates that sufficient levels of endogenous PSM production are needed for dendritic expansion with mucin to occur.

By contrast, supernatants from robust clinical spreaders (*S. aureus* L0021-02 and *S. epidermidis* L0021-06 in Fig. 4.2) greatly stimulated dendritic expansion of *S. aureus* JE2 in the presence of mucin (Fig. 4.5A). The supernatants had no effect on the spreading and dendritic expansion of colonies grown on control plates without mucin (Fig. 4.5A). Thus, both PSMs and mucins cooperate to facilitate the rapid movement of staphylococcal cells on the semisolid

surface. Supernatants from *S. aureus* L0021-02 had the greatest stimulatory effect (Fig. 4.5B), consistent with the more robust dendritic expansion of this clinical isolate on mucin plates (Fig. 4.2). However, the supernatants did not have any effect on the spreading of Tn::agrA mutant (Fig. 4.5A and B), supporting our earlier conclusion that some basal endogenous production of PSMs via the agr quorum sensing system is needed to stimulate this motile behavior. Further supporting of this, the supernatants did not promote dendritic expansion of the *S. hominis* clinical isolates either, which are strains that do not produce lubricating PSMs [37]. Interestingly, *S. aureus* L0021-02 supernatants suppressed the motility of *S. epidermidis* L0021-06 colonies (Fig. 4.5C). Given the cross-talk reported for the quorum sensing systems of these two species [38, 39], this antagonistic effect could have resulted from the presence in the *S. aureus* supernatants of inhibitors of the *S. epidermidis* agr system. Hence, *S. aureus* may target this social behavior to interfere with the spreading of competing strains, an antagonistic behavior that maximizes resource utilization.

DISCUSSION

The results presented herein demonstrate that mucins can induce the spreading and dendritic expansion of *S. aureus* and *S. epidermidis* colonies. We demonstrated this in plate assays with semisolid agar (0.3% w/v) typically used to study swarming motility (movement of flagellated bacteria on viscous surfaces) [25]. These agar concentrations supported the passive spreading of staphylococcal colonies as they grew, albeit slowly and without the formation of dendrites (Fig. 4.1). Yet, addition of mucin, greatly stimulated colony spreading of clinical *S. aureus* and *S. epidermidis* strains and triggered the dendritic expansion of cells from the colony edge (Fig. 4.1). Like the clinical isolates (Fig. 4.1), all the laboratory strains tested in our study spread slowly as they grew on the 0.3% agar surface but spread very rapidly when mucin was

present in the medium (Fig. 4.3). Mucin-induced spreading was not regulated by quorum sensing regulation because *agr*-defective mutants of *S. aureus* JE2 spread like the WT on the plates without mucin (Fig. 4.4B). This contrasts with the colony spreading reported for this bacterium on 0.24% TSA, which requires an active quorum sensing system and lubrication by PSMs [10, 12, 14]. By contrast, the dendritic expansion triggered by mucin was a social behavior requiring lubrication by not only mucin but also PSMs secreted by the cells moving in trails from the colony periphery (Fig. 4.4).

A time-course study of the spreading and dendritic expansion of clinical and laboratory strains of *S. aureus* and *S. epidermidis* helped differentiate these two types of surface movement and the contributions of mucins and quorum sensing regulatory networks to both. Overnight (18 h) incubation in the presence of mucin was sufficient for the clinical strains of *S. aureus* and *S. epidermidis* to spread dendritically, typically expanding the colony diameter 1-2 cm compared to the no mucin controls (Fig. 4.1B). Increasing the incubation time enhanced surface expansion by the clinical isolates and promoted the growth consolidation of the spreading dendrites (Fig. 4.1B). This was also observed in *S. aureus* JE2 as colonies with markedly undulated edges after 42 h of incubation (Fig. 4.4), which resulted from the consolidated growth of the thin dendritic trails that emerged from the periphery of 18-h colonies (Fig. 4.3). Inactivation of the *agr* system and PSM synthesis produced colonies that spread as much as the WT with mucin but were unable to form dendrites. As a result, these *agr*-deficient colonies had smooth edges and smaller perimeters than the WT (Fig. 4.3). This suggests that mucin provides lubrication for rapid colony spreading and dendritic expansion. However, the latter also required an active *agr* quorum sensing system (Fig. 4.4) and the production of surfactant-active PSMs (Fig. A2.4A).

The lubricating properties of mucin reduce the adhesion of the cells to the surface and facilitated the spreading of the staphylococcal colonies. Yet, mucin glycosylation influenced the charge and structural conformation of the glycoproteins in the hydrogel, its wettability and the mucin-induced response (Fig. 4.3C). Thus, highly glycosylated mucins such as the porcine stomach type used in our study increase the wettability and surface lubrication of mucin hydrogels [18]. Water carriage is also important to mobilize nutrients and facilitate growth on the surface. This could explain why we see increased motility in laboratory strains when plated on soft agar plates supplemented with gastric mucin yet inhibition of colony growth and spreading in the presence of the less glycosylated submaxillary mucin (Fig 4.3C). The greater negative net charge of the submaxillary mucin glycoproteins [26] may have also contribute to growth inhibition by influencing the adhesion of the bacterial cells to the surface [40]. The distribution of the sialic acid moieties in the two mucin types is also to be considered, as it affects the folding of the glycoprotein and the hydration of the mucin gel [26]. Thus, the gastric mucin adopts a conformation that hinders hydrophobic pockets and exposes the sialic acid moieties, increasing hydration and surface lubrication. Consequently, staphylococcal spreading and dendritic expansion was rapid with this mucin (Fig. 4.3C). Given the different mucin composition of mucosae at each body site [26, 41], mucin-mediated hydration and lubrication may ultimately determine the ability of staphylococci such as *S. aureus* to rapidly disperse and infect.

Although *S. epidermidis* was previously reported to passively spread via darting (ejection of aggregates from the colony as it grows) [15], mucin also induced the rapid surface expansion of clinical (Fig. 4.2) and laboratory (Fig. 4.3) strains of *S. epidermidis*. Colony expansion in these strains did not always correlate with mucin growth. For example, *S. epidermidis* B0021-03 spread dendritically on mucin plates although it did not grow with the glycoprotein substrate

(Fig. 4.2B). Thus, although darting may contribute to the spreading of *S. epidermidis* colonies, mucin's stimulatory effect on colony spreading is not due to growth. There was however a general correspondence between mucin growth and robust surface translocation among the strains tested, particularly for those of clinical origin (Fig. 4.2). Mucin availability as a substrate supports growth on the surface. Thus, strains that grow with the mucin have a growth advantage and can more rapidly reach the high cell density needed to activate the quorum sensing pathways that control dendritic expansion.

Isolates of *S. hominis* (Fig. 4.1 and 2) or closely related laboratory strains (Fig. 4.3) did not show a mucin-induced response even after extended incubation. The reported inability of *S. hominis* commensals to produce PSMs [37] suggests that mucins do not provide enough lubrication to promote colony expansion in these strains. By contrast, mucin stimulated colony spreading of *S. aureus* strains even when carrying inactivating mutations that prevented PSM secretion (Fig. 4.4B). These mutants did not expand dendritically (Fig. 4.4A) and, as a result, had partial defects in mucin-induced expansion compared to the WT (Fig. 4.4B) *S. aureus* secretes two surfactant-active PSMs (PSMα3 and PSMγ) [14]. We adapted an atomized oil assay to measure the surfactant activity of PSM peptides released by *S. aureus* JE2 and various mutants (Fig. A2.4A) and demonstrated the correlation between dendritic expansion and PSM-mediated surfactant activity (Fig. 4.4). The surfactant activities of PSMs have previously been linked to comet movement of *S. aureus* on agar plates (0.3% TSA) such as the ones used in our study [11]. The production of PSM surfactants at high cell densities on the colony edge facilitates the dispersal of cells and the formation of slimeless trails (“comets”) that grow into dendrites once they stop moving. Consistent with this, supernatants from robust clinical spreaders of *S. aureus* and *S. epidermidis* stimulated the dendritic expansion of *S. aureus* JE2.

Strain domestication may have contributed to the reduced formation of dendrites by the laboratory strain compared to the clinical isolates. It is also plausible that clinical strains produce different arrays of PSMs, including surfactant-active types that are essential for mucosal dispersal. Other functions for PSM surfactants in the survival of staphylococci in perioral regions cannot be excluded either. Given the antimicrobial properties of some PSMs [42], the peptides may facilitate niche expansion and antagonize competitors. In support of this, supernatants from a robust *S. aureus* spreader (L0021-02) stimulated the expansion of *S. aureus* JE2 colonies but inhibited the growth of *S. epidermidis* L0021-06 (Fig. 4.5). Therefore, cross-talk between staphylococcal PSM peptides may play a key role in recognizing friend from foe and determining niche co-inhabitance or exclusion. More studies are needed to fully understand the roles of PSMs in staphylococcal crosstalk and how mucins influence these social behavior.

Taken together, these results show that mucin stimulates staphylococcal motility, both enhancing colony spreading and promoting the dispersal of cell trails via PSM-mediated mechanisms. Mucin lubrication has previously shown to stimulate swarming motility by flagellated bacteria [43]. Here we show that mucins can also induce rapid surface movement of non-flagellated staphylococci in a process that can be regulated at high cell densities via the production of PSM surfactants. Membrane-bound, rather than secreted, gell-forming mucins such as the gastric type used in our study, can have the opposite effect and promote the adhesion of staphylococcal cells to specific mucosa of the nasal-respiratory mucosal lining [44-46]. This seemingly contrasting interactions highlight the various roles that mucins play in the dispersal of staphylococci on perioral mucosal surfaces and the ability of the cells to colonize specific mucosae with specificity. Future studies will need to examine the integration of mucin signaling in social behaviors and coordination of PSM secretion during dendritic expansion. Also

important is to evaluate how the viscoelastic properties and hydration of mucin hydrogels and analogs (e.g., methyl cellulose or polyethylene glycol gels [47]) contribute to staphylococcal motility or how mucin metabolism influences surface expansion. Given the robust motility of clinical isolates with mucin, it is also important to study the arrays and levels of PSMs secreted by the strains and their physicochemical properties. HPLC-QTOF analysis of PSM-containing supernatants could help characterize PSM biochemistry and expression levels compared to close laboratory relatives, as previously described [48]. The robust motility of clinical staphylococcal strains is also consistent with increased production of surfactant-active PSMs. This, in turn, impacts staphylococcal pathogenesis and the enhanced virulence noted for some strains [49, 50]. Thus, perioral regions may be reservoirs of invasive and potentially pathogenic strains of staphylococci. By stimulating spreading, mucins enhance the invasiveness of these strains and their ability to breach the protective mucus barrier of respiratory epithelia. This is particularly important in the middle ear, where inflammation of the Eustachian tube leads to mucin hypersecretion and increased risk of infections by otopathogens, including *S. aureus* and *S. epidermidis*. Findings from this work thus help explain how staphylococcal species colonize the middle ear mucosa in patients suffering from tubal disfunctions and/or respiratory viral or bacterial infections that lead inflammation. Mechanistic understanding of mucin-induced motility can however identify targets to neutralize staphylococcal cells in perioral reservoirs and prophylactically treat patients such as children with a history of otitis media, who are most at risk of staphylococcal infections.

DECLARATIONS

Acknowledgments

The authors would like to thank Dr. Neal Hammer at Michigan State University for providing staphylococcal laboratory strains for controls used in this study. Additionally, we would like to thank Dr. Andrew VanAlst and the lab of Dr. Victor DiRita at Michigan State University for supplying purified porcine gastric mucin used in this study. Finally, we would also like to thank Drs. Batsirai Mabvakure and Heather Blankenship at the Michigan Department of Health and Human Services for assistance with bioinformatic analysis of Illumina sequences.

Funding

This research was funded by grants N00014-17-2678 and N00014-20-1-2471 from the Office of Naval Research (ONR) to GR. KJ acknowledges support from a summer 2020 G. D. Edith Hsiung and Margaret Everett Kimball Endowed fellowship from the department of Microbiology and Molecular Genetics at Michigan State University. The funders had no role in study design, data collection and analysis, decision to publish or manuscript preparation.

APPENDIX

Figure 4.1: Mucin-enhanced surface expansion of (peri)oral Staphylococcus isolates. (**A**) Effect of mucin (M, 0.4% purified porcine gastric mucin) on the surface expansion of staphylococcal colonies on the surface of 0.5% TSA (swarming plate assay) or 0.3% TSA (flagellar motility plate assays). (**B**) Surface expansion (average diameter in cm and standard deviation of triplicate plate assays) of the staphylococcal isolates at 18 or 42 h on 0.3% TSA media without (–M) or with mucin (purified porcine gastric mucin, +M).

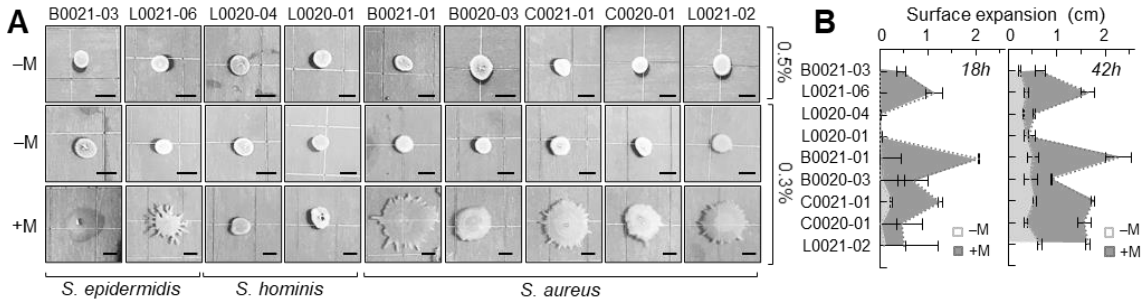

Figure 4.2: Colony spreading (A), planktonic growth (B) and mucinase activity (C) of staphylococcal isolates with commercial mucin (Mc). (**A**) Colony expansion on 0.3% TSA supplemented with 0.4% (w/v) commercial porcine gastric mucin (Mc). Incubation was at 37ºC for 18 h. (**B**) Growth (A_{600}) of *Staphylococcus* isolates in 50% (w/v) TSB with (+Mc) or without (–Mc) commercial grade mucin (0.4%, w/v). Clear diauxic growth transitions to mucin growth are marked with an arrow. (**C**) Mucin degradation on 1.5% TSA supplemented with 0.5% (w/v) commercial porcine gastric mucin and incubated at 37°C for 24 h. The edges of the zones of mucin degradation, when present, are highlighted in white.

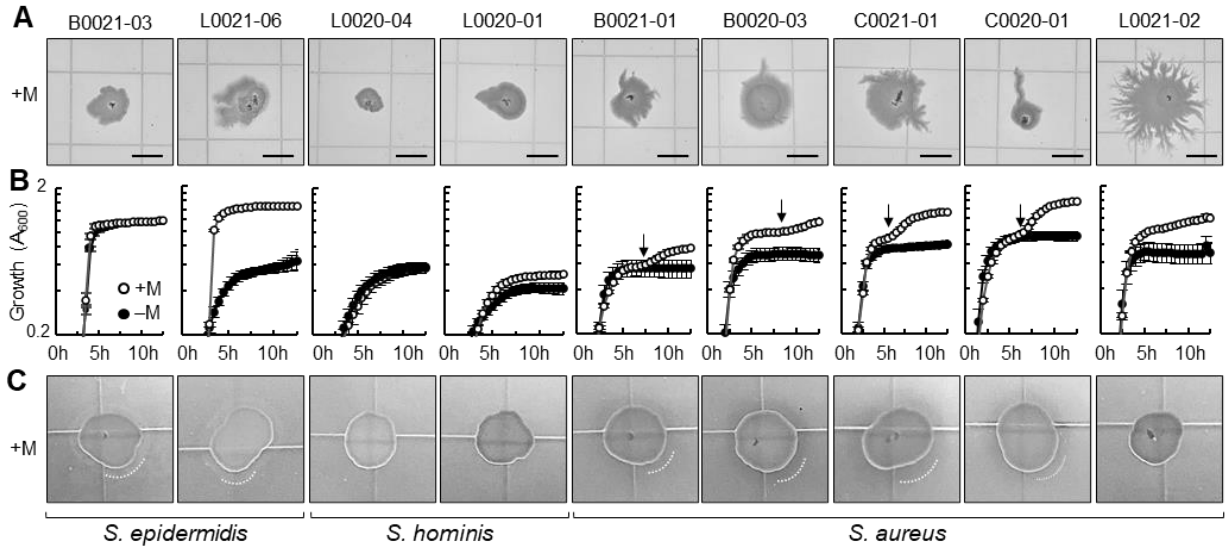

Figure 4.3: Effect of mucin on spreading and growth by laboratory strains most closely related to (peri)oral isolates. (A) Surface expansion (18 h) on 0.3% TSA agar with or without 0.4% commercial grade porcine gastric mucin (–M and +psM, respectively) of *S. epidermidis* (*Se*), *S. lugdunensis (Sl*), *S. haemolyticus* (*Sh*) and *S. aureus* JE2 (*Sa*). The bottom panel shows the mucinase activity of the strains (white line added to the edge of the clearing zone, when present). (**B**) Time-course expansion of the staphylococcal colonies (diameter in cm) on 0.3% TSA without mucin (–M) or with 0.4% commercial grade porcine gastric (+psM) or bovine submaxilliary (+bsM) mucin. (**C**) Growth of the staphylococcal strains in 50% TSB without mucin (–M) or with 0.4% commercial porcine gastric mucin (+Mp). All assays were carried out at 37ºC. Statistical significance between –M and either +psM or +bsM expansion zones were calculated using t-test (type 2) analysis, where statistical significance of ≤0.05 (*), ≤0.005 (*), ≤0.0005 (*) are reported.

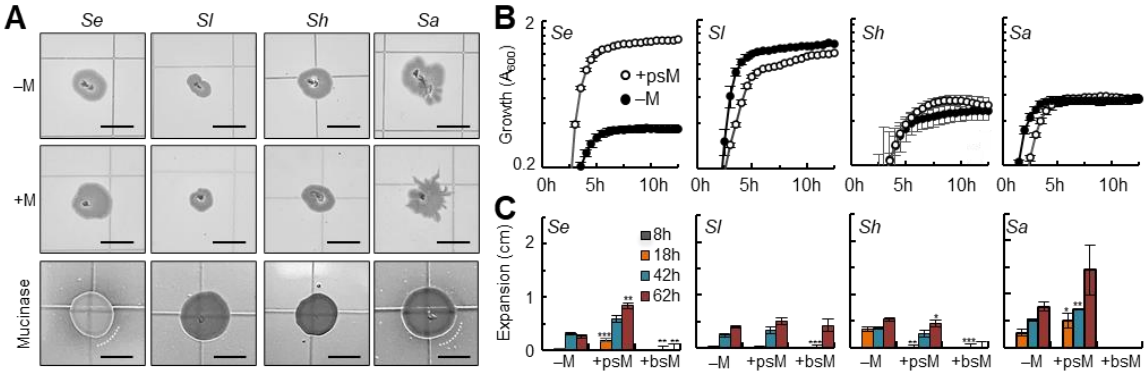

Figure 4.4: Effect of mucin on surface spreading of *S. aureus* JE2 and quorum sensing mutants. The figure shows representative images (**A**) and perimeters (average and standard deviation of 5-6 replicates from two independent experiments) of 42-h colonies of the WT and mutants on plates without (–M) or with (+M) porcine stomach mucin. The mutants included in the plate assays carried deletions in quorum sensing (AgrB transporter, AgrC histidine kinase for autoinducer sensing, AgrA response regulator, SarA enhancer of AgrA binding, and Rot transcriptional regulator). Statistical significance perimeters (cm) of transposon mutants against wild-type *S. aureus* JE2 were calculated using t-test (type 2) analysis, where statistical significance of ≤0.05 (*), ≤0.005 (*), ≤0.0005 (*) are reported.

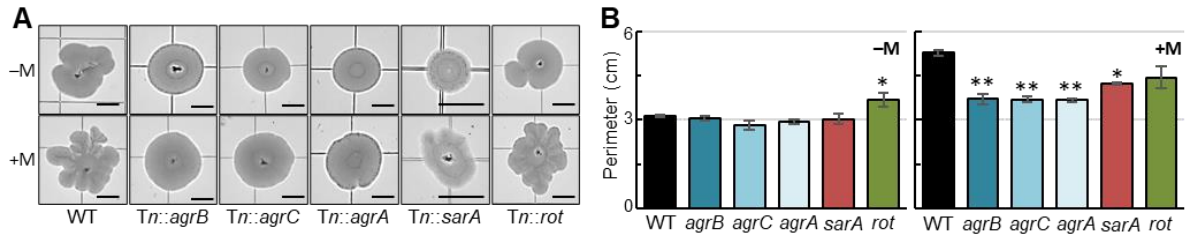

Figure 4.5: Effect of PSM-containing supernatants on dendritic motility. (A) Representative images of 18-h colonies of laboratory strains (WT and Δ*agrA* mutant of *S. aureus* JE2) and clinical strains of *S. hominis* (L0020-01 and L0020-04), *S. aureus* (L0021-02) and *S. epidermidis* (L0021-06). The strains were grown overnight before spot plating 1 µl on 0.3% TSA without (–M) or with (+M) mucin. Rows of cells spot plated after resuspension in PSM-containing supernatants of the L0021-02 or L0021-06 clinical strains are also shown. (**B-C**) Perimeter (average and standard deviation of triplicates) of *S. aureus* JE2 WT and Δ*agrA* mutant (**B**) or clinical strains of *S. aureus* (L0021-02) and *S. epidermidis* (L0021-06) of colonies shown in (**A**). Statistical significance perimeters (cm) strains challenged with supernatant addition to non-supernatant controls were calculated using t-test (type 2) analysis, where statistical significance of ≤0.05 (*), ≤0.005 (*), ≤0.0005 (*) are reported.

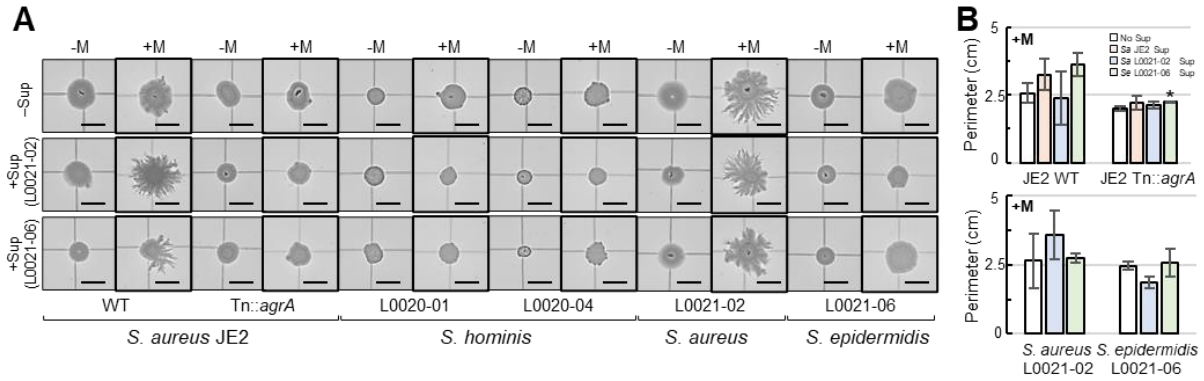

Figure 4.6: 16S rRNA phylogeny of otic, buccal and oropharyngeal staphylococci.

Maximum likelihood tree constructed of staphylococci isolated from otic (L), buccal (B) or oropharyngeal (C) secretions, and closest relative reference sequences (accession numbers). Scale bar indicates 2% sequence divergence filtered to a conservation threshold above 79% using the Living Tree Database (24, 25). Bootstrap probabilities by 1000 replicates at or above 50% are denoted by numbers at each node. Squares identify motile phenotypes characterized either in literature (blue), or apart of this study on tryptic soy motility agar (0.3%) supplemented with (red) or without (green) 0.4% purified porcine gastric mucin after 18 hours of growth at 37°C.

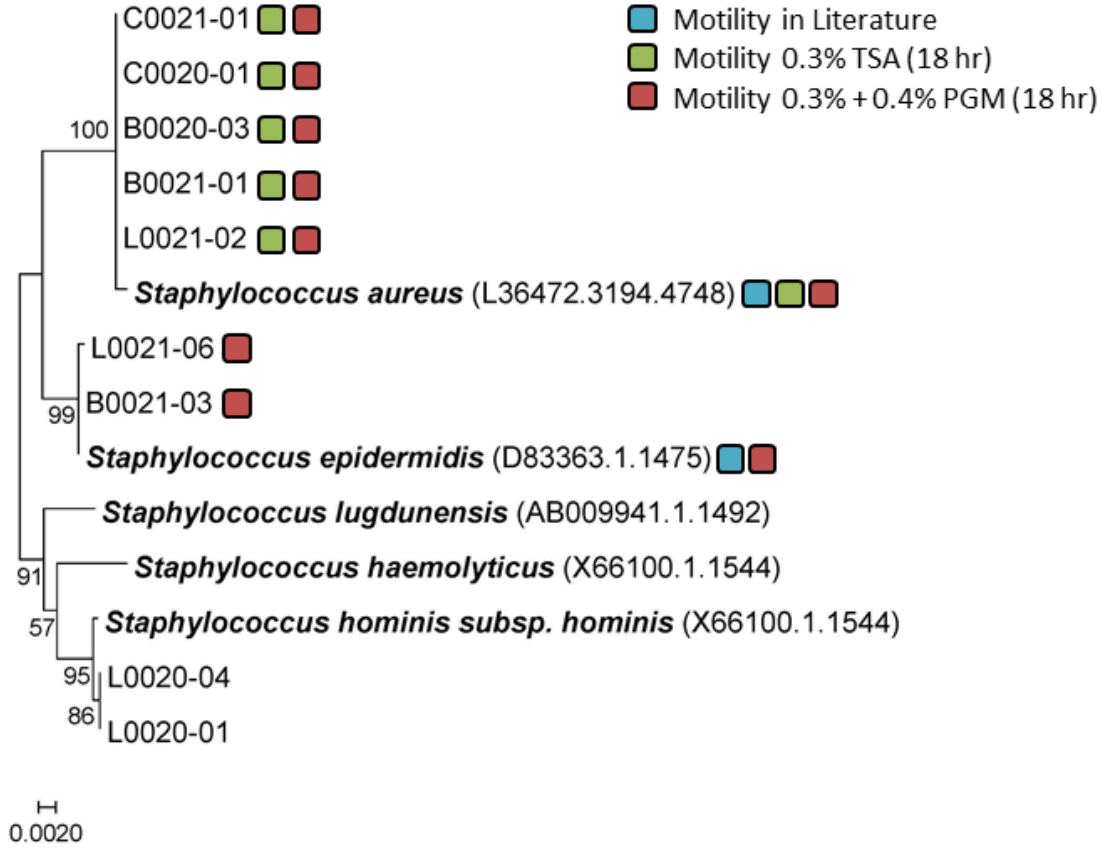

Figure 4.7: Regulatory pathway of *S. aureus agr*-quorum sensing system. Cartoon representation of regulatory pathway depicting the interactions of the *agr*-quorum sensing (QS) system with SarA and Rot regulatory proteins adapted from [27]. The *agr*-QS system is made up of the AgrD AIP precursor protein, AgrB transporter protein, AgrC histidine kinase and AgrA response regulator. AgrA directly regulates phenol-soluble modulin (PSM) expression, and indirectly regulates genes under RNAIII/*hld* regulation, including inhibition of Rot. Additionally, *agrBDAC* operon is autoregulated by AgrA binding. SarA acts as an enhancer protein, resulting in conformational change of AgrA fro optimum binding to the P2/P3 promotor region.

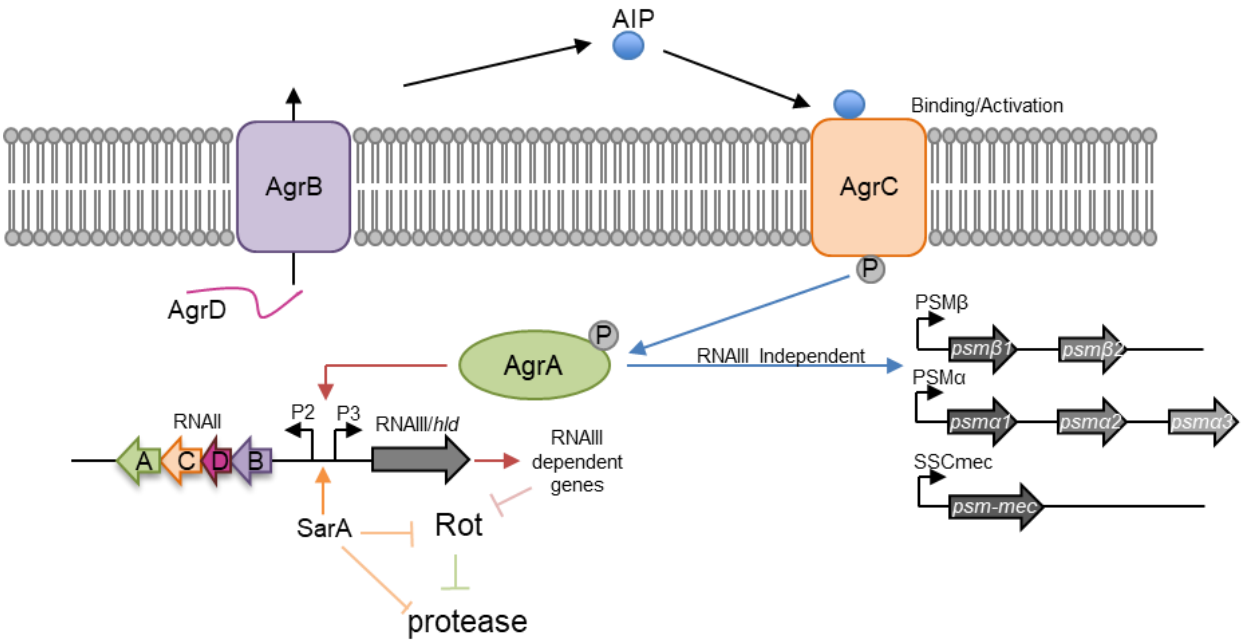

Figure 4.8: Effect of mucin on surface spreading of *S. aureus* LAC and a protease defective mutant (ΔESPN). The figure shows representative images (A) and perimeters (average and standard deviation of 3 replicates from 3 independent experiments) of 42-h colonies of the WT and mutants on plates without (–M) or with (+M) porcine stomach mucin (B). Mucinase activity (haloes of mucin degradation on 1.5% TSA plates supplemented with 0.5% mucin]) and surfactant activity (atomized oil assay) of the mucin-grown colonies is also sown (**C**). Statistical significance (T-test) of parameter expansion between mucin and no mucin controls are depicted by p-values of ≤0.05 (*), ≤0.005 (**) or ≤0.0005 (***).

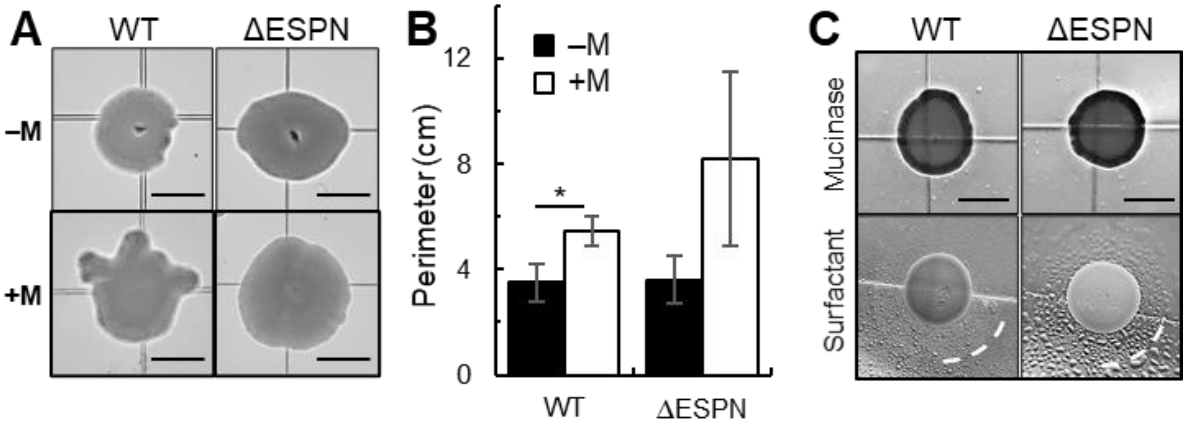

Figure 4.9: Phenotypic characterization of *S. aureus* mutants. (A) Plate assays showing the mucinase activity (mucin clearings on 1.5% TSA plates supplemented with 0.5% mucin) and surfactant activity (haloes of mineral oil dispersion around PSM-producing colonies) of *S. aureus* JE2 strains. (B-C) Planktonic growth (B) and biofilm formation (crystal violet assay) (**C**) of WT and mutant strains of *S. aureus* JE2 or LAC in the presence (+M) or absence (–M) of porcine stomach mucin measured with the crystal violet assay. Statistical significance (T-test) of biofilm formation between mucin and no mucin controls are depicted by p-values of ≤0.05 (*), ≤0.005 (**) or ≤0.0005 (***).

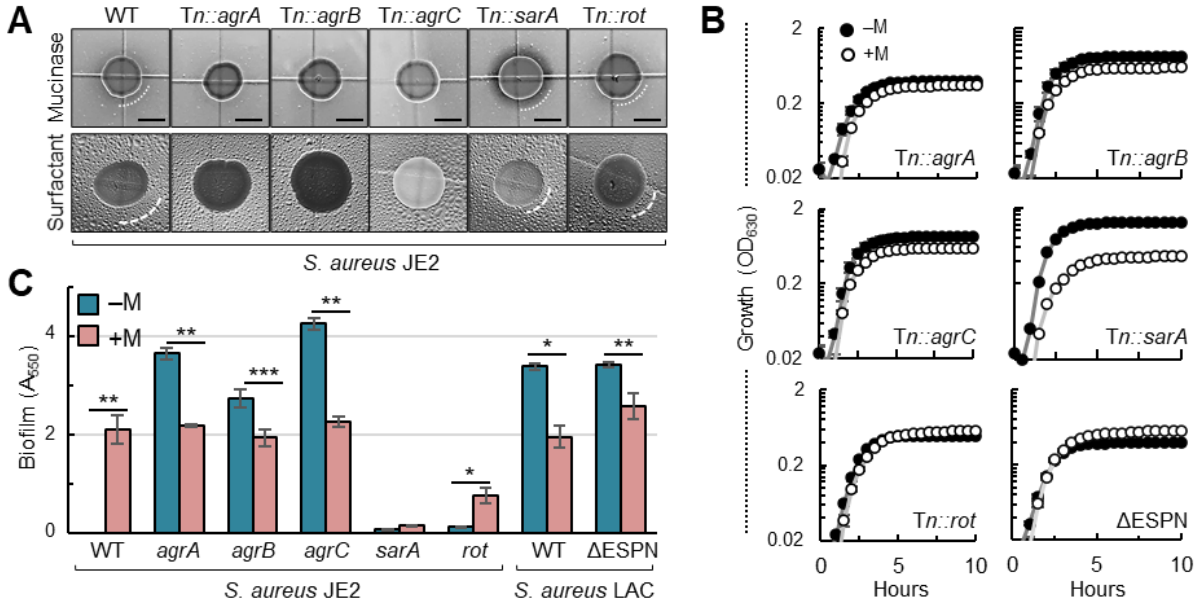

Figure 4.10: Effect of JE2 supernatant on colony expansion of the WT and quorum-sensing mutants on 0.3% TSA. (A) Colony phenotypes at 8, 18 and 42h. (B) Perimeter (average and standard deviation of triplicate colonies) of 18-h colonies in the presence (+M) or absence (–M) of 0.4% commercial porcine stomach mucin, with (black) or without (white) supernatant additions.

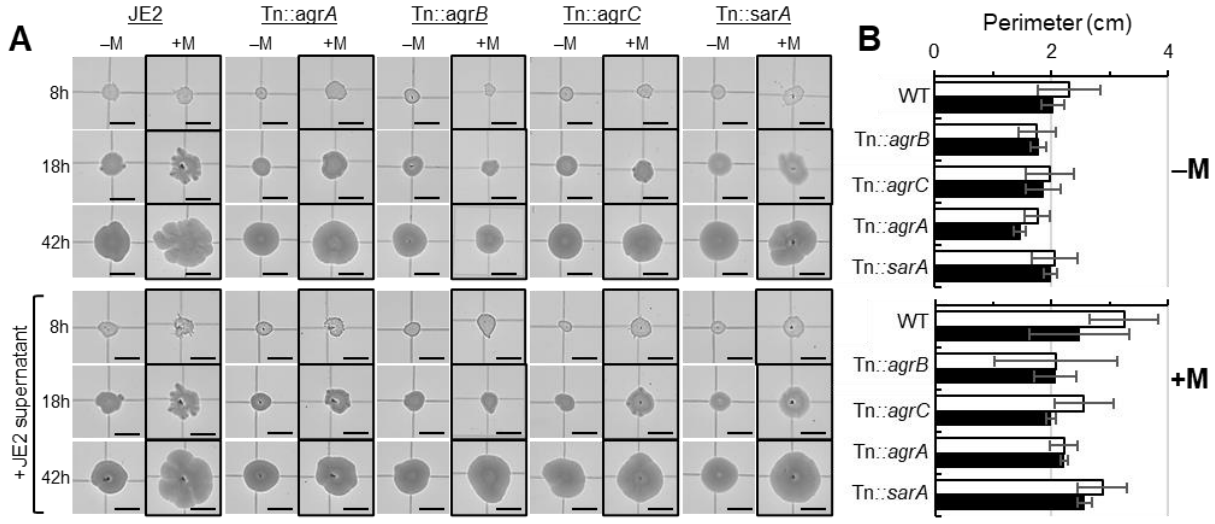

Table 4.1: **Presences (+) or absence (-) of either surfactant production or mucin degradation phenotypes in clinical and laboratory isolates used in this study.** The presence of a faint halo, or inconclusive results between clinical isolates is denoted by (+/-). NCBI accession numbers of clinical isolates and references for laboratory strains are indicated.

Strain	Surfactant Production (+/-)	Mucin Degradation (+/-)	NCBI Accession Number	Reference
Staphylococcus spp. B0020-03	-	+/-	MW866510	This Study
Staphylococcus spp. B0021-01	+	+/-	MW866509	This Study
Staphylococcus spp. B0021-03	+	+	MW866508	This Study
Staphylococcus spp. C0020-01	+	+/-	MW866512	This Study
Staphylococcus spp. C0021-01	-	+/-	MW866511	This Study
Staphylococcus spp. L0020-01	+	-	MW866488	This Study
Staphylococcus spp. L0020-04	-	-	MW866491	4
Staphylococcus spp. L0021-02	-	-	MW866496	4
Staphylococcus spp. L0021-06	-	+	MW866498	4
Staphylococcus aureus JE2	+	+/-	---	59
Staphylococcus aureus JE2 agrA::Tn erm NE1532	-	-	---	59
Staphylococcus aureus JE2 agrB::Tn erm NE95	-	-	---	59
Staphylococcus aureus JE2 agrC::Tn erm NE873	-	-	---	59
Staphylococcus aureus JE2 sarA::Tn erm NE1193	+/-	+	---	59
Staphylococcus aureus JE2 rot::Tn erm NE386	+	+/-	---	59

Table 4.1 (cont'd)

Staphylococcus aureus LAC	**+**	**-**	**---**	**51**
Staphylococcus aureus LAC strain AH1919 (ΔESPN)	+	-	---	52
Staphylococcus epidermidis RP62a	+	+/-	---	55
Staphylococcus lugdunensis N920143	+	-	---	56
Staphylococcus haemolyticus NRS9	+	-	---	57

REFERENCES

REFERENCES

1. Bomar, L., S.D. Brugger, and K.P. Lemon, Bacterial microbiota of the nasal passages across the span of human life. Curr. Opin. Microbiol., 2018. 41: p. 8-14.

2. Ohara-Nemoto, Y., et al., Occurrence of staphylococci in the oral cavities of healthy adults and nasal oral trafficking of the bacteria. J. Med. Microbiol., 2008. 57(Pt 1): p. 95-9.

3. McCormack, M.G., et al., *Staphylococcus aureus* and the oral cavity: an overlooked source of carriage and infection? Am. J. Infect. Control, 2015. 43(1): p. 35-7.

4. Lee, J.-Y., et al., Oral seeding and niche-adaptation of middle ear biofilms in health. Biofilm, 2021. 3: p. 100041.

5. Bluestone, C.D., The Eustachian Tube: Structure, function, and role in the middle ear. 2005, Hamilton, Ontario: BC Decker Inc.

6. Jacob, K.M. and G. Reguera, Competitive advantage of oral streptococci for colonization of the middle ear mucosa. Biofilm, 2022: p. 100067.

7. Ding, Y.L., et al., Molecular characterization and antimicrobial susceptibility of *Staphylococcus aureus* isolated from children with acute otitis media in Liuzhou, China. BMC Pediatrics, 2018. 18(1): p. 388.

8. Kurono, Y., K. Tomonaga, and G. Mogi, *Staphylococcus epidermidis* and *Staphylococcus aureus* in otitis media with effusion. Arch. Otolaryngol. Head Neck Surg., 1988. 114(11): p. 1262-1265.

9. Lin, J., et al., Mucin production and mucous cell metaplasia in otitis media. International Journal of Otolaryngology, 2012. 2012: p. 745325.

10. Kaito, C. and K. Sekimizu, Colony spreading in *Staphylococcus aureus*. J Bacteriol, 2007. 189(6): p. 2553-7.

11. Pollitt, E.J.G., S.A. Crusz, and S.P. Diggle, *Staphylococcus aureus* forms spreading dendrites that have characteristics of active motility. Sci. Rep., 2015. 5(1): p. 17698.

12. Tsompanidou, E., et al., Requirement of the agr locus for colony spreading of *Staphylococcus aureus*. J Bacteriol, 2011. 193(5): p. 1267-72.

13. Pollitt, E.J.G. and S.P. Diggle, Defining motility in the Staphylococci. Cell Mol Life Sci, 2017. 74(16): p. 2943-2958.

14. Tsompanidou, E., et al., Distinct roles of phenol-soluble modulins in spreading of *Staphylococcus aureus* on wet surfaces. Appl. Environ. Microbiol., 2013. 79(3): p. 886-95.

15. Henrichsen, J., Bacterial surface translocation: a survey and a classification. Bacteriol. Rev., 1972. 36(4): p. 478-503.

16. Rupp, C.J., C.A. Fux, and P. Stoodley, Viscoelasticity of *Staphylococcus aureus* biofilms in response to fluid shear allows resistance to detachment and facilitates rolling migration. Applied and Environmental Microbiology, 2005. 71(4): p. 2175-2178.

17. Lin, J., et al., Expression of mucins in mucoid otitis media. J. Assoc. Res. Otolaryngol., 2003. 4(3): p. 384-393.

18. Crouzier, T., et al., Modulating mucin hydration and lubrication by deglycosylation and polyethylene glycol binding. Advanced Materials Interfaces, 2015. 2(18): p. 1500308.

19. Yeung, A.T., A. Parayno, and R.E. Hancock, Mucin promotes rapid surface motility in *Pseudomonas aeruginosa*. MBio, 2012. 3(3).

20. Sun, E., S. Liu, and R.E.W. Hancock, Surfing Motility: A conserved yet diverse adaptation among motile bacteria. J Bacteriol, 2018. 200(23).

21. Sun, E., S. Liu, and R.E.W. Hancock, Surfing motility: a conserved yet diverse adaptation among motile bacteria. J. Bacteriol., 2018. 200(23).

22. Jacob, K.M. and G. Reguera, Competitive advantage of oral streptococci for colonization of the middle ear mucosa. Biofilm, 2022.

23. Joo-Yong Lee, K.M.J., Kazem Kashefi, Gemma Reguera Oral seeding and niche-adaptation of middle ear biofilms in health. Biofilm, 2021. 3: p. e10041.

24. Partridge, J.D., Surveying a Swarm: experimental techniques to establish and examine bacterial collective motion. Appl Environ Microbiol, 2021: p. AEM0185321.

25. Partridge, J.D. and R.M. Harshey, Swarming: Flexible roaming plans. J. Bacteriol., 2013. 195(5): p. 909-918.

26. Madsen, J.B., et al., Structural and mechanical properties of thin tilms of tovine Submaxillary mucin versus porcine gastric mucin on a hydrophobic surface in aqueous solutions. Langmuir, 2016. 32(38): p. 9687-96.

27. Jenul, C. and A.R. Horswill, Regulation of *Staphylococcus aureus* virulence. Microbiol Spectr, 2019. 7(2).

28. Painter, K.L., et al., What role does the quorum-sensing accessory gene regulator system play during *Staphylococcus aureus* bacteremia? Trends Microbiol, 2014. 22(12): p. 676-85.

29. Tan, L., et al., Therapeutic Targeting of the *Staphylococcus aureus* Accessory Gene Regulator (agr) system. Front Microbiol, 2018. 9: p. 55.

30. Zielinska, A.K., et al., Defining the strain-dependent impact of the Staphylococcal accessory regulator (sarA) on the alpha-toxin phenotype of *Staphylococcus aureus*. J Bacteriol, 2011. 193(12): p. 2948-58.

31. Said-Salim, B., et al., Global regulation of *Staphylococcus aureus* genes by Rot. J Bacteriol, 2003. 185(2): p. 610-9.

32. Wu, X., et al., Expression and regulation of phenol-soluble modulins and enterotoxins in foodborne *Staphylococcus aureus*. AMB Express, 2018. 8(1): p. 187.

33. Burch, A.Y., et al., Novel high-throughput detection method to assess bacterial surfactant production. Appl. Environ. Microbiol., 2010. 76(16): p. 5363-72.

34. Loughran, A.J., et al., Impact of sarA and phenol-soluble modulins on the pathogenesis of osteomyelitis in diverse clinical isolates of *Staphylococcus aureus*. Infect Immun, 2016. 84(9): p. 2586-94.

35. Peschel, A. and M. Otto, Phenol-soluble modulins and staphylococcal infection. Nature Reviews Microbiology, 2013. 11(10): p. 667-673.

36. Solano, C., M. Echeverz, and I. Lasa, Biofilm dispersion and quorum sensing. Curr Opin Microbiol, 2014. 18: p. 96-104.

37. Rautenberg, M., et al., Neutrophil responses to staphylococcal pathogens and commensals via the formyl peptide receptor 2 relates to phenol-soluble modulin release and virulence. FASEB J, 2011. 25(4): p. 1254-63.

38. Otto, M., et al., Pheromone cross-inhibition between *Staphylococcus aureus* and *Staphylococcus epidermidis*. Infect Immun, 2001. 69(3): p. 1957-60.

39. Canovas, J., et al., Cross-Talk between *Staphylococcus aureus* and other staphylococcal species via the agr quorum sensing system. Front Microbiol, 2016. 7: p. 1733.

40. Caldara, M., et al., Mucin biopolymers prevent bacterial aggregation by retaining cells in the free-swimming state. Current Biology, 2012. 22(24): p. 2325-2330.

41. Park, M.S., et al., Viscosity and wettability of animal mucin solutions and human saliva. Oral Dis, 2007. 13(2): p. 181-6.

42. Cogen, A.L., et al., Selective antimicrobial action is provided by phenol-soluble modulins derived from *Staphylococcus epidermidis*, a normal resident of the skin. J Invest Dermatol, 2010. 130(1): p. 192-200.

43. Yeung, A.T.Y., A. Parayno, and R.E.W. Hancock, Mucin promotes rapid surface motility in *Pseudomonas aeruginosa*. mBio, 2012. 3(3): p. e00073-12.

44. Trivier, D., et al., The binding of surface proteins from *Staphylococcus aureus* to human bronchial mucins. European Respiratory Journal, 1997. 10(4): p. 804-810.

45. Shuter, J., V.B. Hatcher, and F.D. Lowy, *Staphylococcus aureus* binding to human nasal mucin. Infection and Immunity, 1996. 64(1): p. 310-318.

46. Thomas, V.L., B.A. Sanford, and M.A. Ramsay, Calcium- and mucin-binding proteins of staphylococci. J Gen Microbiol, 1993. 139(3): p. 623-9.

47. Co, J.Y., et al., Mucins trigger dispersal of *Pseudomonas aeruginosa* biofilms. NPJ Biofilms Microbiomes, 2018. 4: p. 23.

48. Wu, X. and C. Zhang, Determination of Staphylococcal Phenol-Soluble Modulins (PSMs) by a high-resolution HPLC-QTOF System. 2017.

49. Wang, R., et al., Identification of novel cytolytic peptides as key virulence determinants for community-associated MRSA. Nat Med, 2007. 13(12): p. 1510-4.

50. Kobayashi, S.D., et al., Comparative analysis of USA300 virulence determinants in a rabbit model of skin and soft tissue infection. J Infect Dis, 2011. 204(6): p. 937-41.

51. Diep, B.A., et al., Complete genome sequence of USA300, an epidemic clone of community-acquired meticillin-resistant *Staphylococcus aureus*. The Lancet, 2006. 367(9512): p. 731-739.

52. Wormann, M.E., et al., Proteolytic cleavage inactivates the *Staphylococcus aureus* lipoteichoic acid synthase. J Bacteriol, 2011. 193(19): p. 5279-91.

53. Merritt, J.H., D.E. Kadouri, and G.A. O'Toole, Growing and analyzing static biofilms. Curr Protoc Microbiol, 2005. Chapter 1: p. Unit 1B 1.

54. Van Alst, A.J. and V.J. DiRita, Aerobic metabolism in *Vibrio cholerae* is required for population expansion during infection. mBio, 2020. 11(5).

55. Schindelin, J.A.-c., I. & Frise, E. et al., Fiji: an open-source platform for biological-image anlaysis. Nature methods, 2012. 9(7): p. 682.

56. Vitko, N.P., et al., Expanded glucose import capability affords *Staphylococcus aureus* optimized glycolytic flux during infection. mBio, 2016. 7(3): p. e00296-16.

57. Haley, K.P., et al., *Staphylococcus lugdunensis* IsdG liberates iron from host heme. Journal of Bacteriology, 2011. 193(18): p. 4749-4757.

58. Pishchany, G., et al., Specificity for Human Hemoglobin Enhances *Staphylococcus aureus* Infection. Cell Host & Microbe, 2010. 8(6): p. 544-550.

59. Fey, P.D., et al., A Genetic Resource for rapid and comprehensive phenotype screening of nonessential *Staphylococcus aureus* Genes. mBio, 2013. 4(1): p. e00537-12.

CHAPTER 5

CONCLUSIONS AND FUTURE DIRECTIONS

The long-standing dogma of a sterile middle ear in health is incongruent with the periodic opening (~400 ms/min) of the Eustachian tube, which functions as a conduit between the tympanic cavity and the naso- and oropharynx [1]. Previous studies failed to conclusively demonstrate whether the middle ear is indeed sterile or colonized by a commensal microbiome [2-6]. These early studies (1) collected samples from patients with no history of otic infections but underlying otic conditions (i.e. perforated eardrum, cochlear implants) that can affect otic ventilation, (2) used invasive sampling techniques, often relying on transcanal surgery which exposes the otic cavity to high levels of oxygen and risks contamination, and (3) lacked appropriate control groups to account for contamination [2-7]. To bypass these limitations, I was part of a research team that developed a non-invasive method to collect otic secretions non-invasively (through the mouth) as they drain through the nasopharyngeal orifice of the Eustachian tube. In an effort to better understand the microbiology of the middle ear in health, I carried out dissertation studies to culture otic and (peri)oral bacteria and and gain insights into their ecophysiology. The main goals were to (1) recover in pure culture otic commensals, (2) compare their physiology to that of transient migrants to identify adaptive responses needed for middle ear colonization, and (3) define conditions that allow otopathogens from the nasal cavity to breach the middle ear defenses and infect.

In Chapter 2, I describe the sequencing of 16S rRNA-V4 amplicons from otic secretions and neighboring regions (buccal and oropharyngeal samples) by my teammate, Dr. Joo-Young Lee, using samples we collected from 19 healthy young adults in 2017. The sequencing survey identified a diverse bacterial community in otic secretions distinct from the nasal microbiome [8] and more similar to the oral (oropharyngeal and buccal) microbiomes. Indeed, the otic oral microbiomes included the same phyla but differed in the enrichment in otic secretions of

anaerobic genera in the phyla Bacteroidetes (Prevotella and Alloprevotella), Fusobacteria (*Fusobacterium* and Leptotrichia) and firmicutes (*Veillonella*). Facultative anaerobes in the genus *Streptococcus* (Firmicutes) were also abundant in otic secretions. These findings showed that the otic and oral microbiomes are related, yet the limited ventilation of the middle ear selected for a bacterial community adapted to anaerobiosis. Given the dynamics of the Eustachian tube, the middle ear mucosa is likely seeded by saliva aerosols from the oropharynx. This process introduces oral bacteria in the middle ear periodically. While some migrants are transient and cleared from the middle ear with air or via mucociliary and muscular clearance, specific groups colonize and grow in the otic mucosa as a commensal community. This model is analogous to the establishment of the lung microbiome [9-14]. As with the middle ear, the lower airways and lungs had been proposed to be sterile, yet the inhalation of salivary microaerosols seeds the respiratory mucosae with oral migrants [9-14]. Further surveys would need to consider greater sample sizes and demographic (e.g, race, ethnicity) physiological (diet, pulmonary capacity) factors that could influence the otic microbiome. Our team has also used shotgun-sequencing to recover the metagenomes from additional participants, which is critical to obtain a more in-depth view of the otic community structure, including species level identification and metabolic function.

My contribution to Chapter 2 was the recovery in pure culture of otic and oral (buccal and oropharyngeal) strains (n=39) using samples collected from an additional 4 participants. Sequencing of 16S rRNA amplicons from the otic cultivars (n=20) confirmed the recovery primarily *Streptococcus* species (60%). The remaining isolates belonged to rare otic taxa, including *Staphylococcus* (20%), *Micrococcus* (5%), *Neisseria* (10%) and *Corynebacterium* (5%). Oropharyngeal (n=9) and buccal (n=10) cultivars did not include actinobacteria

(*Micrococcus* and *Corynebacterium*). Phylogenetic analysis of partial 16S rRNA gene sequences from all the cultivars showed a similar taxonomic distribution, consistent with the oral ancestry of the otic isolates. Yet, the separation of *Streptococcus* strains by sample site (otic, oropharyngeal, and buccal) suggested that this abundant otic group may have undergone ecological diversification from oral ancestors once in the middle ear. The isolation procedure used only samples from 4 individuals and selected for facultatively or strictly aerobic, heterotrophic bacteria. Future cultivation studies to recover otic commensals will need to consider the strictly anaerobic metabolism of most of these bacteria. Of particular interest is the recovery of representatives from the most abundant otic phylum, Bacteroidetes, which is a strictly anaerobic group predicted to degrade mucin glycoproteins to sustain the otic trophic webs. Having a broader range of clinical otic isolates could also facilitate studies of microbe-microbe interactions in the middle ear communities (e.g., syntrophic, and competitive behaviors). The metabolic characterization of the isolates could lead to a better understanding of how the native bacteria interact in the otic trophic webs and how these consortia contribute to regulating mucosal health and homeostasis. Lastly, 16S amplicon sequencing isn't sensitive enough to provide species level identification. Whole-genome sequencing of the isolates could improve phylogenetic and metabolic predictions and permit genome-level comparisons between otic and oral genera for predictive identification of the selective forces that select for specific groups of oral migrants in the middle ear.

Chapter 3 focused on investigating adaptive responses of otic isolates (n=9) that contribute to the enrichment of specific groups of oral migrants in the middle ear mucosa. Partially assembled whole-genome sequences of commensal (*Streptococcus*) and migrant (*Staphylococcus*, *Micrococcus*, *Corynebacterium*, and *Neisseria*) strains provided full length 16S

rRNA sequences for species-level taxonomic identification and phylogenetic analysis. The taxonomic and phylogenetic studies were congruent with results shown in chapter 2, which revealed close evolutionary relationships between otic and oral streptococcal commensals. Physiological functions examined in this study included traits important for mucosal colonization (motility, surfactant production, biofilm formation), nutrient acquisition (mucin and protein degradation) and growth under anoxic flux. Though these traits were widespread among otic isolates, the streptococcal isolates stood out for their enhanced biofilm-forming abilities under oxic and anoxic conditions. Additionally, the streptococci degraded mucin glycoproteins and proteins, the main growth substrates in the middle ear mucosa, and produced lactate as the main product of their fermentative metabolism, which is critical for the establishment of metabolically co-dependent consortia. Streptococci are pioneer species during the establishment of oral biofilm communities [15-17]. In these communities, the streptococcal cells provide anchorage to host cells and ferment substrates into byproducts that syntrophic partners can feed on. The metabolic co-dependence between *Streptococcus*, *Veillonella* and Bacteroidetes is predicted to control carbon flow in the otic commensal communities. In this model, streptococci ferment sugars and proteins, such as mucin or mucin byproducts, into lactate, sustaining propionate and acetate production in *Veillonella* spp. [17, 18], which was identified in chapter 2 as being among the most abundant bacteria in otic samples. Furthermore, the mucinolytic metabolism of Bacteroidetes could sustain streptococcal fermentation of sugars and the growth of *Veillonella* spp. via acetate [19-22]. Importantly, this chapter describes the ability of otic streptococci to inhibit the growth of common otopathogens (*Haemophilus influenzae*, *Streptococcus pneumoniae*, and *Moraxella catarrhalis*) in overlay assays, an antagonistic behavior that could exclude competitors and protect the otic mucosa from infection. This finding provides a plausible

explanation to the beneficial effect that alpha-hemolytic *Streptococcus* species in the prevention of acute and chronic otitis media once reintroduced via nasal sprays [23]. The results presented in chapter 3 describe adaptive responses in some streptococcal isolates that make them suitable for similar preventive treatments. These strains have a competitive advantage for the colonization of the middle ear mucosa and are highly aggregative, which facilitates immunoescape, firmly attaches the cells to the underlying epithelium, and promotes co-aggregation with syntrophic partners. Furthermore, they inhibit the growth of otopathogens. Thus, they are promising candidates for bacterial replacement therapies of the middle ear. Closing and annotating the genomes of the streptococcal isolates could provide further insights into the physiology of these bacteria and could help assess their probiotic potential. Preliminary studies show the suitability of bioinformatic analysis (i.e. DRAM, MAUVE) for metabolic predictions and genome comparisons, which is also important to evaluate genomic adaptations in otic bacteria compared to the oral ancestors. Additionally, competitive assays between otopathogens and otic streptococcal strains could help understand the mechanisms that drive their antagonism. Furthermore, animal studies are important to evaluate the protective role of streptococci in vivo. Though animal models are available for the study of otitis media [24, 25], model conditions would need to be adapted for the evaluation of the protective role of streptococci when challenged with otopathogens.

The final chapter of my dissertation describes a novel mode of surface translocation by staphylococci in the presence of mucin that could contribute to the invasiveness of these pathobionts into the middle ear. A common nasopharyngeal inhabitant, staphylococci disperse into perioral regions and are frequently isolated from perioral samples. Aerial dispersal also introduces staphylococci into the middle ear though transiently. Yet, staphylococci are a

common cause of otitis media and are typically enriched in the effusion of patients with chronic otitis media [26-29]. Using clinical staphylococcal isolates (n=9) and related laboratory strains, chapter 4 describes the enhanced surface motility of isolates closely related to *Staphylococcus aureus* (n=5) and *Staphylococcus epidermidis* (n=2) in the presence of mucin. The motile behavior was controlled by quorum sensing and dependent on the endogenous secretion of surfactant-active phenol-soluble modulins (PSMs such as PSMα3 and PSMγ). These results provide novel insights into the mechanisms that trigger the rapid movement of staphylococci such as *S. aureus* and *S. epidermidis* on surfaces [30-33]. Additionally, the results strengthen the notion that PSM secretion is critical for staphylococcal motility, as previously reported for colony spreading and comet formation by *S. aureus* [30]. The work presented in chapter 4 also shows that mucin did not expansion of clinical isolates closely related to *Staphylococcus hominis* (n=2), further confirming other studies that classified *S. hominis* as non-motile. This result is also consistent with the inability of *S. hominis* commensals to produce PSMs (PMSα, PSMβ, or PSMγ), particularly those with surfactant activity (PMSα3 and PSMγ). Moreover, the results support with the notion that PSM secretion is most commonly associated with pathogenic species of *Staphylococcus*, rather than with commensal species [34]. Interestingly, the addition of PSM-containing supernatants from clinical strains that showed robust spreading greatly stimulated dendritic expansion of the laboratory *S. aureus* JE2 strain but did not promote the expansion of the *S. hominis* strains, further supporting the notion that endogenous PSM production is essential. When challenged against each other, supernatants from the clinical strains had different effects: while *S. aureus* L0021-02 was unaffected by *S. epidermidis* L0021-06 supernatants, *S. epidermidis* colony spreading was suppressed by the *S. aureus* supernatant. Future studies will need to investigate whether PSMs re involved in cross-species competition, as reported for the

bactericidal effect of *S. epidermidis* PSMs on *S. aureus* [35, 36]. Moreover, HPLC-QTOF analysis of supernatants could shed light on the biochemical and functional diversity of PSMs among the clinical isolates in comparison to laboratory strains and how mucin controls PSM synthesis under conditions previously reported to trigger motility [37]. The effect of mucin types also needs to be examined, as the glycosylation levels, net charge and/or structural conformation in hydrogels could affect the staphylococcal response. Similarly, RNA sequencing analysis could be useful to identify whether mucin activates specific signaling pathways. Particularly important is the co-regulation of genes encoding virulence factors, mucinases and agr-quorum sensing pathways and the integration of physical and chemical cues to modulate motile responses. Additionally, whole-genome sequences could be mined for homolous PSM genes, which are important for mucin-induced motility. Further understanding the metabolism of mucin by staphylococci is important as well. Although mucin growth is not required for mucin-induced motility in *S. aureus* JE2, we observed positive correlations between the robustness of the spreading response in clinical isolates and their ability to use mucin as a growth substrate. In chapter 4, I developed protocols to test for mucin growth in staphylococcal cultures with commercial porcine stomach mucin, but assays with purified mucin would be useful to control the concentration of the glycoproteins and the viscoelastic properties of the mucin-containing medium. Similarly, it is important to investigate how the viscoelastic properties of mucin hydrogels affect dendritic expansion and compare to gel-forming chemicals such as methyl cellulose or polyethylene glycol [38]. Also important is to develop assays that mimic the viscoelastic and hydration properties of the otic mucus layer in health or under conditions (e.g., inflammation of the Eustachian tube) that lead to mucin hyperproduction. Finally, clinical staphylococcal species may target this social behavior for competitive advantages. Competition

assays in the presence of supernatant extracted from either *S. aureus* or *S. epidermidis* clinical isolates may aid in understanding specific molecular components that could contribute to inhibition of either strain's viability. These results identify potential mechanisms and environmental factors that are utilized by staphylococcal species in the middle ear environment to establish and cause disease and afford opportunities for therapeutical interventions.

In summary, the findings described in this dissertation provide novel insights into the adaptive responses that contribute to the colonization of the middle ear and site-specific adaptations of otic commensals. The work also describes syntrophic and antagonistic relationships that could help build, support and regulate a healthy bacterial commensal community in the otic mucosa. Finally, this study revealed a hitherto unknown role for mucin in the spread of staphylococcal otopathogens. Future studies of the otic microbiome are however needed to elucidate the inter-connections of the otic and (peri)oral microbial communities and the environmental factors that disrupt the otic commensal communities and trigger infections.

REFERENCES

REFERENCES

1. Bluestone, C.D., Eustachian tube: structure, function, role in otitis media, ed. M.B. Bluestone. 2005, Hamilton; Lewiston, NY: BC Decker. 219.

2. Hall-Stoodley, L., et al., Direct detection of bacterial biofilms on the middle-ear mucosa of children with chronic otitis media. JAMA, 2006. 296(2): p. 202-11.

3. Jervis-Bardy, J., et al., Examining the Evidence for an Adult Healthy Middle Ear Microbiome. mSphere, 2019. 4(5).

4. Minami, S.B., et al., Microbiomes of the normal middle ear and ears with chronic otitis media. Laryngoscope, 2017. 127(10): p. E371-E377.

5. Tonnaer, E.L., et al., Detection of bacteria in healthy middle ears during cochlear implantation. Arch. Otolaryngol. Head Neck Surg., 2009. 135(3): p. 232-7.

6. Nguyen, C.T., et al., Noninvasive in vivo optical detection of biofilm in the human middle ear. Proc Natl Acad Sci U S A, 2012. 109(24): p. 9529-34.

7. Luers, J.C. and K.B. Huttenbrink, Surgical anatomy and pathology of the middle ear. J. Anat., 2016. 228(2): p. 338-53.

8. Koskinen, K., et al., The nasal microbiome mirrors and potentially shapes olfactory function. Scientific Reports, 2018. 8(1): p. 1296.

9. Wolf, A., et al., The salivary microbiome as an indicator of carcinogenesis in patients with oropharyngeal squamous cell carcinoma: A pilot study. Sc. Rep., 2017. 7.

10. Huffnagle, G.B., R.P. Dickson, and N.W. Lukacs, The respiratory tract microbiome and lung inflammation= a two-way street. Mucosal Immunol, 2017. 10(2): p. 299-306.

11. Dickson, R.P. and G.B. Huffnagle, The lung Microbiome: New principles for respiratory bacteriology in health and disease. PLoS Pathog, 2015. 11(7): p. e1004923.

12. Dickson, R.P., et al., Spatial variation in the healthy human lung microbiome and the adapted island model of lung biogeography. Ann Am Thorac Soc, 2015. 12(6): p. 821-30.

13. Bassis, C.M., et al., Analysis of the upper respiratory tract microbiotas as the source of the lung and gastric microbiotas in healthy individuals. mBio, 2015. 6(2): p. e00037.

14. Venkataraman, A., et al., Application of a neutral community model to assess structuring of the human lung microbiome. mBio, 2015. 6(1).

15. Deo, P.N. and R. Deshmukh, Oral microbiome: Unveiling the fundamentals. J Oral Maxillofac Pathol, 2019. 23(1): p. 122-128.

16. Huang, R., M. Li, and R.L. Gregory, Bacterial interactions in dental biofilm. Virulence, 2011. 2(5): p. 435-44.

17. Chalmers, N.I., et al., Characterization of a *Streptococcus* sp.-*Veillonella* sp. community micromanipulated from dental plaque. J Bacteriol, 2008. 190(24): p. 8145-54.

18. Distler, W. and A. Kröncke, The lactate metabolism of the oral bacterium *Veillonella* from human saliva. Archives of Oral Biology, 1981. 26(8): p. 657-661.

19. Delwiche, E.A., J.J. Pestka, and M.L. Tortorello, The *Veillonella*e: gram-negative cocci with a unique physiology. Annu Rev Microbiol, 1985. 39: p. 175-93.

20. Kandler, O., Carbohydrate metabolism in lactic acid bacteria. Antonie Van Leeuwenhoek, 1983. 49(3): p. 209-24.

21. Selwal, K.K., M.K. Selwal, and Z. Yu, Mucolytic bacteria: prevalence in various pathological diseases. World Journal of Microbiology and Biotechnology, 2021. 37(10): p. 176.

22. Rios-Covian, D., et al., Shaping the metabolism of intestinal bacteroides population through diet to improve human health. Front Microbiol, 2017. 8: p. 376.

23. Tano, K., et al., A nasal spray with alpha-haemolytic streptococci as long term prophylaxis against recurrent otitis media. Recent Advances in Otitis Media, Proceedings, 2001: p. 397-402.

24. Davidoss, N.H., Y.K. Varsak, and P.L. Santa Maria, Animal models of acute otitis media – A review with practical implications for laboratory research. European Annals of Otorhinolaryngology, Head and Neck Diseases, 2018. 135(3): p. 183-190.

25. Park, M.K. and B.D. Lee, Development of animal models of otitis media. Korean J Audiol, 2013. 17(1): p. 9-12.

26. Celin, S.E., et al., Bacteriology of acute otitis media in adults. JAMA, 1991. 266(16): p. 2249-2252.

27. Niedzielski, A., L.P. Chmielik, and T. Stankiewicz, The Formation of biofilm and bacteriology in otitis media with effusion in children= A prospective cross-sectional study. International Journal of Environmental Research and Public Health, 2021. 18(7): p. 3555.

28. Ding, Y.L., et al., Molecular characterization and antimicrobial susceptibility of *Staphylococcus aureus* isolated from children with acute otitis media in Liuzhou, China. BMC Pediatrics, 2018. 18(1): p. 388.

29. Kurono, Y., K. Tomonaga, and G. Mogi, *Staphylococcus epidermidis* and *Staphylococcus aureus* in Otitis Media With Effusion. Archives of Otolaryngology–Head & Neck Surgery, 1988. 114(11): p. 1262-1265.

30. Pollitt, E.J.G. and S.P. Diggle, Defining motility in the Staphylococci. Cell Mol Life Sci, 2017. 74(16): p. 2943-2958.

31. Pollitt, E.J., S.A. Crusz, and S.P. Diggle, *Staphylococcus aureus* forms spreading dendrites that have characteristics of active motility. Sci Rep, 2015. 5: p. 17698.

32. Tsompanidou, E., et al., Distinct roles of phenol-soluble modulins in spreading of *Staphylococcus aureus* on wet surfaces. Appl Environ Microbiol, 2013. 79(3): p. 886-95.

33. Tsompanidou, E., et al., Requirement of the agr locus for colony spreading of *Staphylococcus aureus*. J Bacteriol, 2011. 193(5): p. 1267-72.

34. Rautenberg, M., et al., Neutrophil responses to staphylococcal pathogens and commensals via the formyl peptide receptor 2 relates to phenol-soluble modulin release and virulence. FASEB J, 2011. 25(4): p. 1254-63.

35. Zaman, M. and M. Andreasen, Cross-talk between individual phenol-soluble modulins in *Staphylococcus aureus* biofilm enables rapid and efficient amyloid formation. Elife, 2020. 9.

36. Canovas, J., et al., Cross-Talk between *Staphylococcus aureus* and Other Staphylococcal Species via the agr Quorum Sensing System. Front Microbiol, 2016. 7: p. 1733.

37. Wu, X. and C. Zhang, Determination of Staphylococcal Phenol-Soluble Modulins (PSMs) by a High-Resolution HPLC-QTOF System. 2017.

38. Co, J.Y., et al., Mucins trigger dispersal of *Pseudomonas aeruginosa* biofilms. NPJ Biofilms Microbiomes, 2018. 4: p. 23.